TECHNICAL DOCUMENTARY REPORT

WDL-TR1943
VOLUME III
31 JANUARY 1963

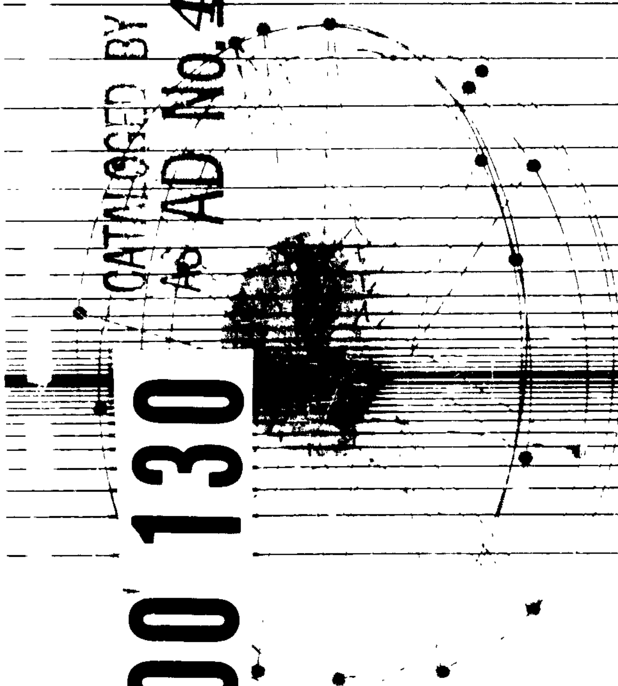

SPECIAL PARAMETER TRACKING SIMULATION STUDY
VOL III - SUMMARIZATION MATERIAL

PREPARED FOR
AIR FORCE SPACE SYSTEMS DIVISION
AIR FORCE SYSTEMS COMMAND
UNITED STATES AIR FORCE
INGLEWOOD, CALIFORNIA

CONTRACT NO. AF04(695)-113

PHILCO WESTERN DEVELOPMENT LABORATORIES
PALO ALTO, CALIFORNIA

63 3-1

PHILCO CORPORATION — Western Development Laboratories

In reply cite: 614-3-71
RWB/EHG:pjc
28 January 1963

SUBJECT: Contract AF04(695)-113
Submission of Technical Report WDL-TR1943, Volume III
As a deliverable item

TO: Commander
Space Systems Division
Air Force Systems Command
United States Air Force
Air Force Unit Post Office
Los Angeles 45, California

ATTENTION: Technical Data Center

INFO COPIES: D. Cowart, CSD #3 (1 copy)
R. Drown, AFSSD/SSOCK (w/o enclosure)

REFERENCE: (a) Contract AF04(695)-113, Exhibit "A"
(b) Section IV, Paragraph 4.2.2 of AFBM Exhibit 58-1
(c) Paragraph 1.2.1.2 of AFSSD Exhibit 61-27A

In accordance with the requirements of references (a), (b), and (c), we are forwarding ten (10) copies of the following document:

Title	No. and Date
Special Parameter Tracking Simulation Study, Volume III - Summarization Material	WDL-TR1943 31 January 1963

PHILCO CORPORATION
Western Development Laboratories

R. W. Boyd
Manager, Contracts Management

WDL-TR1943
Volume III
31 January 1963

TECHNICAL DOCUMENTARY REPORT

SPECIAL PARAMETER TRACKING SIMULATION STUDY VOLUME III - SUMMARIZATION MATERIAL

Prepared by

PHILCO CORPORATION
Western Development Laboratories
Palo Alto, California

Contract AF04(695)-113

Prepared for

SPACE SYSTEMS DIVISION
AIR FORCE SYSTEMS COMMAND
UNITED STATES AIR FORCE
Inglewood, California

FOREWORD

This volume is the third in a series prepared by the Mathematical Analysis Department of Philco WDL to be used as a Design Trade-Off Handbook for error propagation in orbit determination. Using these three volumes, conclusions concerning the effects on down-range prediction accuracy of many pertinent variables can be determined.

Sections 1 through 8 of this volume contain a description of the methods used in arriving at the summary, together with suggestions for its use. More specifically:

Section 1 contains a review of the parameters used to generate Volumes I and II;

Section 2 discusses the purpose of Volume III;

The method used to compare propagated errors is discussed in Section 3;

Sections 4, 5, and 6 describe the trade-off curves that were generated, as well as the method used for their generation;

Section 7 suggests methods for their use.

The summary material itself can be found in Appendix Sections A and B.

ABSTRACT

PHILCO WDL-TR1943	UNCLASSIFIED
SPECIAL PARAMETER	
TRACKING SIMULATION STUDY	
VOL. III, SUMMARIZATION MATERIAL	70 pages
31 January 1963	Contract AF04(695)-113

This volume is the third in a series -- prepared by the Mathematical Analysis Department at Philco WDL -- to be used as a design trade-off handbook for error propagation in orbit determination. Volume I contains all the material derived from the 125 NMI satellite orbit; Volume II contains the same information for the 2000 NMI orbit. This volume summarizes the results of Volumes I and II.

FOREWORD

This Technical Documentary Report on Definitive Contract AF04(695)-113 has been prepared in accordance with Exhibit "A" of that contract and Paragraph 4.2.2 of AFBM Exhibit 58-1, "Contractor Reports Exhibit," dated 1 October 1959, as revised and amended.

This report was prepared by Philco Western Development Laboratories in fulfilling the requirements of Paragraph 1.2.1.2 of AFSSD Exhibit 61-27A, "Satellite Control Subsystem Work Statement," dated 15 February 1962, as revised and amended.

TABLE OF CONTENTS

LIST OF ILLUSTRATIONS

LIST OF TABLES

SPECIAL PARAMETER TRACKING SIMULATION STUDY
VOLUME III - SUMMARIZATION MATERIAL

1. INTRODUCTION

This volume is the third in a series -- prepared by the Mathematical Analysis Department at Philco WDL -- to be used as a design trade-off handbook for error propagation in orbit determination.

Parameter values used in the preparation of Volumes I and II were supplied by AFSSD (See Table 1), and were used as inputs to the Co-Variance Fixed-Bias Simulation Program.* The output of these first two volumes represents results in graphical form of satellite position accuracy as a function of track data, number of passes, station separation, and other pertinent variables. Volume I contains all the material derived from the 125 NMI satellite orbit; Volume II contains the same information for the 2000 NMI orbit.

This volume summarizes the results of Volumes I and II.

1.1 Review of Volumes I and II

Of the cases listed in Table 1, the following combinations were run: Sensors 1 through 6 -- all cases (i.e., A through E, I and II, with all combinations of accuracies).

For Orbit I, one sample per 4 sec was assumed; for Orbit II, two samples per minute was assumed.

All data within 5° of horizon was used; station assumed underneath pass, except for Station Case B, where each pass was 56° from zenith for Orbit Case I and 14° for Orbit Case II.

* For a description of the program, see Philco WDL Technical Note, "A User's Manual for Three Tracking Simulators," to be published.

For Sensor Case 2 only, Cases A and B were run with I and II, for range error 300 ft, angle error 1 milliradian, using all data within 20° of the horizon.

TABLE 1
AFSSD - SUPPLIED PARAMETER VALUES

CONFIGURATIONS*

Station Case A	Single Station	Single Pass
Station Case B	Single Station	Double Pass
Station Case C	Two Stations with 45° latitude separation	each one pass
Station Case D	Two Stations with 90° latitude separation	each one pass
Station Case E	Two Stations with 180° latitude separation	each one pass
Orbit Case I	125 NMI circular orbit 90° inclination	
Orbit Case II	2,000 NMI circular orbit 90° inclination	
Sensor Case 1	θ, ϕ	
Sensor Case 2	S, θ, ϕ	
Sensor Case 3	$\dot{S}$, θ, ϕ	
Sensor Case 4	S	
Sensor Case 5	$\dot{S}$, S, θ, ϕ	
Sensor Case 6	$\dot{S}$	

SENSOR ACCURACIES*

θ and ϕ: 0.1, 1, and 10 milliradians
S: 50, 300 ft
$\dot{S}$: 0.1, 1, 5 ft/sec

* θ means azimuth, ϕ elevation, S range, and $\dot{S}$ range rate.

Outputs of the above simulation are plots of in-track, altitude, and cross-track position and velocity errors vs time, up to three revolutions from the last sighting. These plots have the last sighting on a common axis for ready cross comparison.

For both altitudes and for the various station cases and sensor errors, each graph consists of the standard deviations (or equivalently, the rms) of the orbit's Frenet trihedron coordinate errors plotted against time. The initial time is the last time the satellite is seen by a station. By the orbit's Frenet trihedron coordinates (X, Y, Z) is meant a set of local coordinates in the orbital plane, and orthogonal to it, with the origin at the satellite's position and with direction as follows:

X in the direction of the velocity vector

Y orthogonal at the left (directed counterclockwose thru $\pi/2$ in the orbital plane)

Z perpendicular to (X,Y) by the right-hand rule.

Then (for a circular orbit):

σ_X = the standard deviation of the in-track error,
σ_Y = the standard deviation of the altitude error,
σ_Z = the standard deviation of the cross-track error, and
$\sigma_{\dot{X}}$, $\sigma_{\dot{Y}}$, and $\sigma_{\dot{Z}}$ are the standard deviations of $\dot{X}$, $\dot{Y}$, and $\dot{Z}$.

For quick reference, the graphs are ordered as A, B, C, D, or E and 1 through 37 to refer to, respectively, the station case and sensor errors used. The sensor errors are assumed to be normally distributed with mean zero.

2. PURPOSE OF VOLUME III

When Volumes I and II had been completed, it became obvious that additional work would have to be done to convert the information available in these volumes to a form which would be immediately applicable for the design of tracking systems; in Volume III, an attempt has been made to do this.

In this volume, the data which was generated in the first two volumes has been summarized, and, whenever possible, trade-off curves for different types of tracking accuracies have been determined.

The fundamental problem in reducing and summarizing the great mass of available data in Volumes I and II is that the large number of parameters can significantly affect the final results. These parameters are of three general types:

a. The tracking station and orbital shape configuration (i.e., the number of stations and their location, as well as the nominal orbit of the vehicle)

b. Types of tracking sensors used in the analysis (Volumes I and II considered range, range rate, azimuth and elevation information)

c. The errors associated with each type of tracking measurement

To convert the information to a useful form, it is necessary to hold fixed all but two of the parameters, because when a level curve is drawn on a piece of paper, there are only two dimensions.

3. ERROR MEASUREMENT

The graphs in volumes I and II presented the propagation of error as a function of time during the first three revolutions after the vehicle was last tracked. One of the first parameters which had to be eliminated was the time variation. After careful consideration, it was decided that the measure of error which would be used in this summarization volume would be the maximum of the trace of the covariance matrix for position determination. This maximum is a function of the tracking errors, as well as the geometry and type of tracking error. For the remainder of this report, this function will be designated by

$$f(\sigma_S, \sigma_{\dot{S}}, \sigma_{\phi,\theta})$$

where σ_S is the standard deviation in range, $\sigma_{\dot{S}}$ range rate, and $\sigma_{\phi,\theta}$ elevation and azimuth.* If any of the σ's are missing, this indicates that that particular type of tracking data was not used. For example, $f(\sigma_S)$ means that only range data was considered.

Hence, for a fixed station and orbital configuration,

$$f = \max_{3\ \text{rev}} \sqrt{\sigma_X^2 + \sigma_Y^2 + \sigma_Z^2}$$

where σ_X^2, σ_Y^2, σ_Z^2 are the diagonal elements in the co-variance matrix.

To further describe the functional independence between f and the independent σ variables, if time were added as an additional variable, then

$$\sqrt{\sigma_X^2 + \sigma_Y^2 + \sigma_Z^2} \quad (t)$$
$$= \sqrt{\text{trace}\left\{B\left(\frac{1}{\sigma_S^2} F_S + \frac{1}{\sigma_{\dot{S}}^2} F_{\dot{S}} + \frac{1}{\sigma_{\phi,\theta}^2} F_{\phi,\theta}\right)^{-1} B^T\right\}} \quad (1)$$

---

* It is assumed that, if one angular measurement is taken, the other one is also taken, and that both measurements have the same Gaussian noise content.

where the F's are sums of the partial derivatives of the tracking data with respect to initial conditions (summed over all the tracking data) and B is a matrix of partial derivatives of downrange position with respect to the initial conditions.*

The rms error considered in this report is the maximum of this time-varying quantity over the first three revolutions after the last observational pass.

Because the error propagation is assumed to be linear, the following relationship exists:

$$\alpha f(\sigma_S, \sigma_{\dot{S}}, \sigma_{\phi,\theta}) = f(\alpha\sigma_S, \alpha\sigma_{\dot{S}}, \alpha\sigma_{\phi,\theta}) \qquad (2)$$

for a suitable range of α (i.e., sufficiently small that the error propagation remains linear).**

Because of the nature of f, if a particular type of tracking data is not considered, the f function for this type of tracking data is equivalent to the original f function where the appropriate σ has become infinitely large. Hence, asymptotes exist for the trade-off curves. For example, if the trade-off curve is between range and angles, and if no angle information is used, there will be a value of σ_S that will produce the fixed maximum three-orbit error.

---

* For a derivation and further explanation of these equations, see Philco Technical Note, "A User's Manual for Three Tracking Simulators," to be published.

** The range for α is a function of the geometry of the orbit, station and data configuration.
See Appendix B of the above-named Philco Technical Note.

Because of the properties of f, it is also true that

$$f(\sigma_S, \sigma_{\dot{S}}, \sigma_{\phi,\theta}) \leq f(\sigma_S, \sigma_{\dot{S}}) \tag{3}$$

$$f(\sigma_S, \sigma_{\phi,\theta}) \leq f(\sigma_S)$$

and similarly for other combinations of the independent variables.

4. DESCRIPTION OF THE TRADE-OFF CURVES

It was decided that useful trade-off curves could be constructed by determining 2-dimensional cuts from the 4-dimensional surface

$$f = \text{constant}. \tag{4}$$

Such curves had been constructed for the 10 orbital and station configurations, with five orbital and station configurations for each of two altitudes (see Table 1).

5. TYPES OF TRADE-OFF CURVES

For each of the 10 orbital and station configurations, five families of curves were to be generated. The form of these trade-off curves is shown in Table 2.

6. TECHNIQUES USED IN THE GENERATION OF TRADE-OFF CURVES

The tabulated results used to generate the curves can be found in Appendix B. To form curves I and II for the 10 orbital and tracking configurations, all that was required was the use of the linearity property of f (see equation 2). And, to obtain better shapes for the curves, the existing asymptotes were also used.

TABLE 2

TRADE-OFF CURVE FORMS

CURVE NO.	CURVE DESCRIPTION
I	Errors in range vs errors in angle, i.e., level curves of $f(\sigma_S, \sigma_{\phi,\theta}) = \text{constant}$
II	Errors in range rate vs errors in angles, i.e., level curves of $f(\sigma_{\dot{S}}, \sigma_{\phi,\theta}) = \text{constant}$.
III	Errors in range rate vs errors in angles for particular values of errors in range and values of f.
IV	Errors in range vs errors in range rate for particular values of errors in angles and values of f.
V	Errors in range vs errors in angles for particular values of errors in range rate and f.

Before creating the above curve forms for the 10 orbital and tracking configurations, a set of 12 graphs was drawn for each configuration. These are graphs of the accuracy of one sensor vs rms for fixed sensor accuracy of the other sensors. From these graphs, curves III and IV were constructed.*

6.1 <u>Curve Form III ($\sigma_{\dot{S}}$, $\sigma_{\phi,\theta}$)</u>

Note, first, that $\frac{1}{6} f(300, \sigma_{\dot{S}}, \sigma_{\phi,\theta}) = f(50, \frac{\sigma_{\dot{S}}}{6}, \frac{\sigma_{\phi,\theta}}{6})$.

* For a description of graphs 1-12, see Table 3.

An rms was chosen that was common to several of the graphs 1-6 and such that six times this rms was common to several of the graphs 7-12.* The pairs ($\sigma_{\dot{S}}$, $\sigma_{\phi,\theta}$) were then obtained from graphs 1-12 as follows ($\sigma_{\phi,\theta}$ and $\sigma_{\dot{S}}$ were read from the graphs):

TABLE 3

GRAPHS USED IN CONSTRUCTING
CURVE FORMS III AND IV

GRAPH NO.	SENSOR ACCURACY	FIXED SENSOR ACCURACY
1	$\sigma_{\phi,\theta}$ vs rms	$\sigma_S = 50$, $\sigma_{\dot{S}} = 0.1$
2	$\sigma_{\phi,\theta}$ vs rms	$\sigma_S = 50$, $\sigma_{\dot{S}} = 1$
3	$\sigma_{\phi,\theta}$ vs rms	$\sigma_S = 50$, $\sigma_{\dot{S}} = 5$
4	$\sigma_{\dot{S}}$ vs rms	$\sigma_S = 50$, $\sigma_{\phi,\theta} = 0.1$
5	$\sigma_{\dot{S}}$ vs rms	$\sigma_S = 50$, $\sigma_{\phi,\theta} = 1$
6	$\sigma_{\dot{S}}$ vs rms	$\sigma_S = 50$, $\sigma_{\phi,\theta} = 10$
7	$\sigma_{\phi,\theta}$ vs rms	$\sigma_S = 300$, $\sigma_{\dot{S}} = 0.1$
8	$\sigma_{\phi,\theta}$ vs rms	$\sigma_S = 300$, $\sigma_{\dot{S}} = 1$
9	$\sigma_{\phi,\theta}$ vs rms	$\sigma_S = 300$, $\sigma_{\dot{S}} = 5$
10	$\sigma_{\dot{S}}$ vs rms	$\sigma_S = 300$, $\sigma_{\phi,\theta} = 0.1$
11	$\sigma_{\dot{S}}$ vs rms	$\sigma_S = 300$, $\sigma_{\phi,\theta} = 1$
12	$\sigma_{\dot{S}}$ vs rms	$\sigma_S = 300$, $\sigma_{\phi,\theta} = 10$

* For a description of graphs 1-12, see Table 3.

1. $(0.1, \sigma_{\phi,\theta})$
2. $(1, \sigma_{\phi,\theta})$
3. $(5, \sigma_{\phi,\theta})$
4. $(\sigma_{\dot{S}}, 0.1)$
5. $(\sigma_{\dot{S}}, 1)$
6. $(\sigma_{\dot{S}}, 10)$
7. $\frac{1}{6}(0.1, \sigma_{\phi,\theta})$
8. $\frac{1}{6}(1, \sigma_{\phi,\theta})$
9. $\frac{1}{6}(5, \sigma_{\phi,\theta})$
10. $\frac{1}{6}(\sigma_{\dot{S}}, 0.1)$
11. $\frac{1}{6}(\sigma_{\dot{S}}, 1)$
12. $\frac{1}{6}(\sigma_{\dot{S}}, 10)$

From this data, curve III was constructed.

6.2 Curve Form IV $(\sigma_S, \sigma_{\dot{S}})$

The method used to draw curve IV was a more complicated one than was used in drawing curve III. Graphs 4 and 10, 5 and 11, 6 and 12 were examined for an rms that was common to one of the pairs. Such points gave two points on the graph. Let r be the ratio of the rms to the $\sigma_{\phi,\theta}$ that was chosen. Consider the line $Y = rX$ transposed on 1-3 and 7-9. If this line crossed the curve at, for example, (X_1, Y_1), then $\frac{\sigma_{\phi,\theta}}{X_1}$ was multiplied by

(50, 0 1) for graph 1

(50, [illegible]) for graph 2

(50, 5) for [illegible]

(300, 0.1) for graph 7

(300, 1) for graph 8

(300, 5) for graph 9

From this data, curve form IV was constructed.

6.3 Curve Form V

Because common rms values were lacking in the data in Volumes I and II, it was impossible to construct curve form V for the 10 orbital and tracking configurations.

6.4 General Comments Concerning Curve Forms III, IV and V

Some of the Type III and IV curve form graphs were constructed, using two points and two asymptotes. In general, an even samller amount of data was available for curve number V. Also, since only three points were available for each of the graphs 1-12, interpolation of these graphs was sometimes inaccurate. Because of this lack of data, it is recommended that additional data be created in order that families of graphs can be created for curve forms III, IV, and V (presently, only a single curve may be constructed for curve forms III and IV).

7. USE OF THE GRAPHS

The usefulness of such curves is that they immediately enable a system engineer to determine trade-off between required accuracy and the various types of tracking measurements. They also facilitate the comparision between different station and orbital configurations. For example, the first type of level curve is also constructed of the form (see Fig. 1):

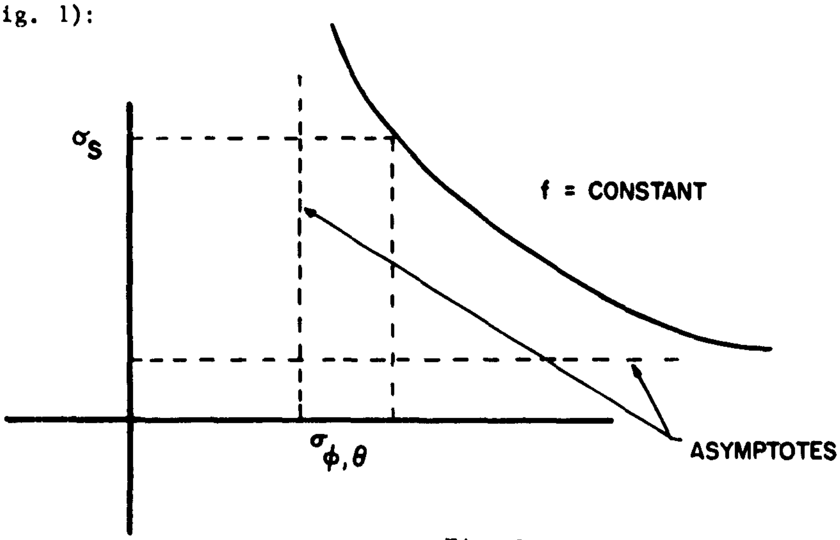

(6)

Fig. 1

This curve can be interpreted and used in the following way. For a given σ_S, it is possible, by projecting over to the curve and then down to the other axis, to immediately determine the necessary angular accuracy to maintain the orbit position accuracy to within a given mission requirement. If the designer has available equipment which is more accurate than the $\sigma_{\phi,\theta}$ read off the graph, he can be assured that the mission requirements will be met. If, on the other hand, this was not the level of accuracy he was contemplating, he must increase the accuracy of either σ_S or $\sigma_{\phi,\theta}$, or both.

For range and angle equipment and/or range-rate and angle equipment, curve forms I and II are quite useful. They can be used as shown in Table 4. For range, range rate, and angle equipment, it should be noted that, because of the limitations of curves numbered III-V (caused by a lack of data), curves numbered 1-12 -- as well as the tabular values to be found in Appendix B -- should generally be used.

8. APPENDIX MATERIAL

Trade-off curves are presented in Appendix A, in the following order:

Page No.'s	Material
A-1 through A-10 and A-21 through A-25	125 NMI orbit: curve forms I through IV for orbital tracking configurations A through E (20 graphs)
A-11 through A-20 and A-26 through A-30	2000 NMI orbit: curve forms I through IV for orbital tracking configurations A through E (20 graphs)
A-31 through A-40	125 NMI orbit: graphs 1 through 12 for configurations A through E (60 graphs)
A-41 through A-50	2000 NMI orbit: graphs 1 through 12 for configurations A through E (60 graphs)

Tracking sensors and errors, together with a list of the rms's that were plotted, are contained in Appendix B.

TABLE 4

	EXAMPLES OF THE TYPE OF INFORMATION DESIRED	HOW TO OBTAIN THE INFORMATION FROM THE GRAPHS
1.	Determine what tolerance in range equipment sensors is necessary (given the value of the angle sensor accuracy) to be sure the error in position is less than β NMI after 3 revolutions.	Can be answered directly by $\beta = \alpha$ in curve form I.
2.	What is the comparable value (to 1 above) in the range-rate equipment.	Can be answered directly by using curve form II and setting $\beta = \alpha$.
3.	How does range and angle sensor accuracy compare with range-rate and angles for various values of the angle sensors?	Use 1. and 2. above, or construct a curve such as Fig. 2 (Taken from I and II).
4.	Compute the maximum expected rms (after 3 revolutions) for a given accuracy in the range and angle equipment.	Let the ratio of the angle error to the range error be r and consider the curve $\sigma_{\lambda,\theta} = r\,\sigma$ going through the curve in I. Where the curves cross, determines the desired value of α, i.e. if it crosses at (X_1, Y_1), then α = the given angle sensor error divided by X_1.

TABLE 4 (Cont'd)

	EXAMPLES OF THE TYPE OF INFORMATION DESIRED	HOW TO OBTAIN THE INFORMATION FROM THE GRAPHS
5.	To compute the maximum rms after 3 revolutions given the range-rate equipment accuracy.	4. above, but $\sigma_{\dot{S}}$ and curve form II instead of σ_S and I.
6.	Compare station case A and B, etc.	Depending on the type of comparison desired, the methods described above can give a great diversity in such types of comparisons.

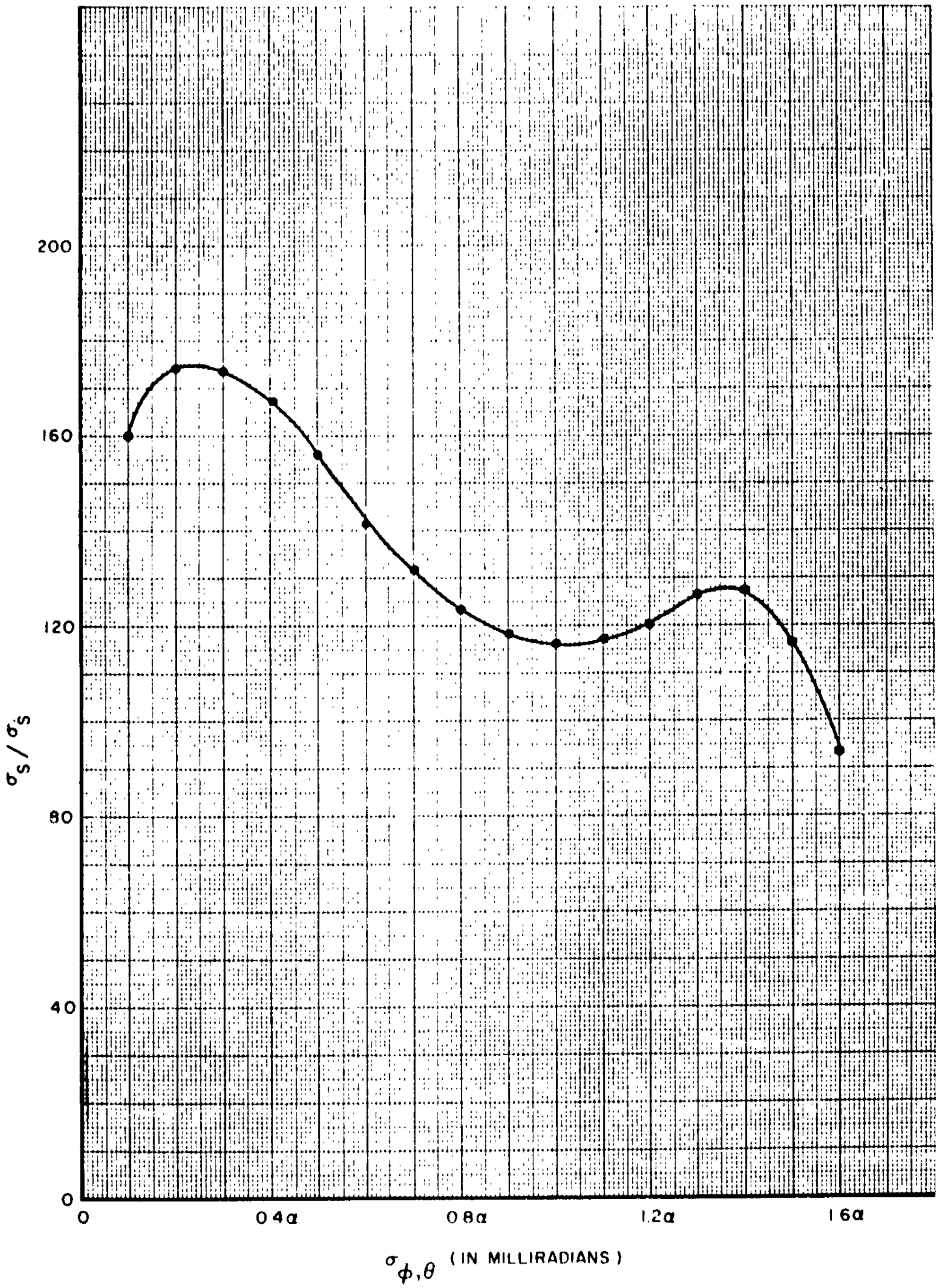

FIG. 2 RANGE AND ANGLES VS RANGE RATE AND ANGLES
125 NMI ORBIT, STATION CASE A, RMS= α NMI

APPENDIX A

TRADE-OFF CURVES

TRADE-OFF CURVES
FOR RANGE AND ANGLE SENSORS
AND
RANGE RATE AND ANGLE SENSORS

CURVE NO. (AT TOP OF GRAPH)	CURVE DESCRIPTION
I	σ_S vs. $\sigma_{\phi,\theta}$
II	$\sigma_{\dot{S}}$ vs. $\sigma_{\dot{\phi},\dot{\theta}}$

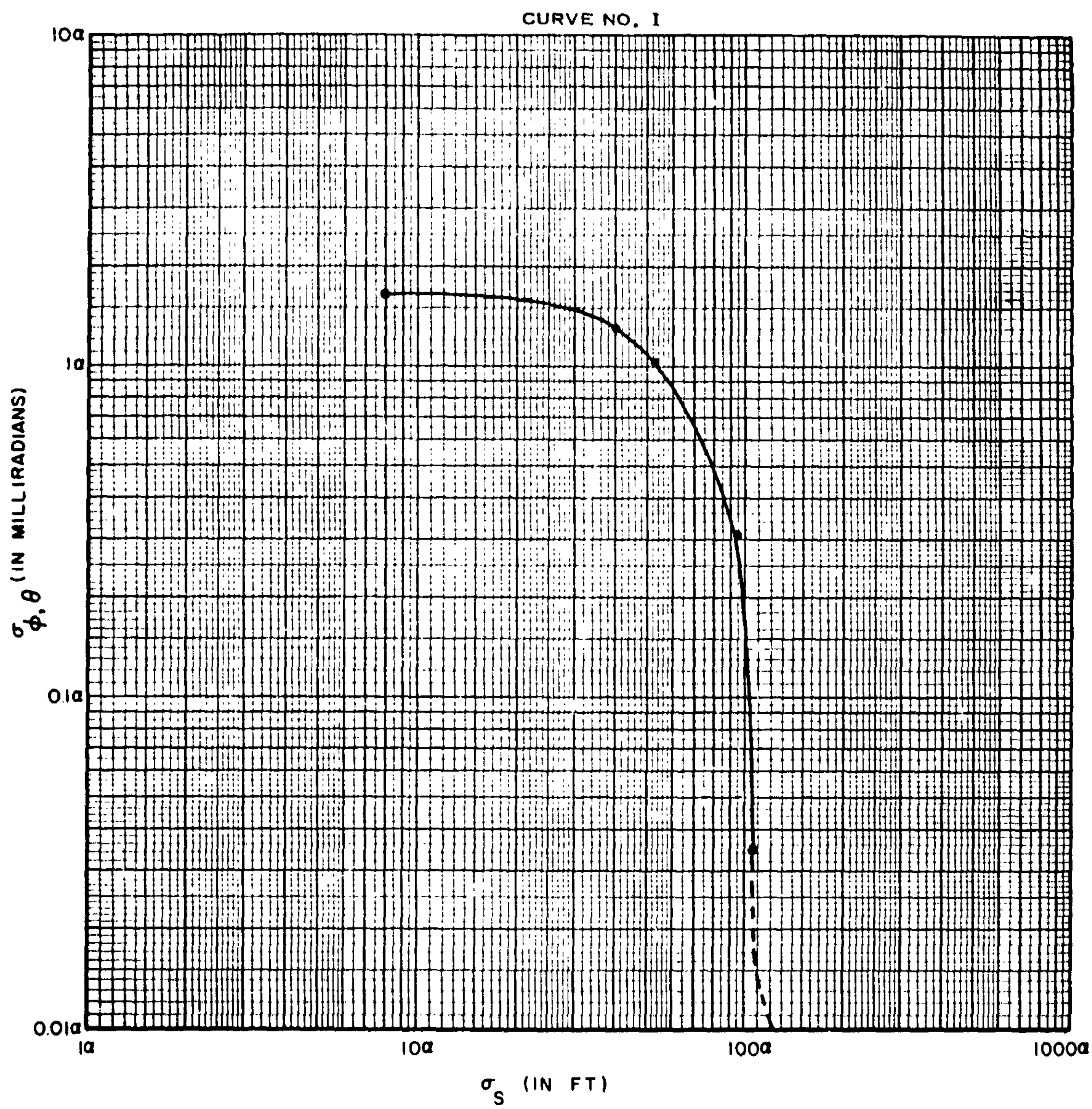

FIG. A-1 125 NMI ORBIT
STATION CASE A, RMS = α NMI

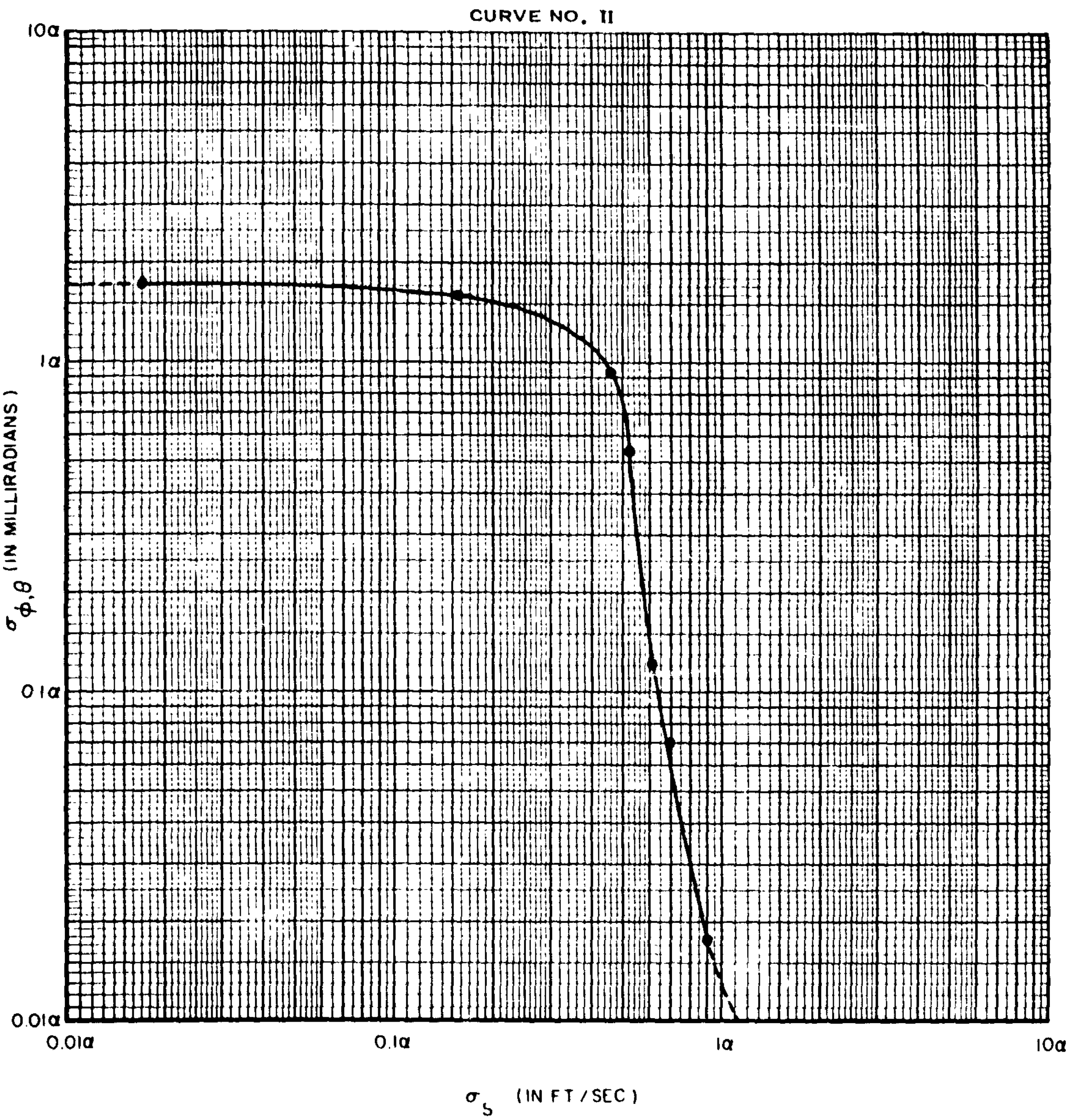

FIG. A-2 125 NMI ORBIT
STATION CASE A, RMS = α NMI

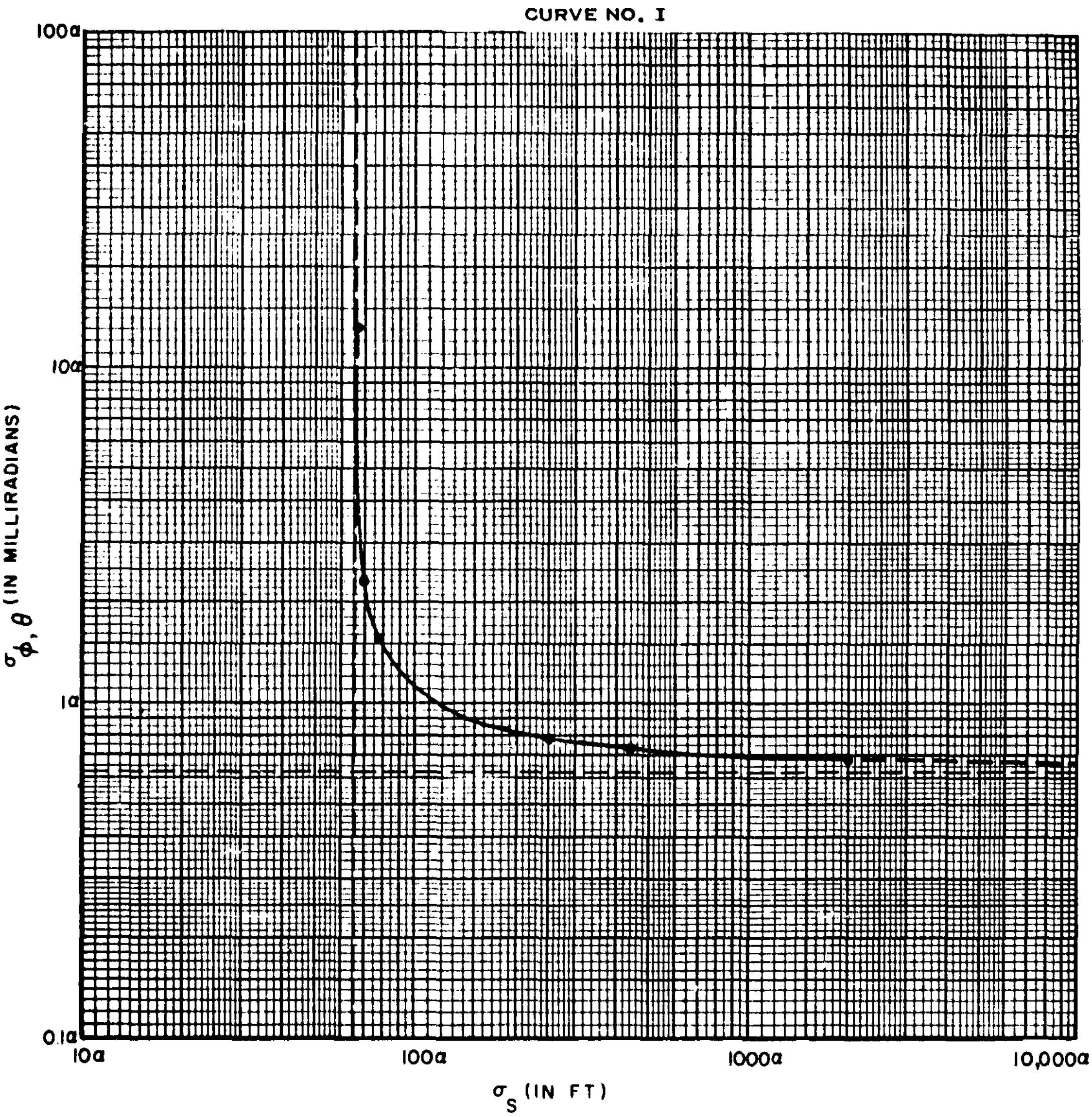

FIG. A-3 125 NMI ORBIT
STATION CASE B, RMS = α NMI

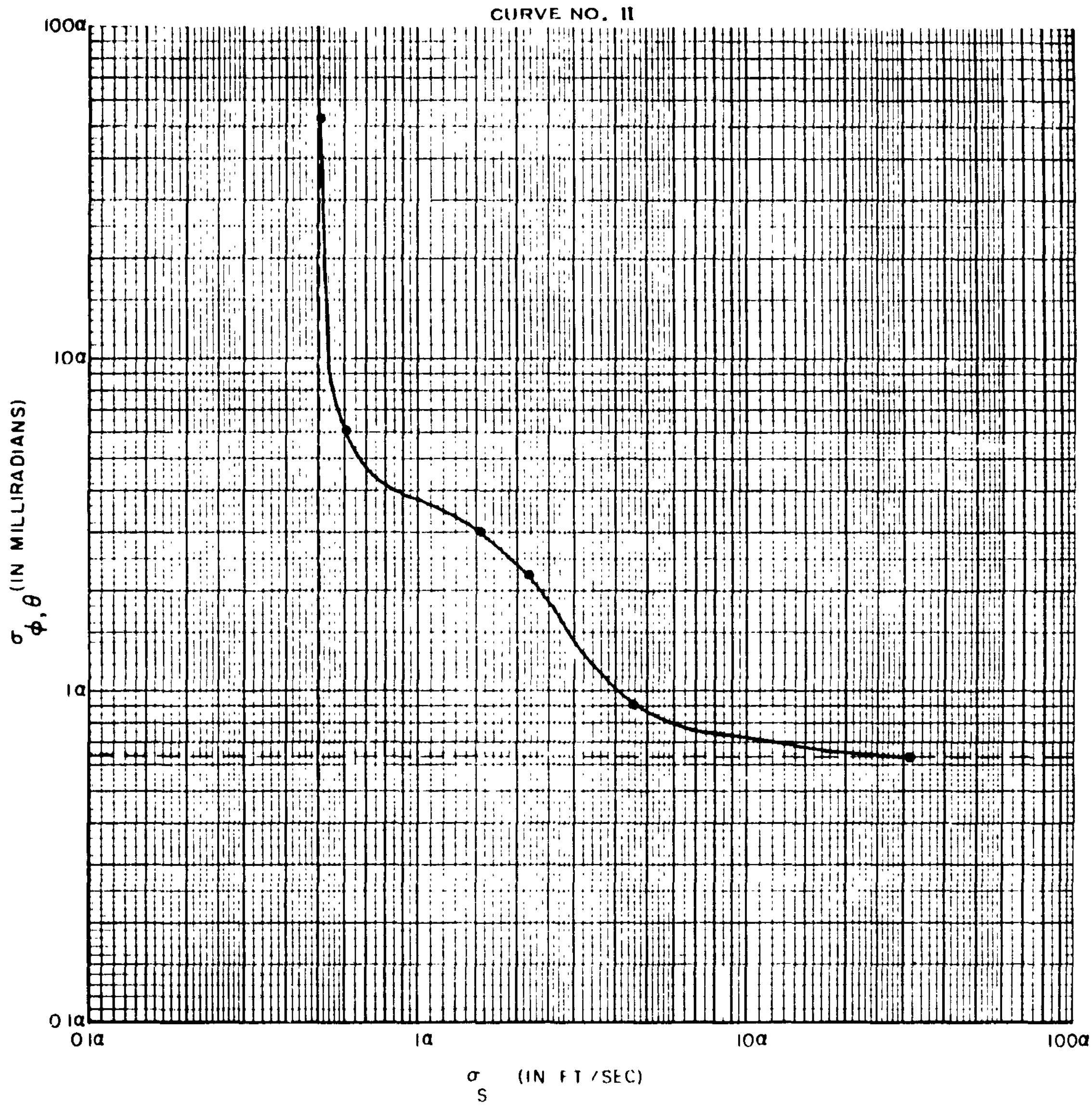

FIG. A-4 125 NMI ORBIT
STATION CASE B, RMS α NMI

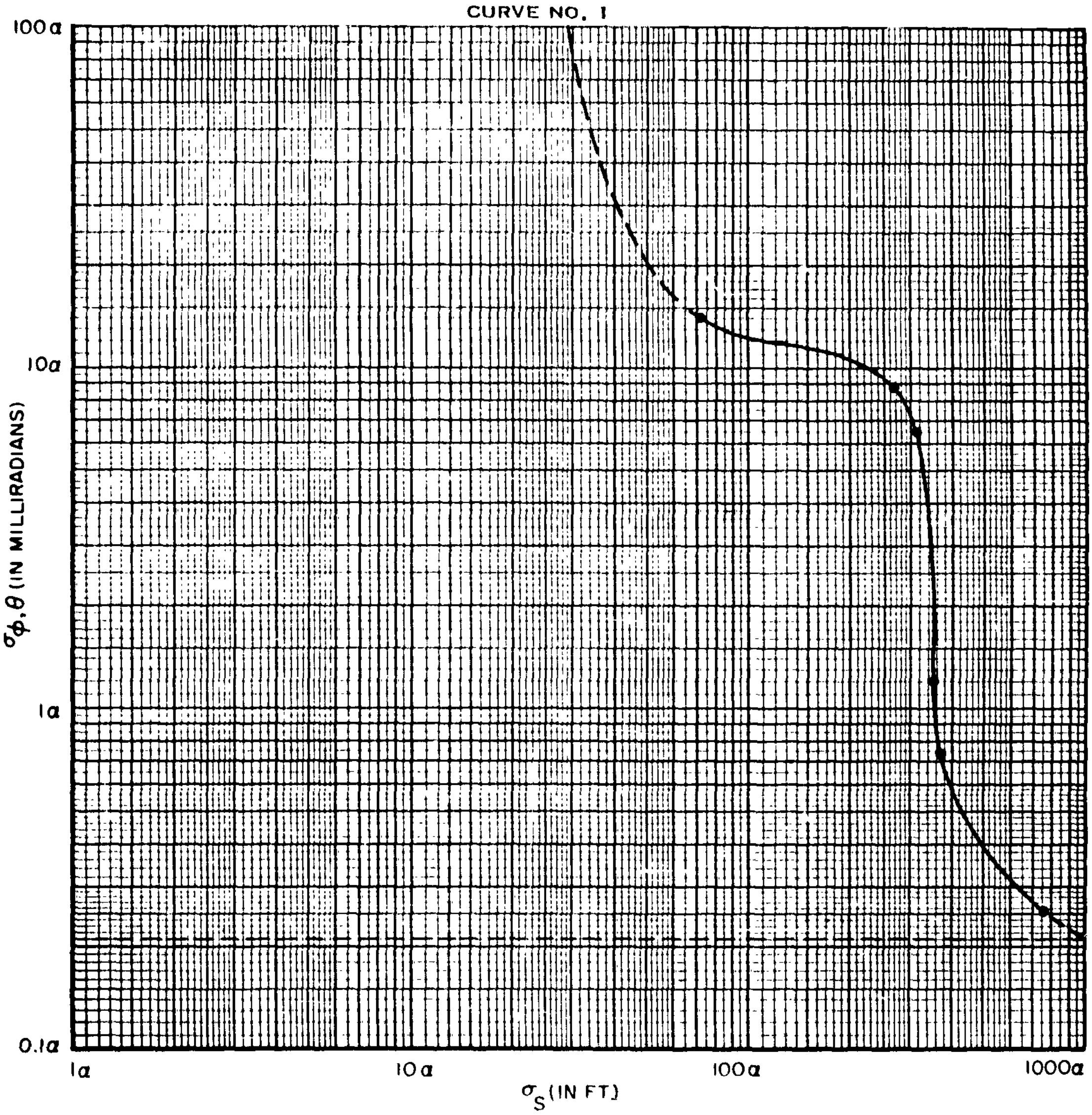

FIG. A-5 125 NMI ORBIT
STATION CASE C, RMS = α NMI

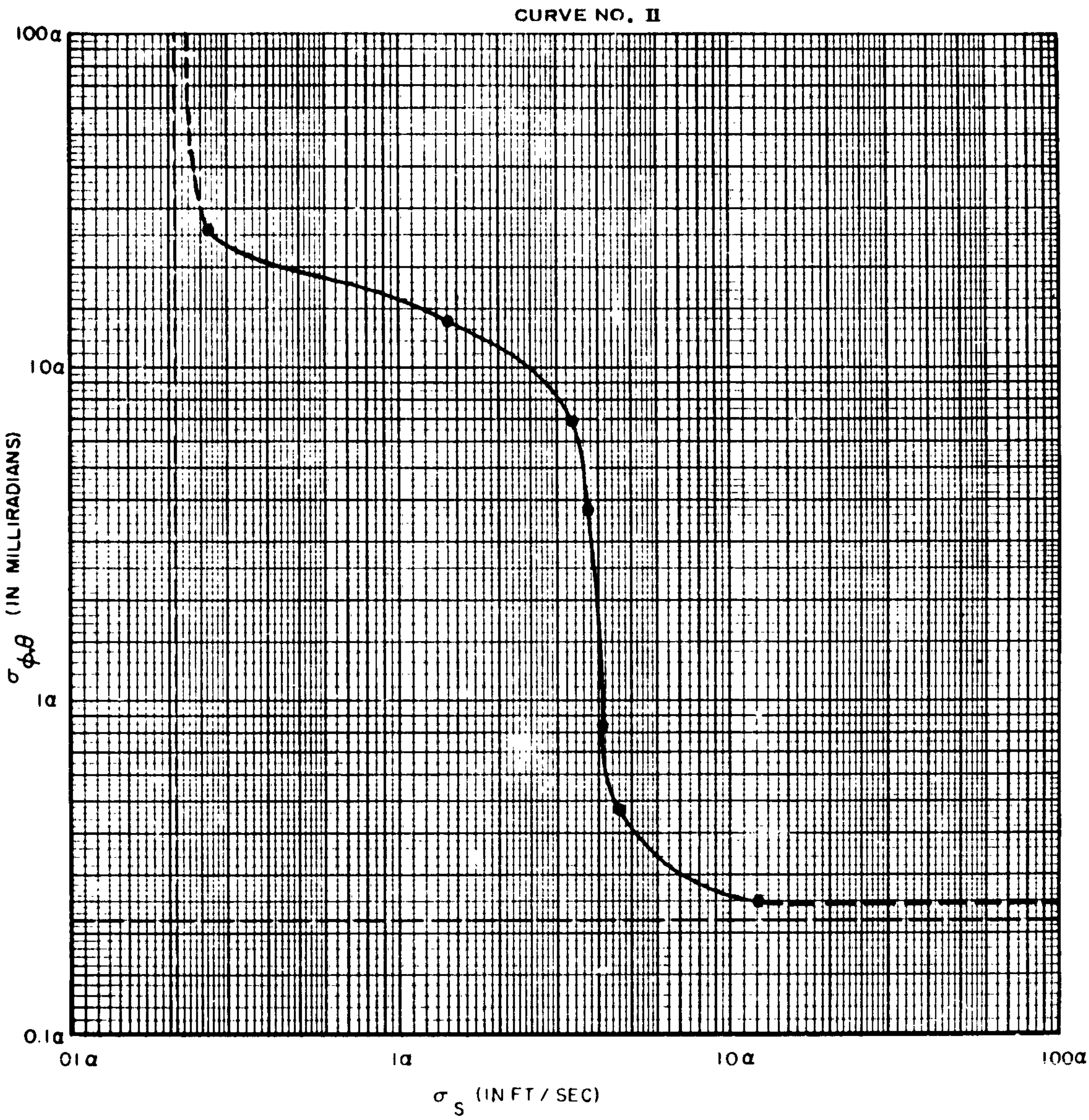

FIG. A 6 125 NMI ORBIT
STATION CASE C, RMS = α NMI

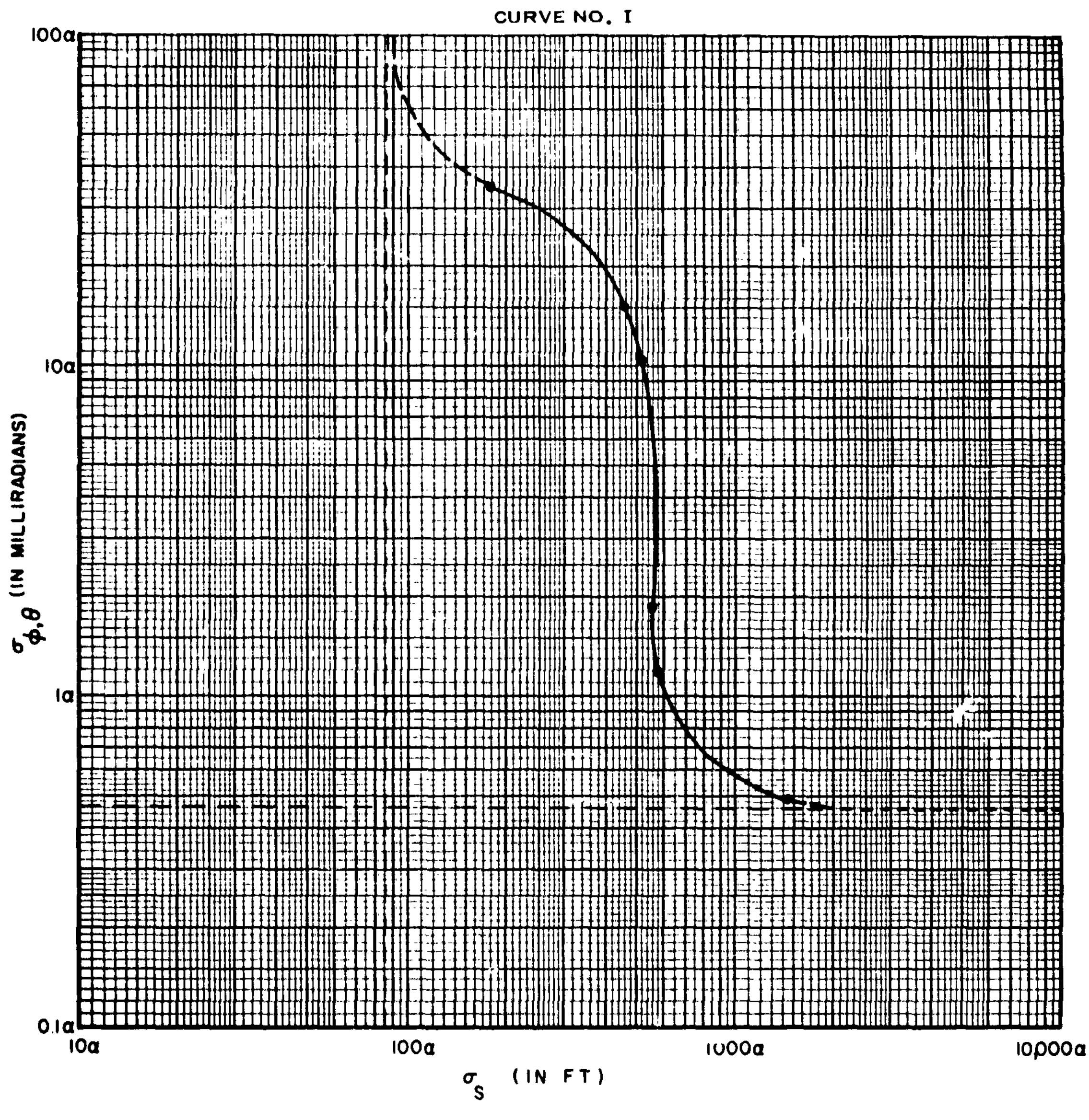

FIG. A-7 125 NMI ORBIT
STATION CASE D, RMS = α NMI

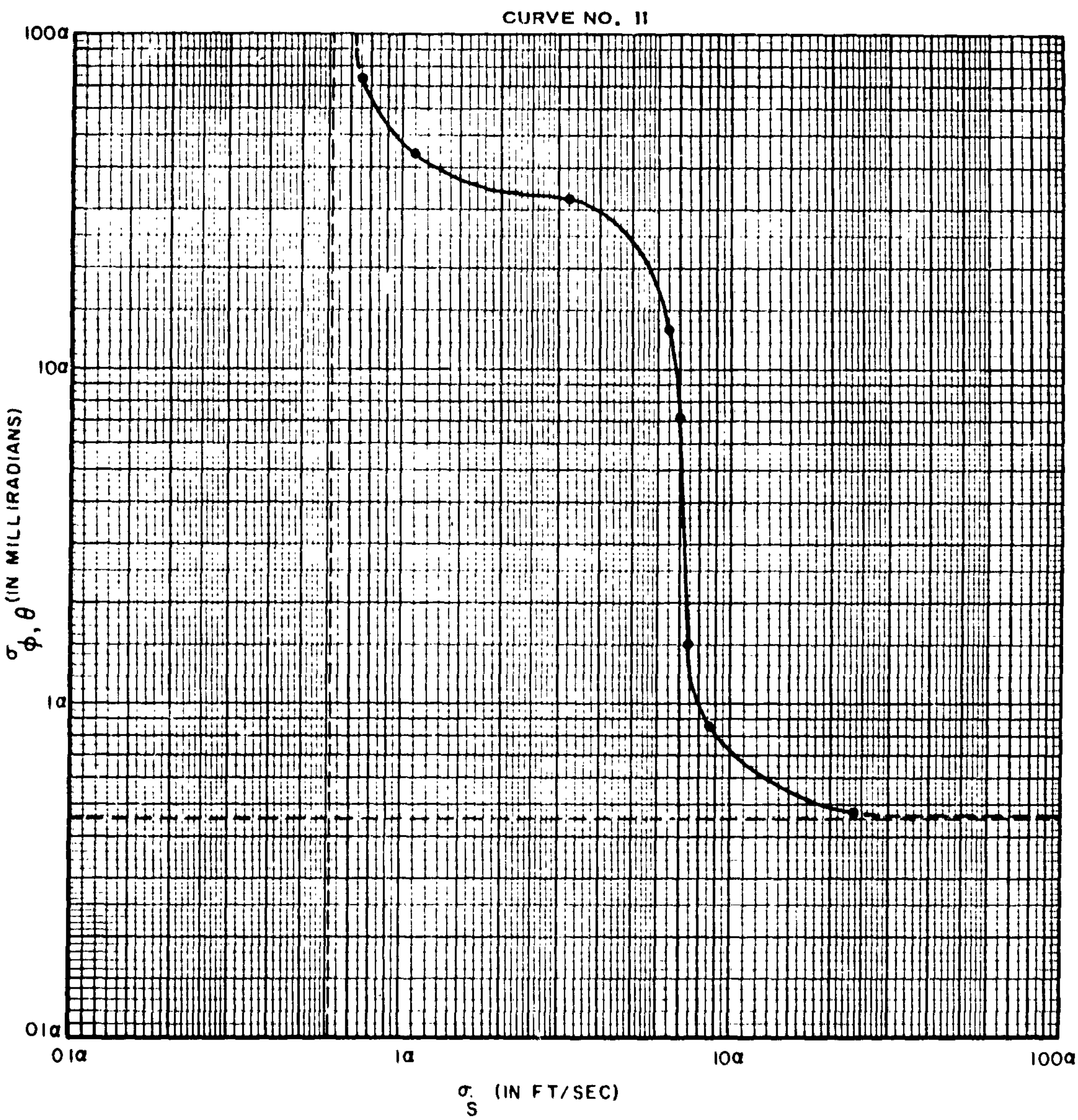

FIG. A-8 125 NMI ORBIT
STATION CASE D, RMS = α NMI

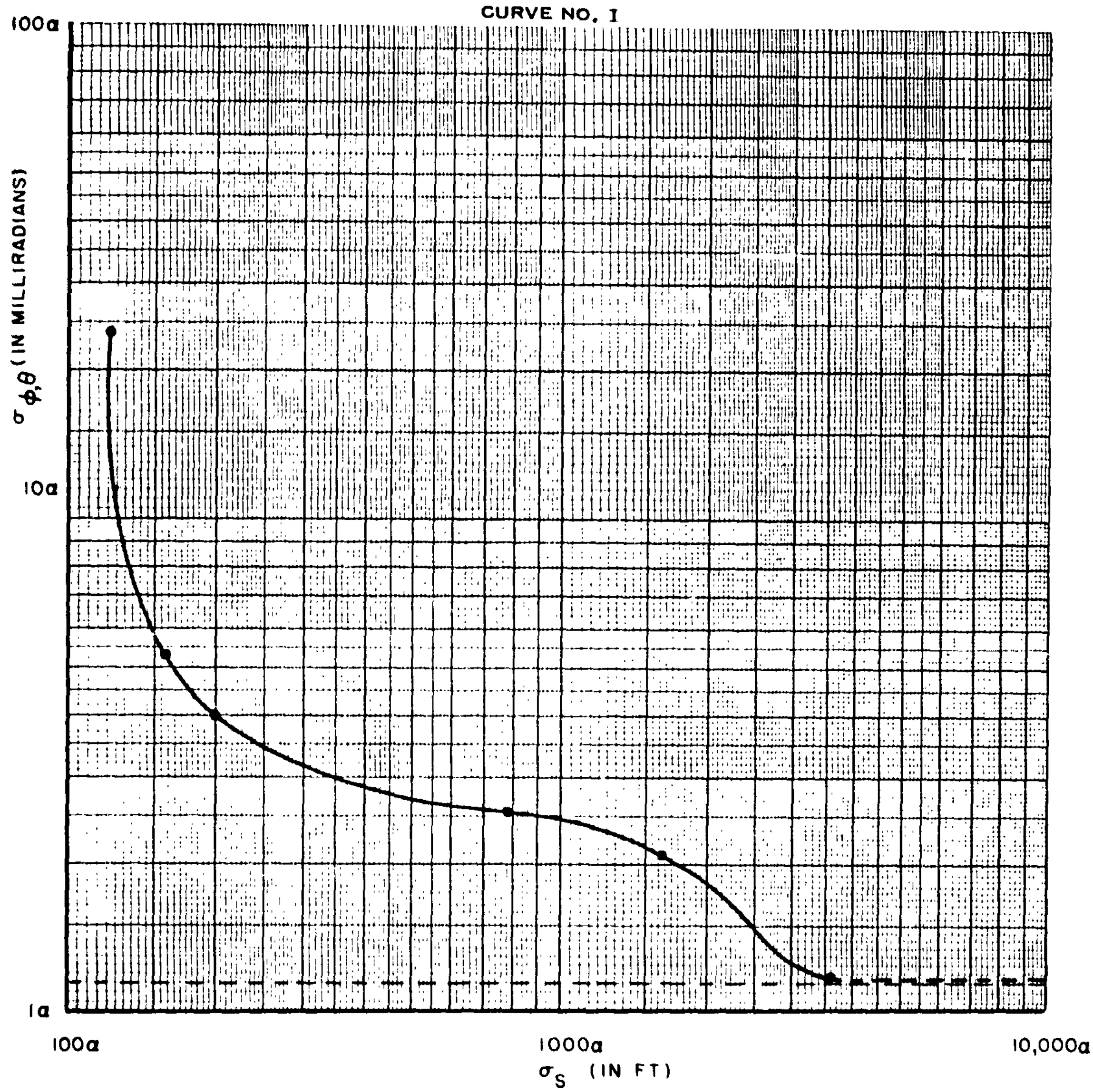

FIG. A-9 125 NMI ORBIT
STATION CASE E, RMS = α NMI

CURVE NO. II

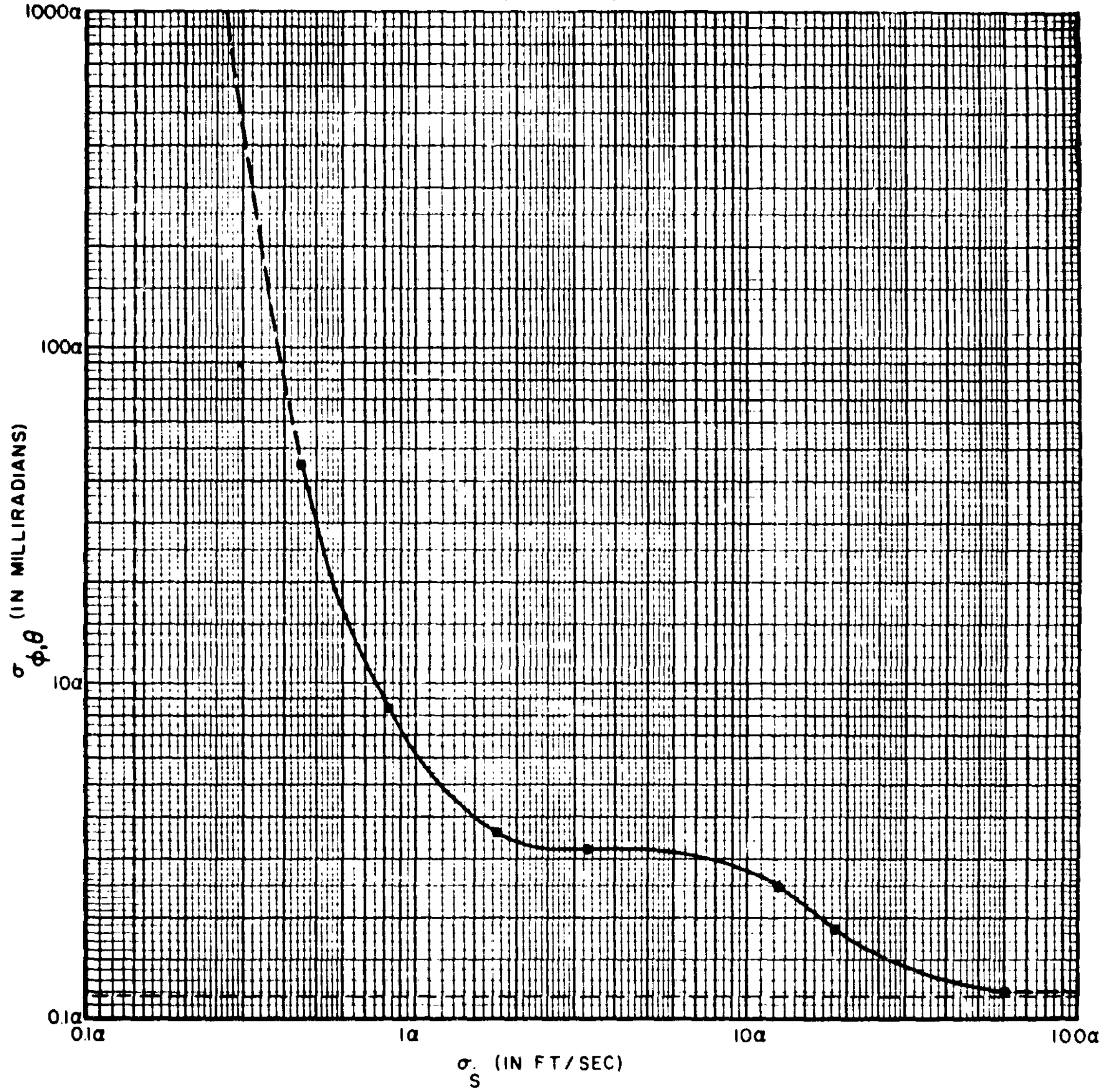

FIG. A-10 125 NMI ORBIT
STATION CASE E, RMS – α NMI

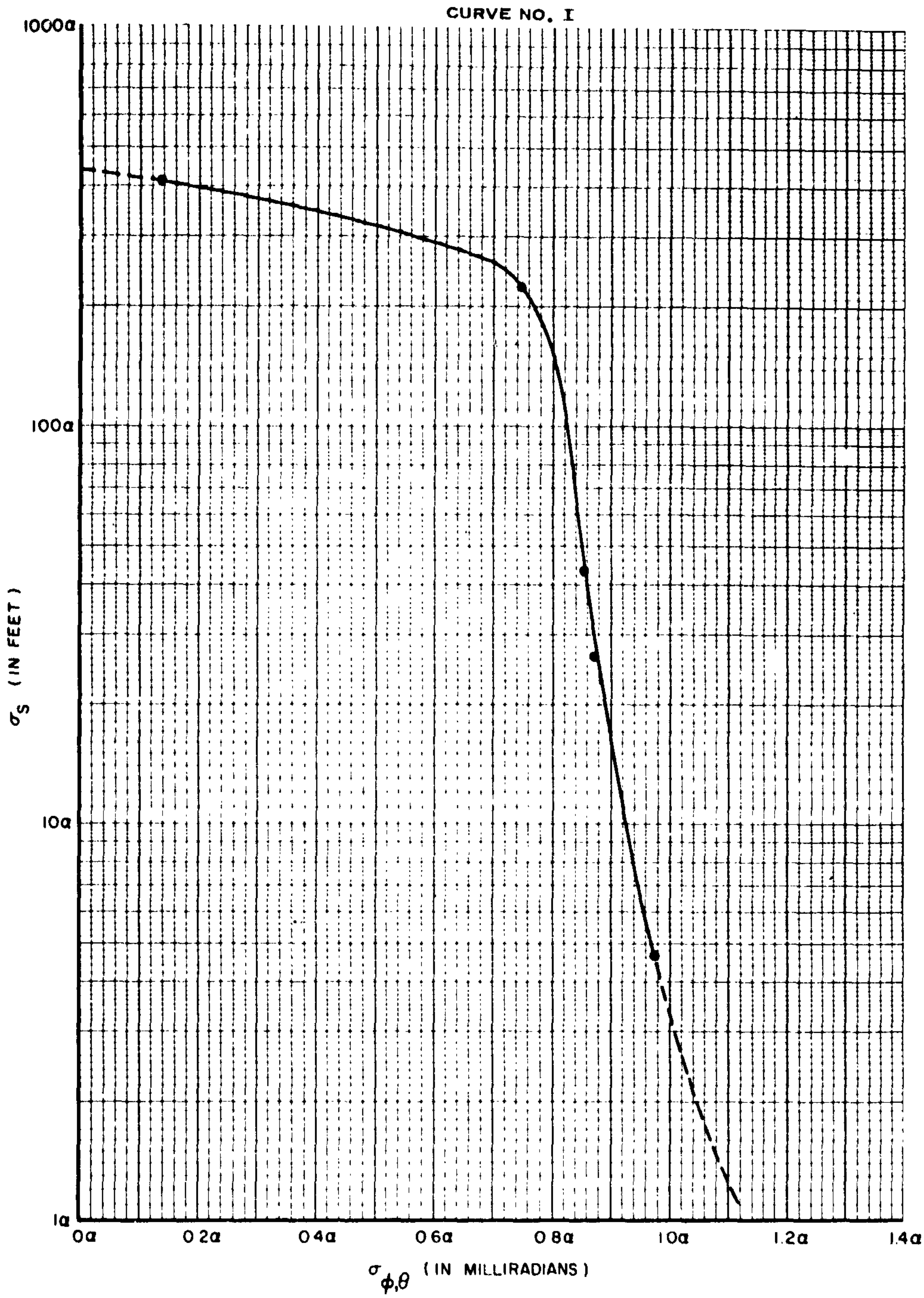

FIG. A-11 2000 NMI ORBIT
STATION CASE A, RMS = α NMI

CURVE NO. II

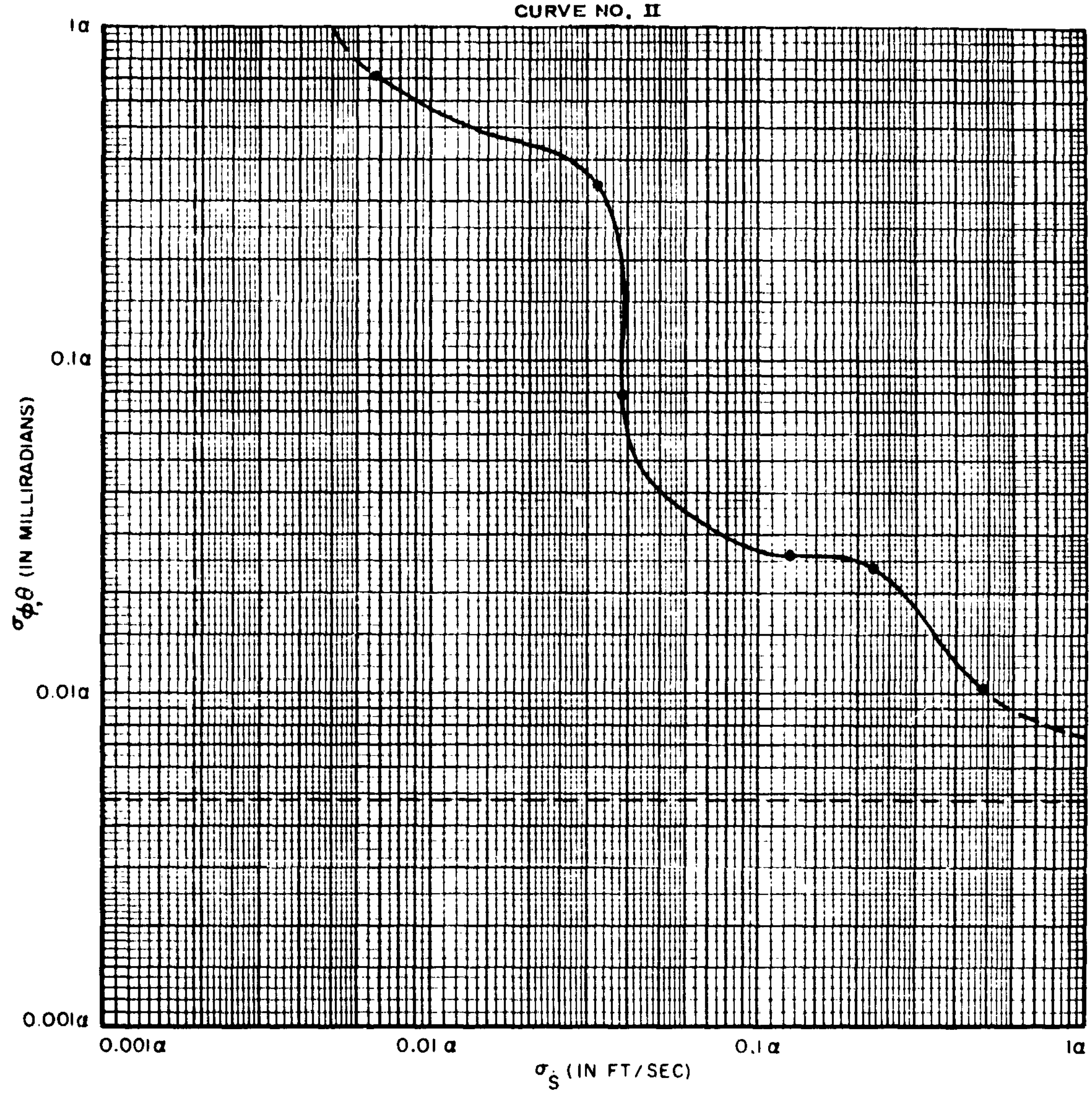

FIG. A-12 2000 NMI ORBIT
STATION CASE A, RMS = α NMI

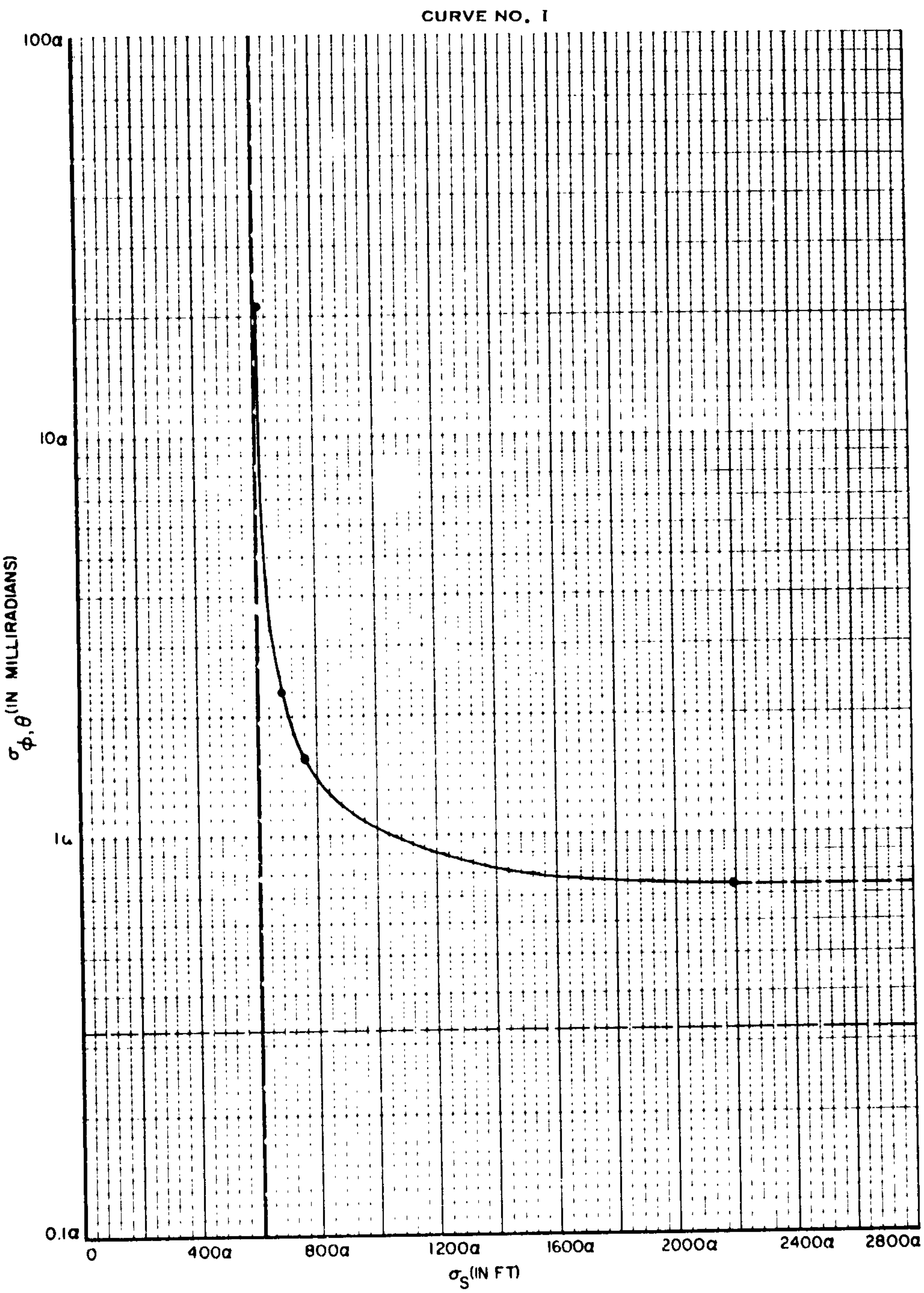

FIG. A-13 2000 NMI ORBIT
STATION CASE B, RMS = α NMI

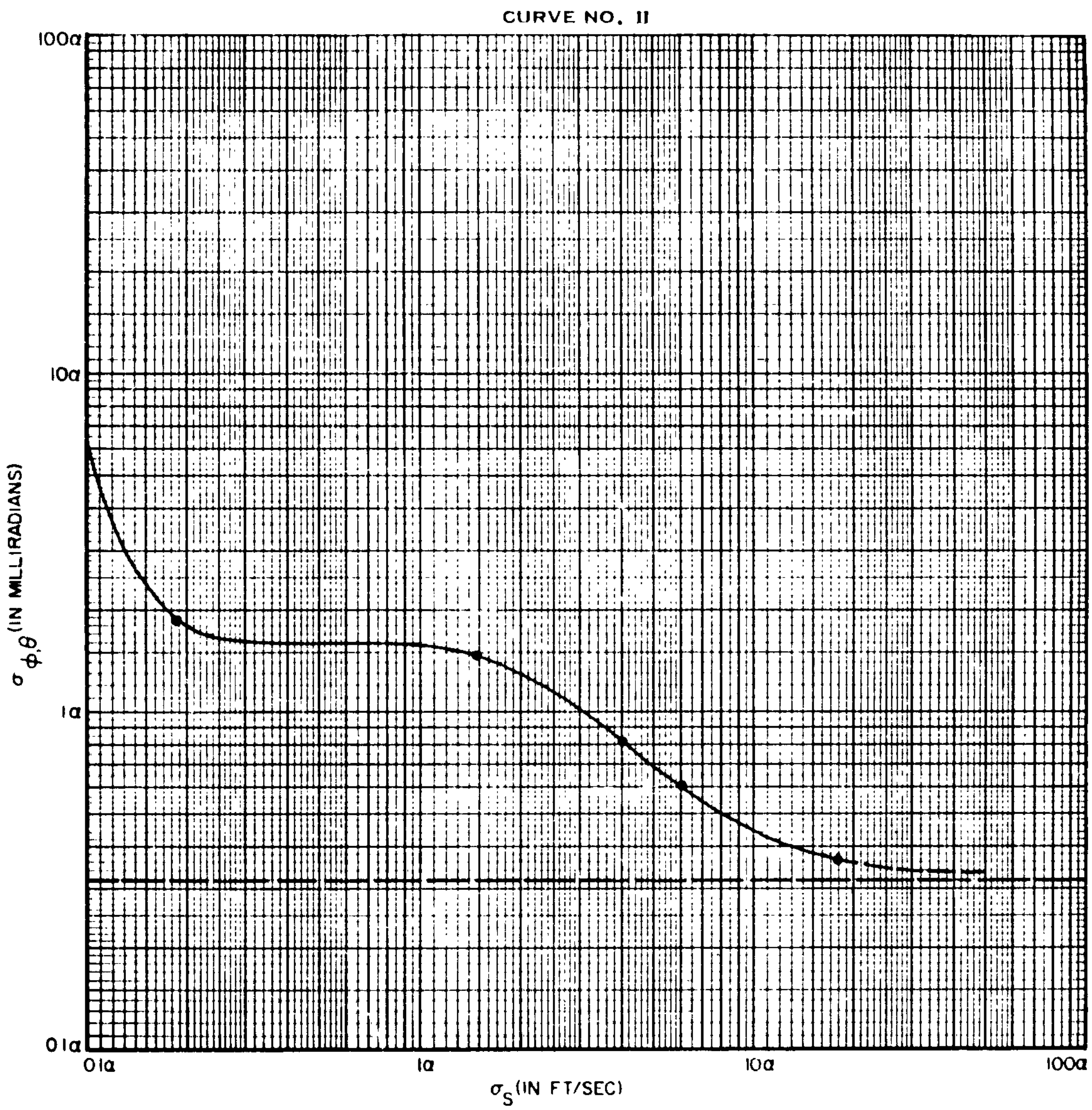

FIG. A-14 2000 NMI ORBIT
STATION CASE B, RMS = α NMI

CURVE NO. 1

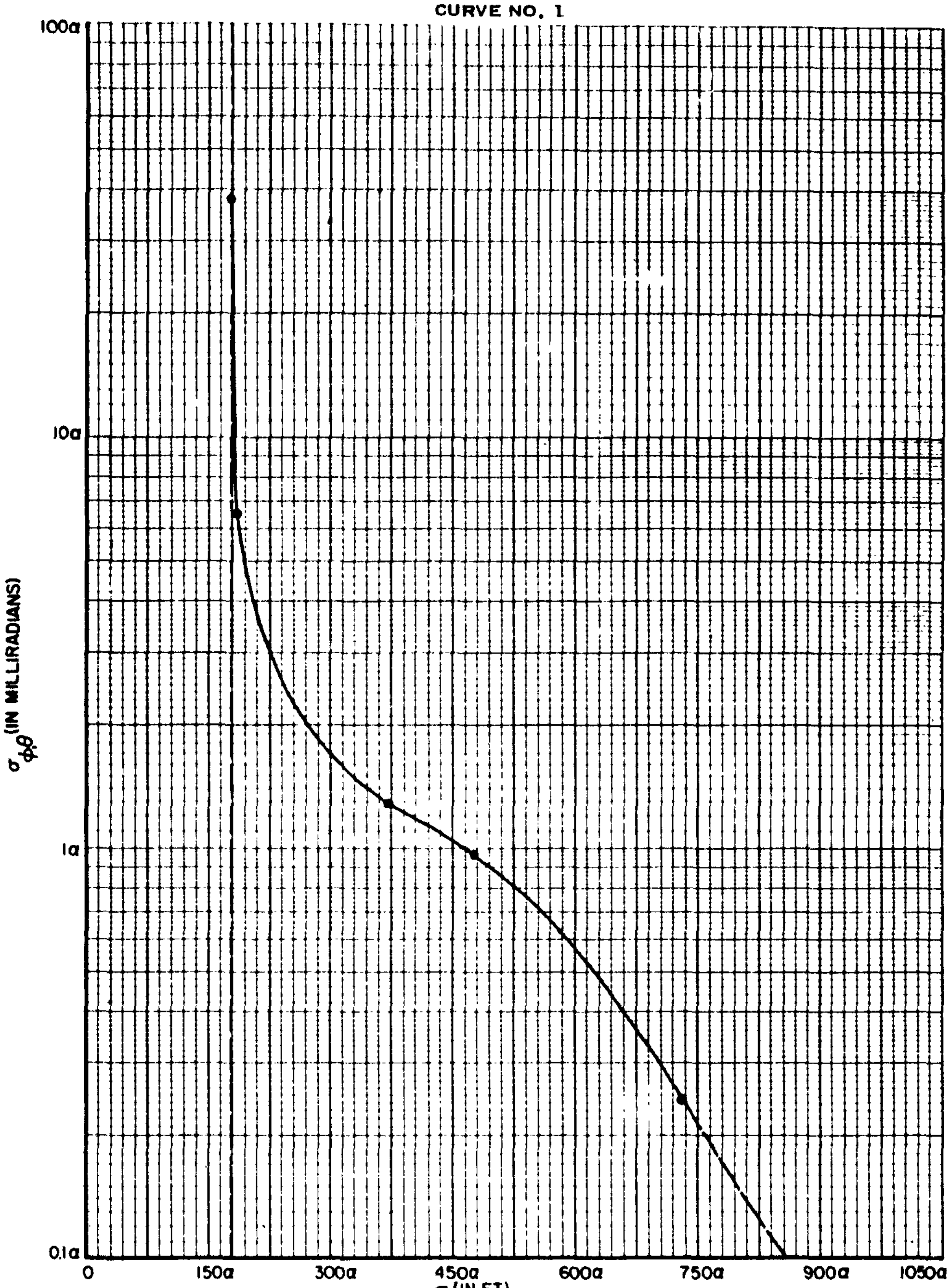

FIG. A-15 2000 NMI ORBIT
STATION CASE C, RMS = α NMI

CURVE NO. II

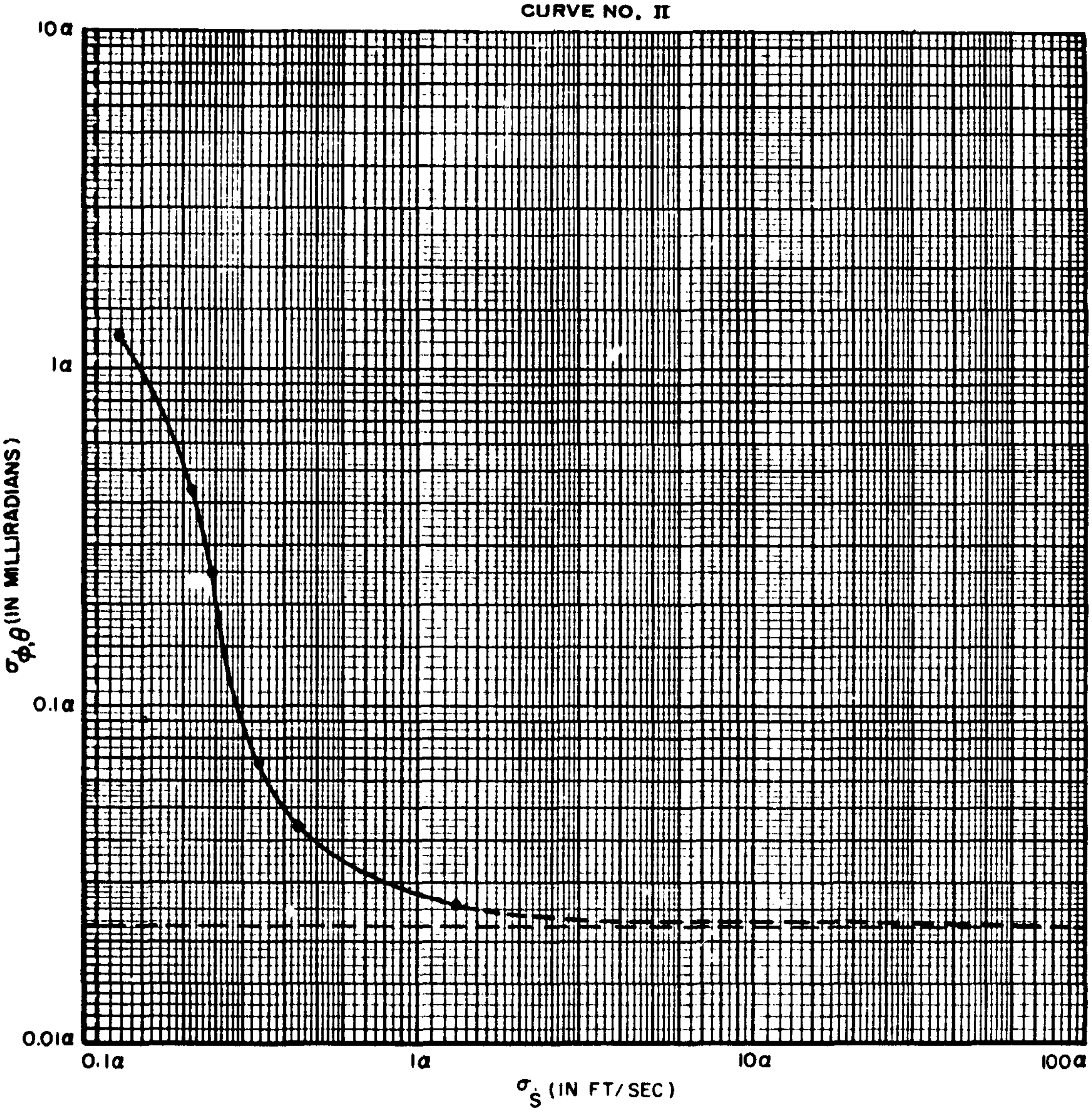

FIG. A-16 2000 NMI ORBIT
STATION CASE C, RMS = α NMI

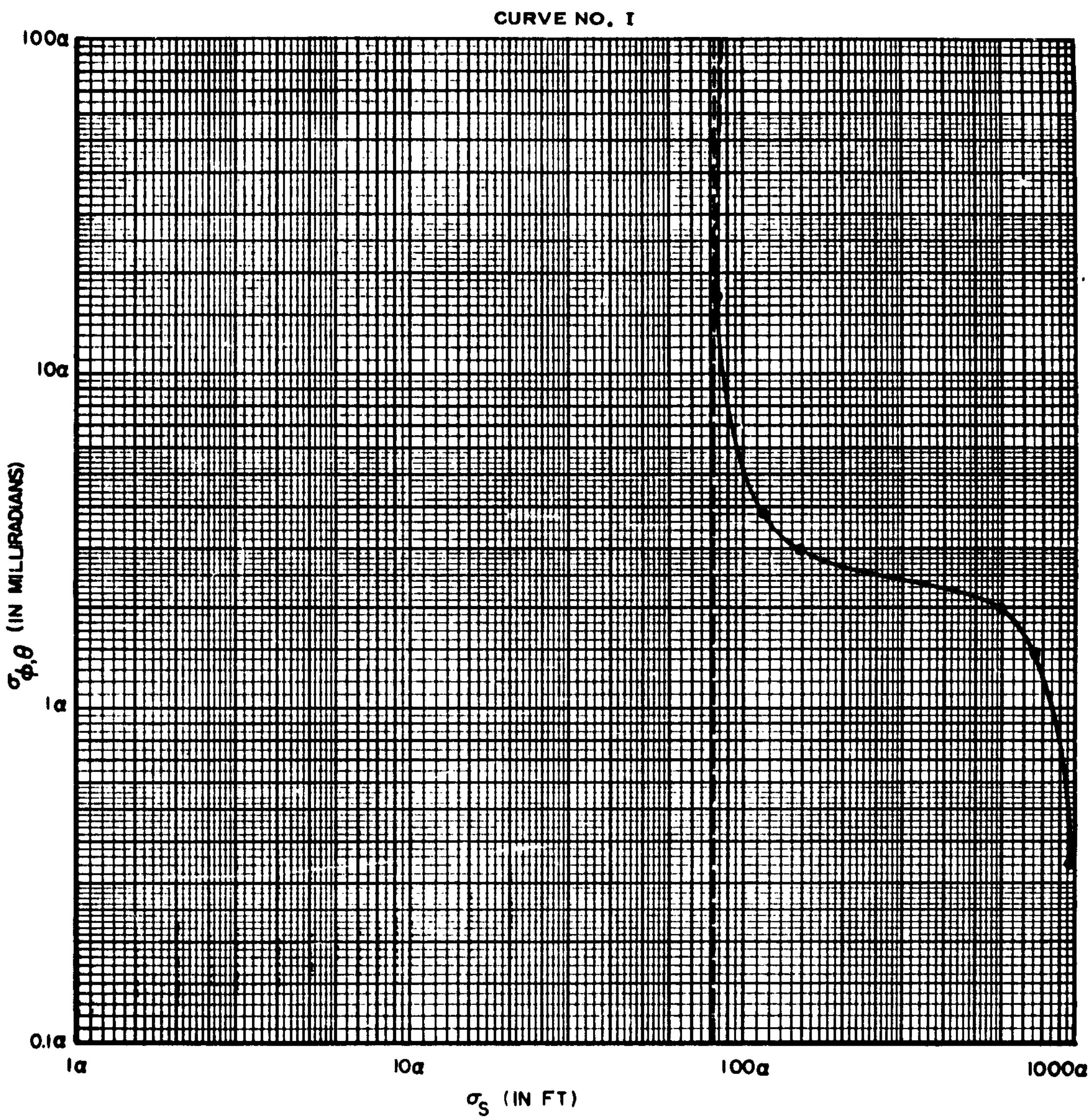

FIG. A-17 2000 NMI ORBIT
STATION CASE D, RMS = α NMI

CURVE NO. 11

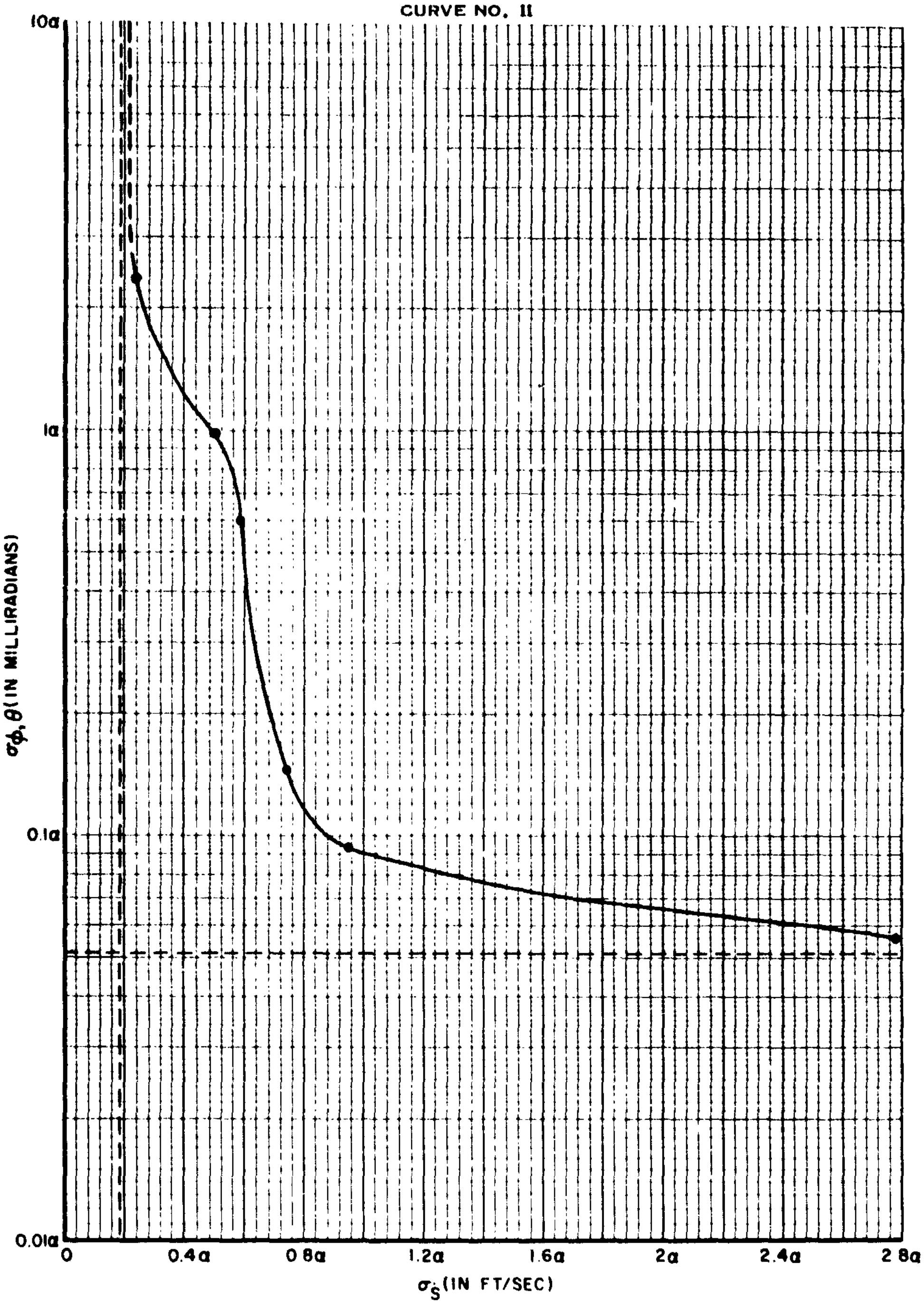

FIG. A-18 2000 NMI ORBIT
STATION CASE D, RMS = α NMI

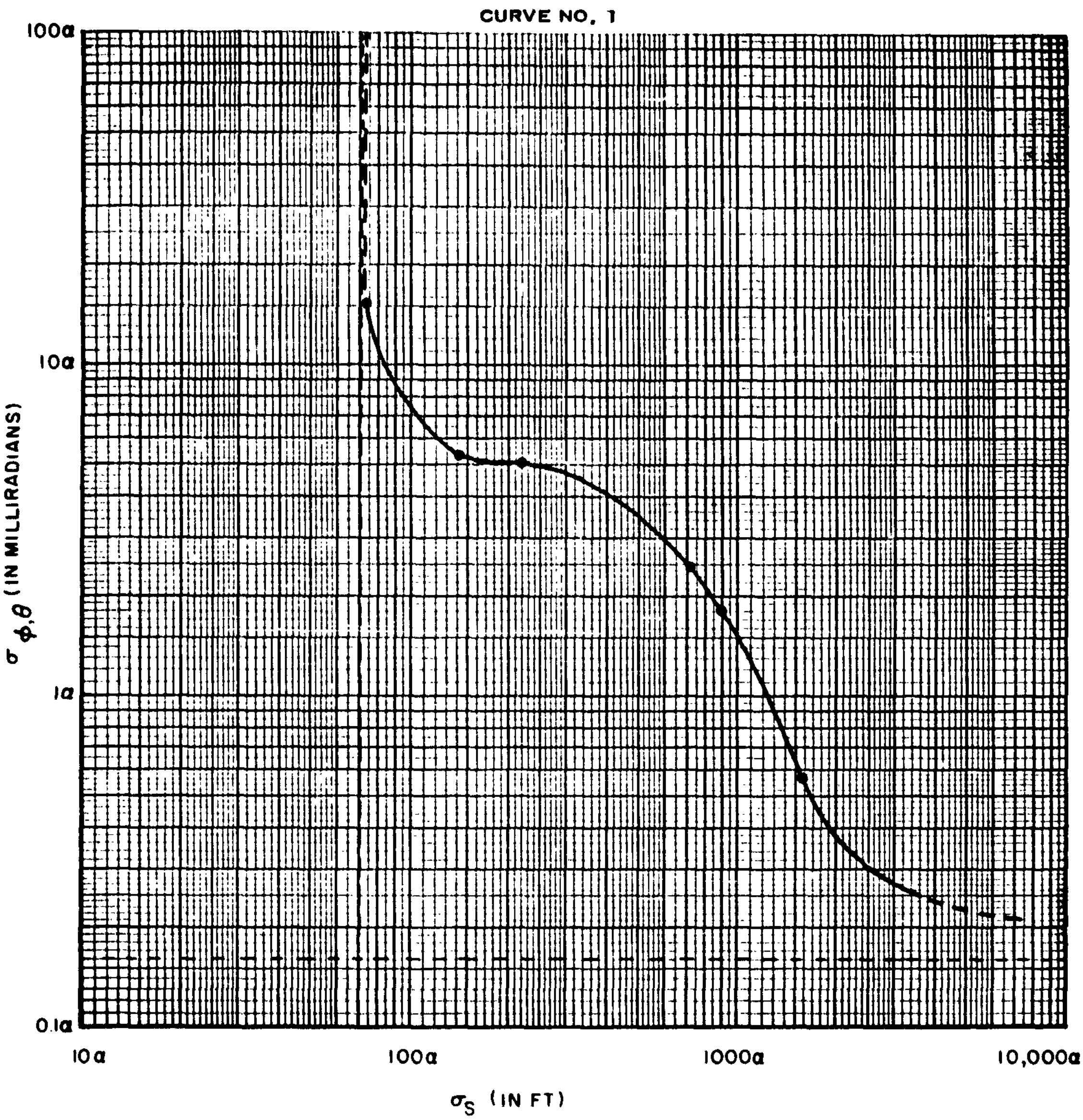

FIG. A-19 2000 NMI ORBIT
STATION CASE E, RMS = α NMI

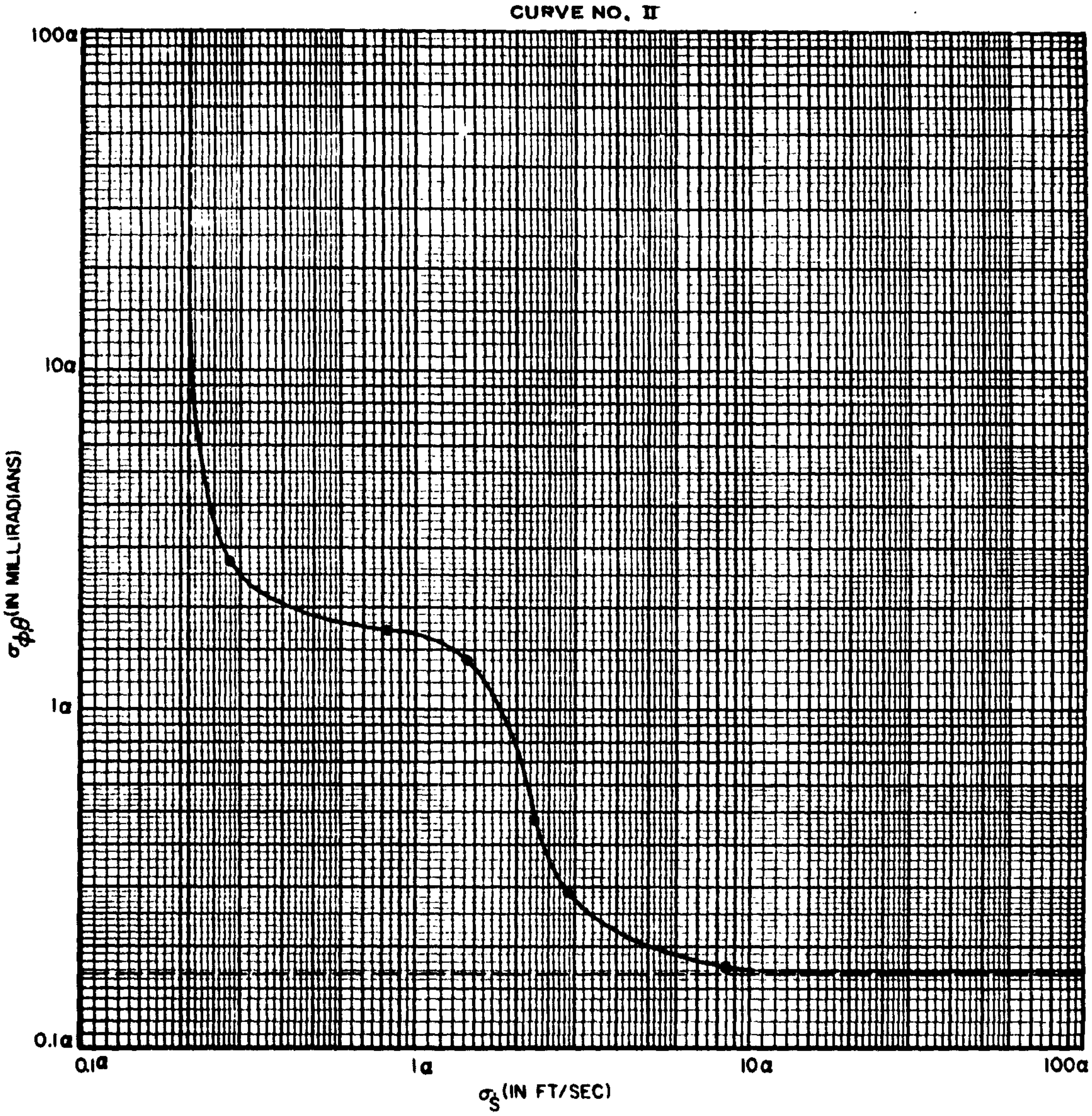

FIG. A-20 2000 NMI ORBIT
STATION CASE E, RMS = α NMI

TRADE-OFF CURVES FOR RANGE, RANGE RATE, AND ANGLE SENSORS

CURVE NO. (TO THE RIGHT OF EACH CURVE)	CURVE DESCRIPTION
III	$\sigma_{\dot{S}}$ vs $\sigma_{\phi,\theta}$ with a fixed σ_S and RMS
IV	σ_S vs $\sigma_{\dot{S}}$ with a fixed $\sigma_{\phi,\theta}$ and RMS

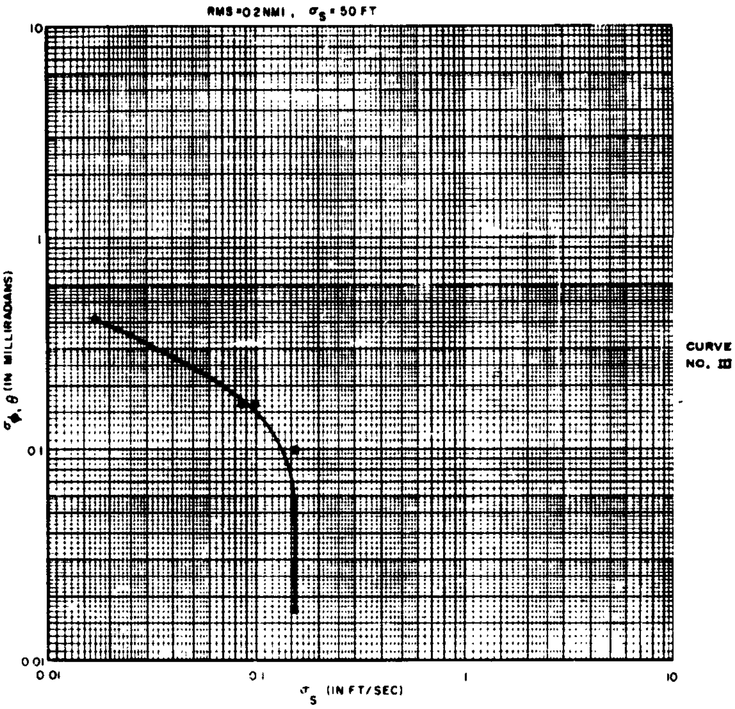

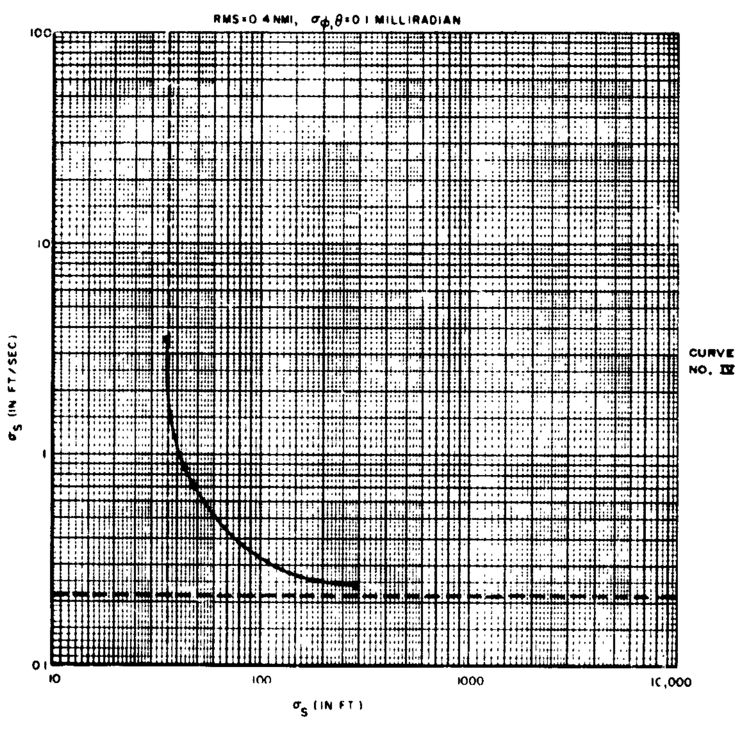

FIG. A-21 125 NMI ORBIT
STATION CASE A

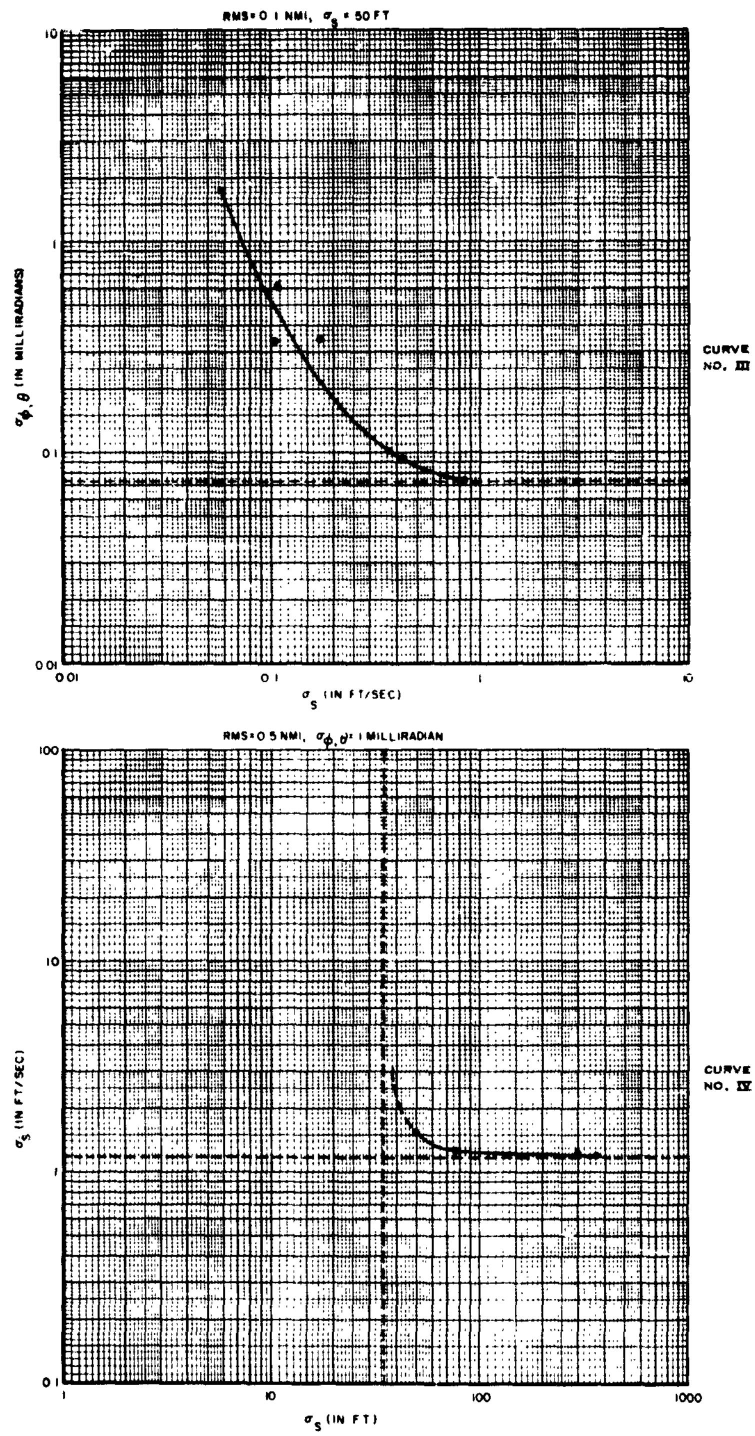

FIG. A-22 125 NMI ORBIT
STATION CASE B

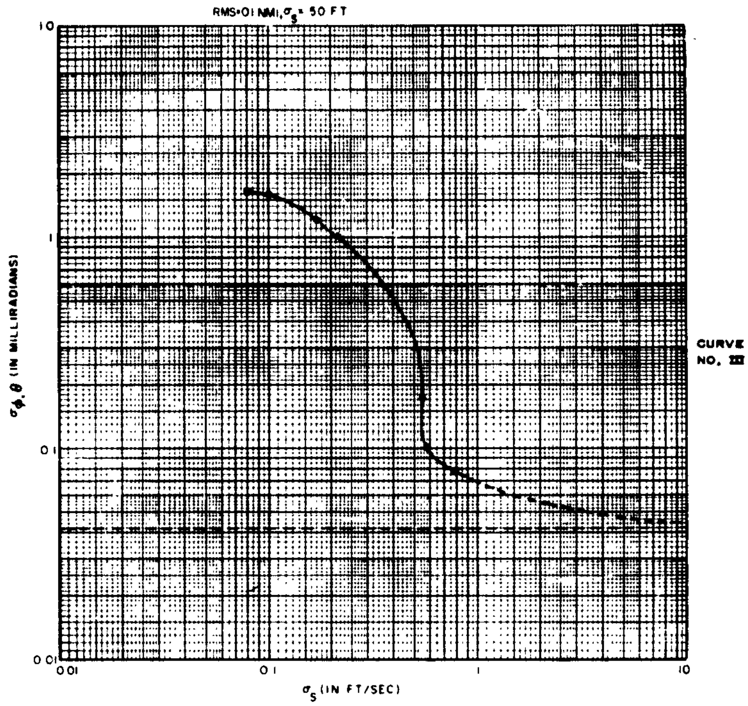

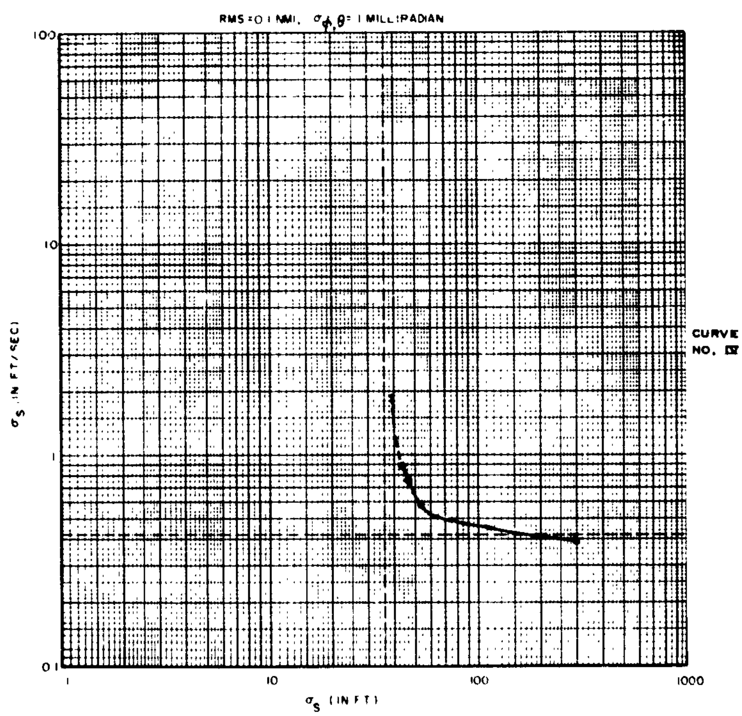

FIG. A-23 125 NMI ORBIT
STATION CASE C

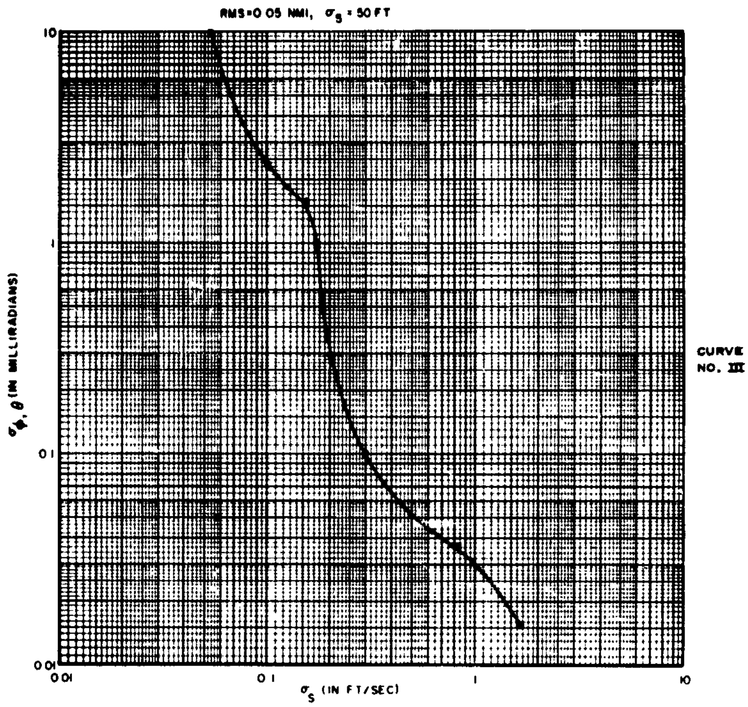

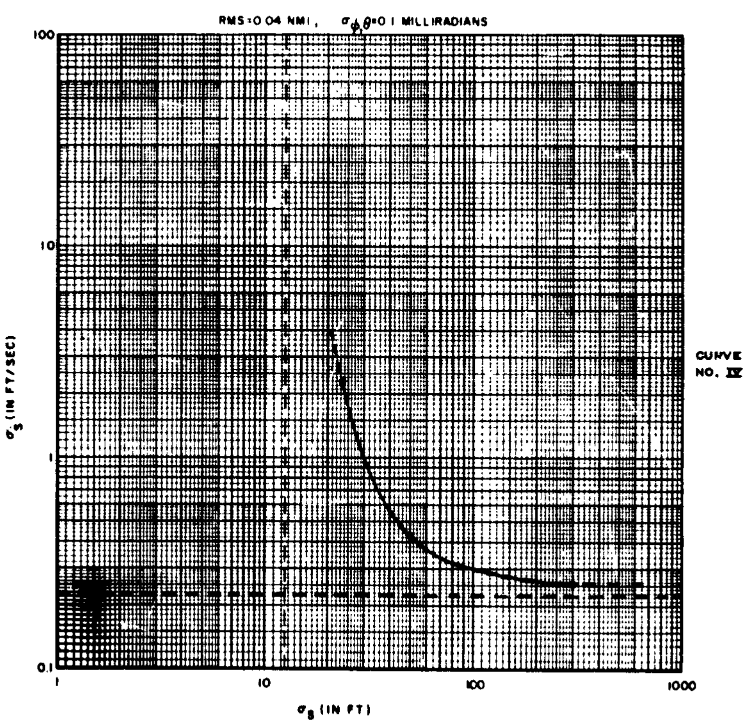

FIG. A-24 125 NMI ORBIT
STATION CASE D

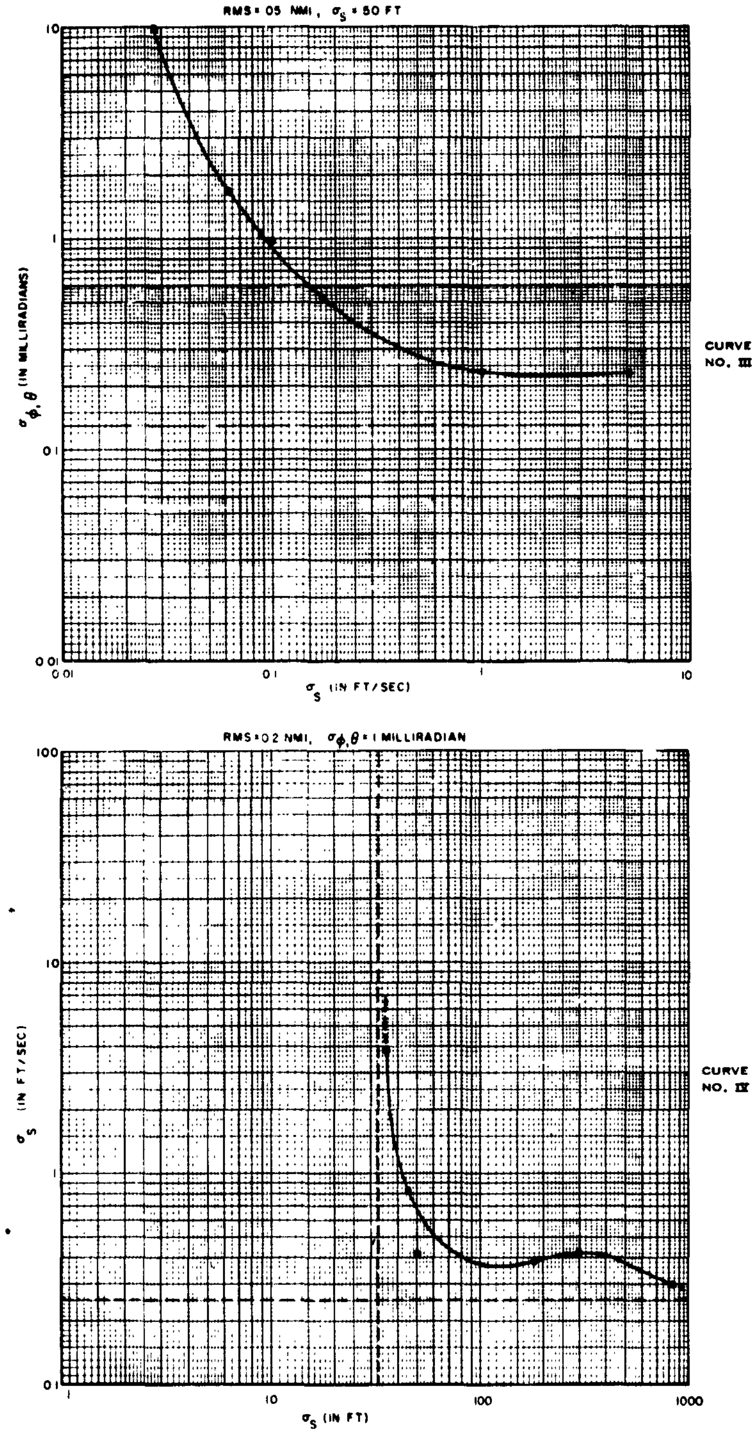

FIG. A-25 125 NMI ORBIT STATION CASE E

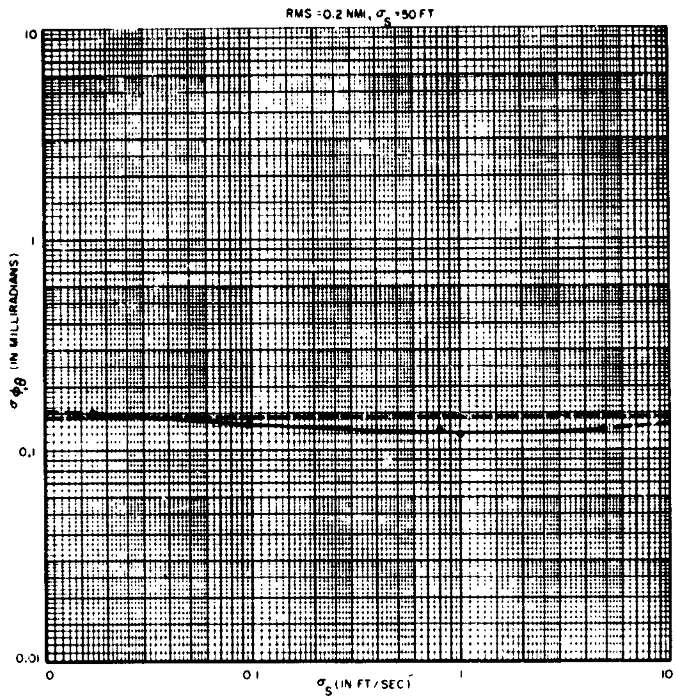

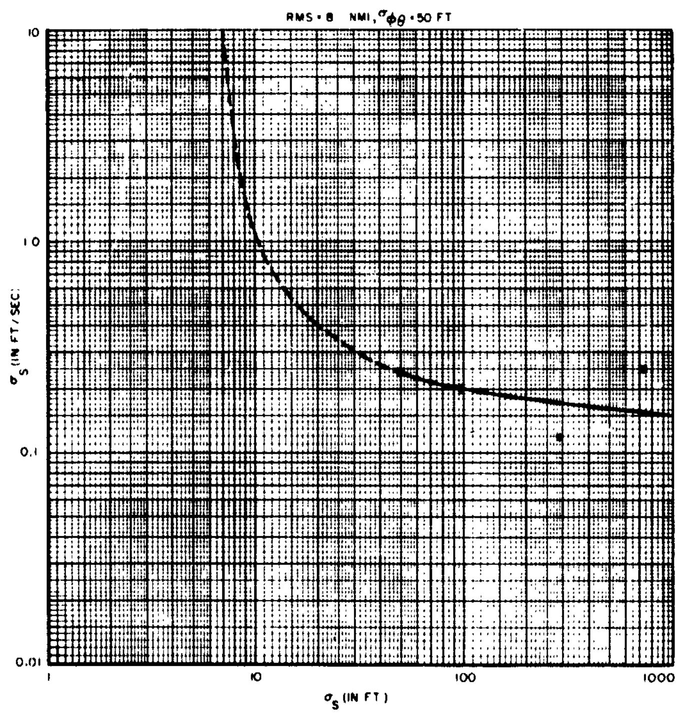

FIG. A-26 2000 NMI ORBIT
STATION CASE A

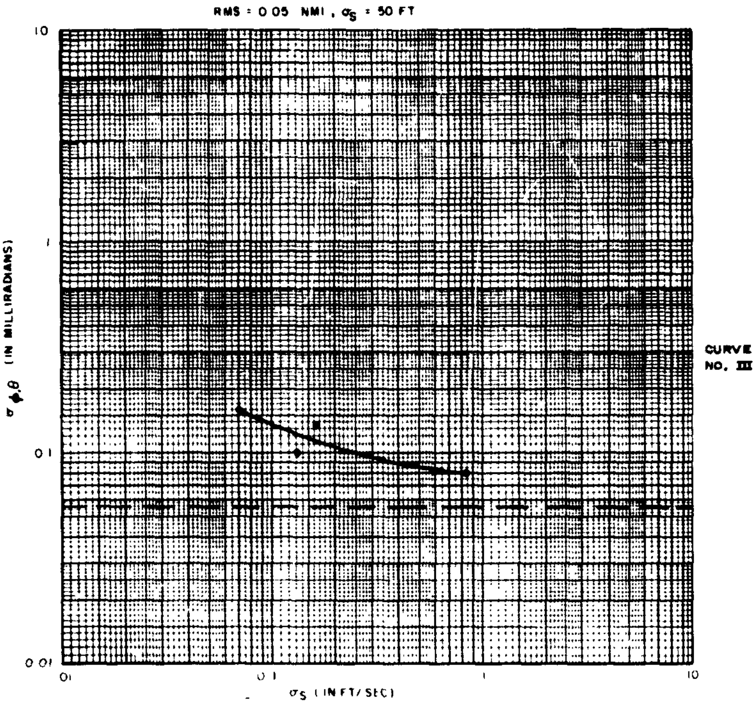

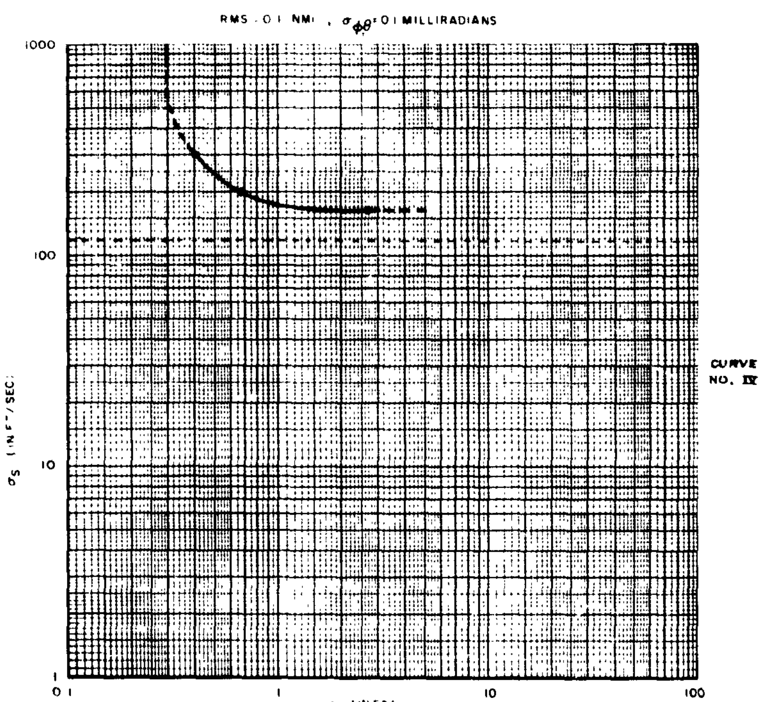

FIG. A-27 2000 NMI ORBIT
STATION CASE B

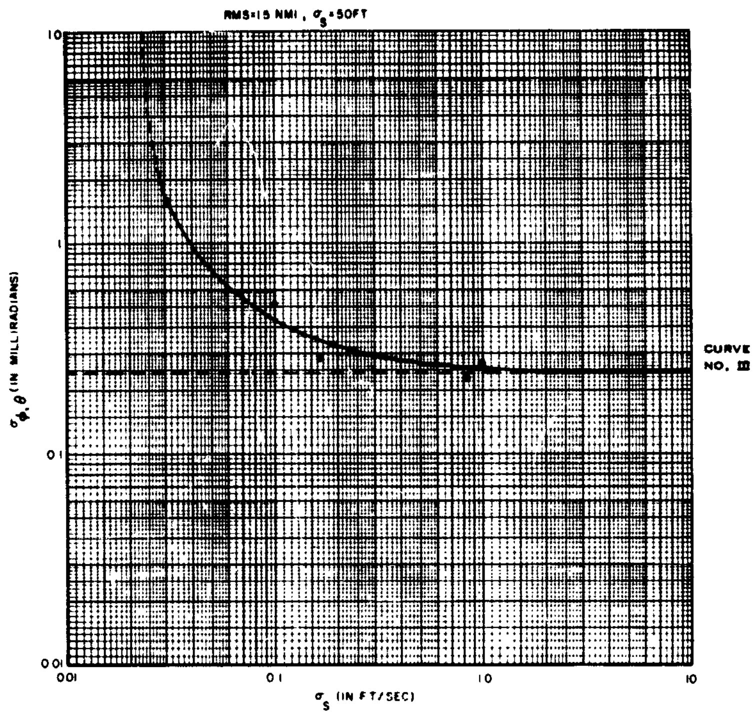

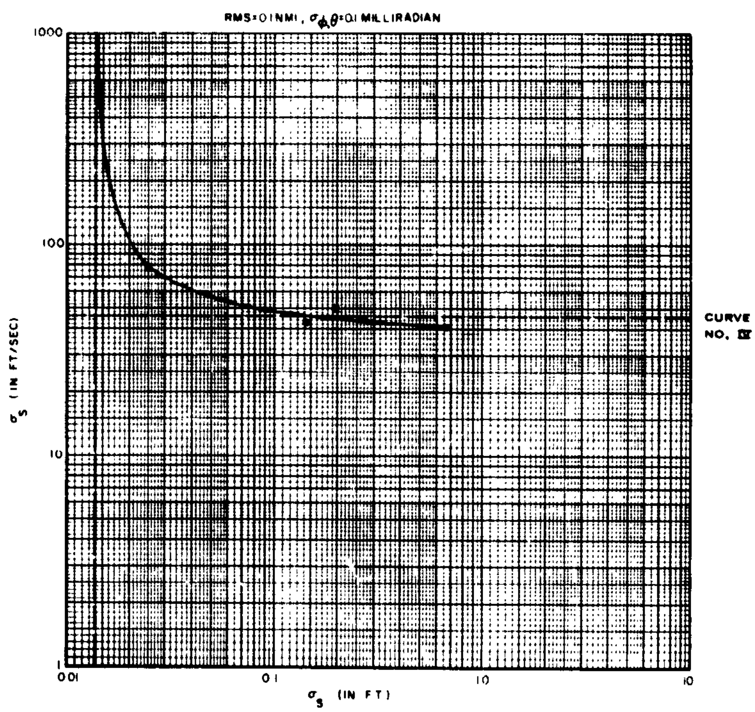

FIG. A-28 2000 NMI ORBIT
STATION CASE C

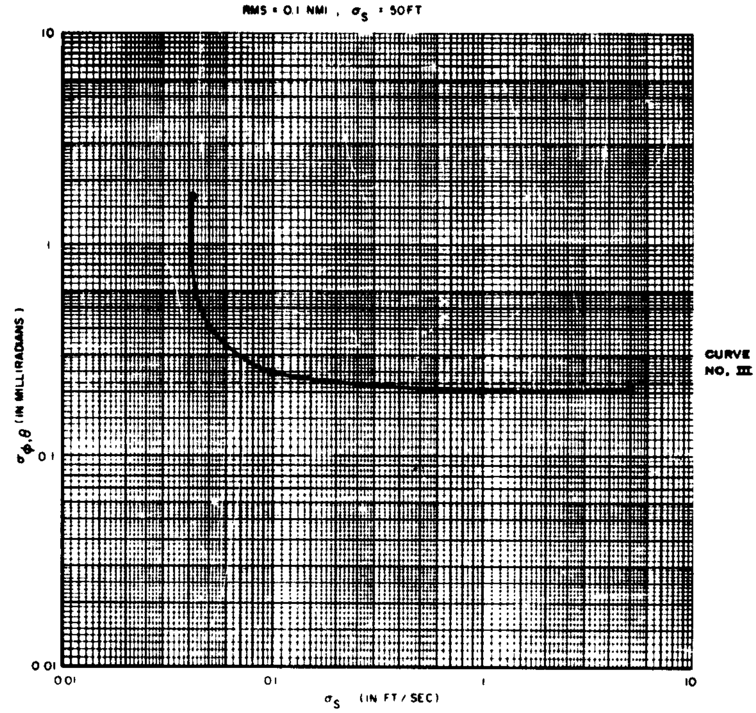

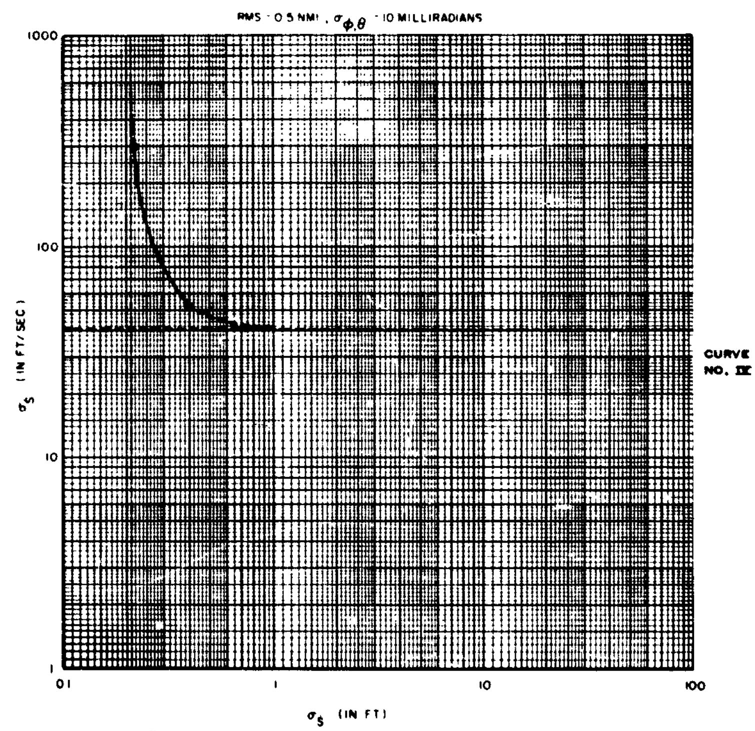

FIG. A-29 2000 NMI ORBIT
STATION CASE D

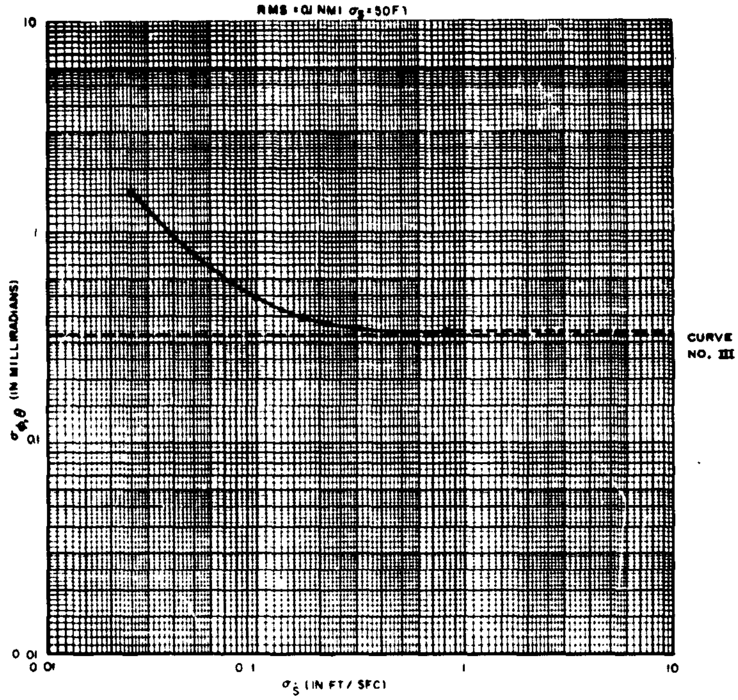

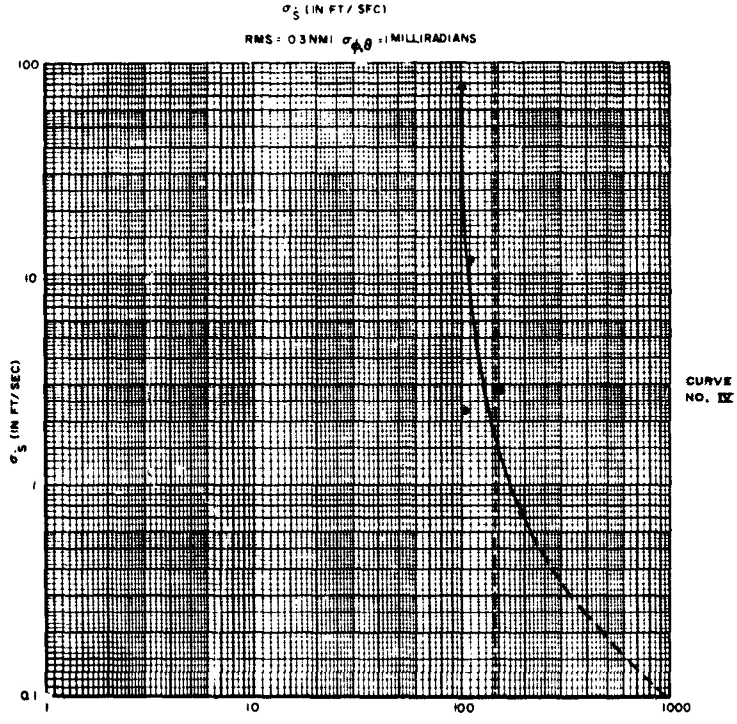

FIG. A-30 2000 NMI ORBIT
STATION CASE E

GRAPHS OF ANGLE OR RANGE RATE ERRORS VERSUS THE RMS, WHEN USING SENSORS OF RANGE, RANGE RATE AND ANGLES. (See Page 9 for a description of the curve no. that is written above each curve.)

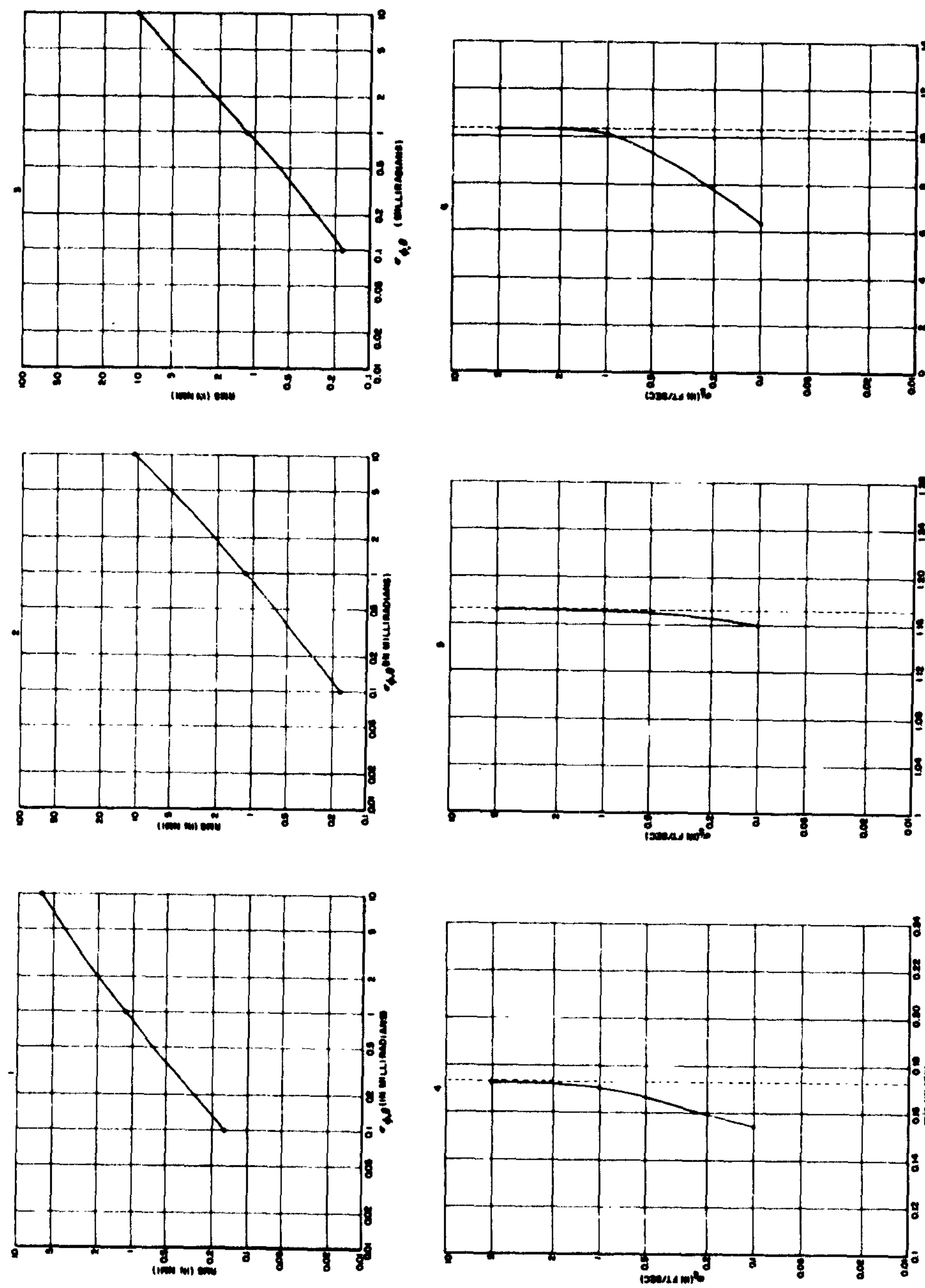

FIG. A-31 2000NMI ORBIT STATION CASE A, σ_S=50FT

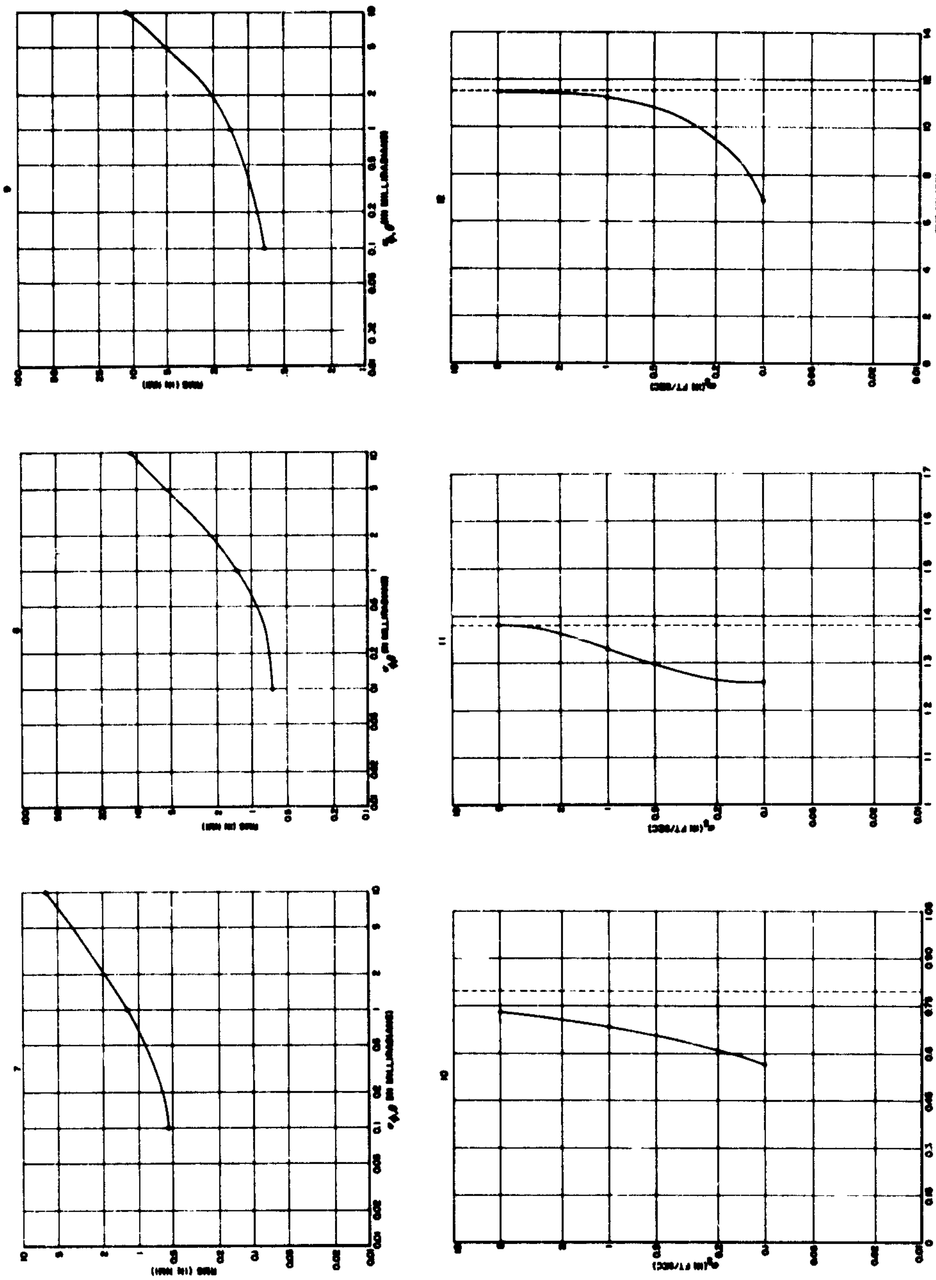

FIG. A-32 2000NMI ORBIT STATION CASE A, σ_S=300FT

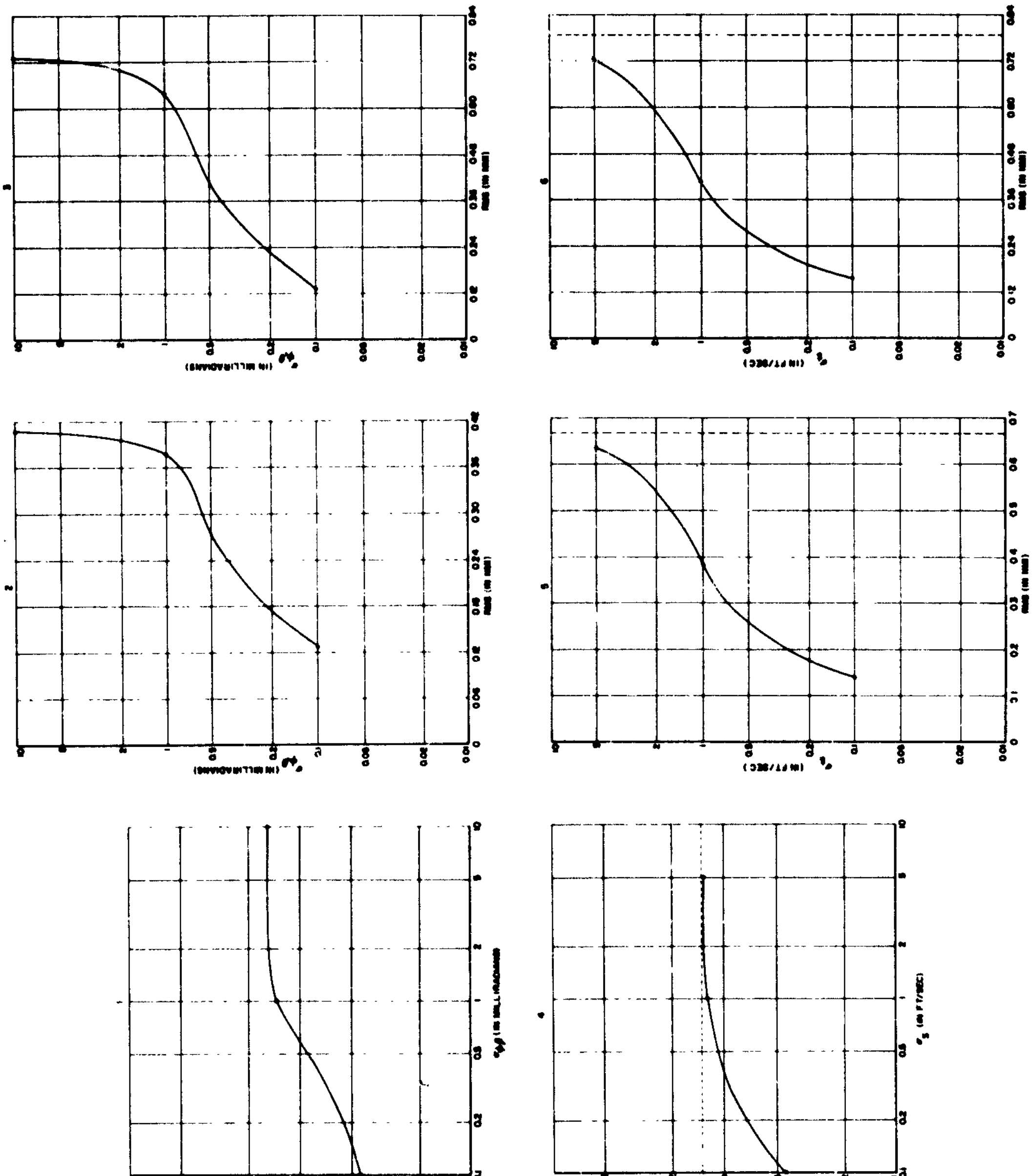

FIG. A-33 125 NMI ORBIT STATION CASE B, σ_S = 50FT

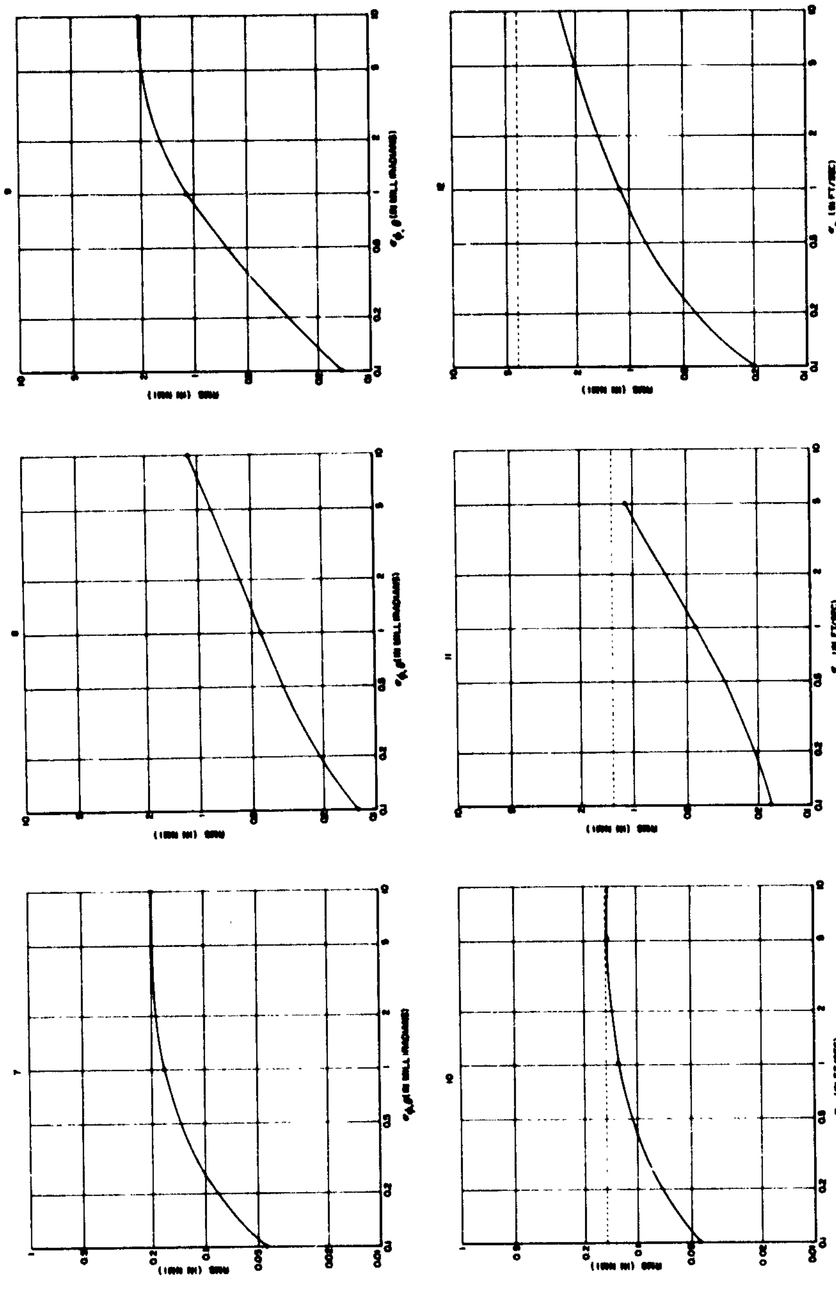

FIG. A-34 125NMI ORBIT STATION CASE B, σ_S=300FT

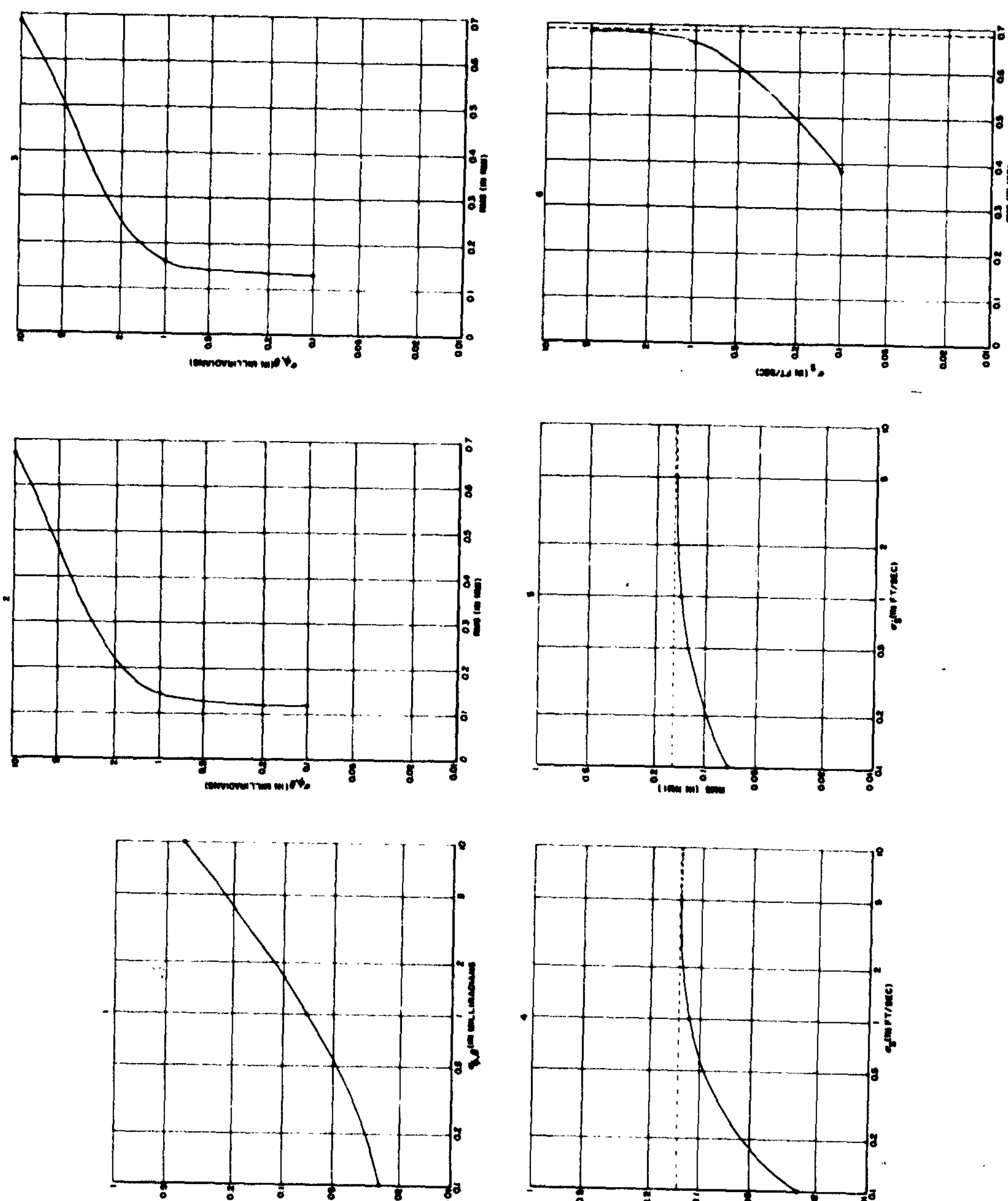

FIG. A-35 125 NMI ORBIT STATION CASE C, $\sigma_S = 50$ FT

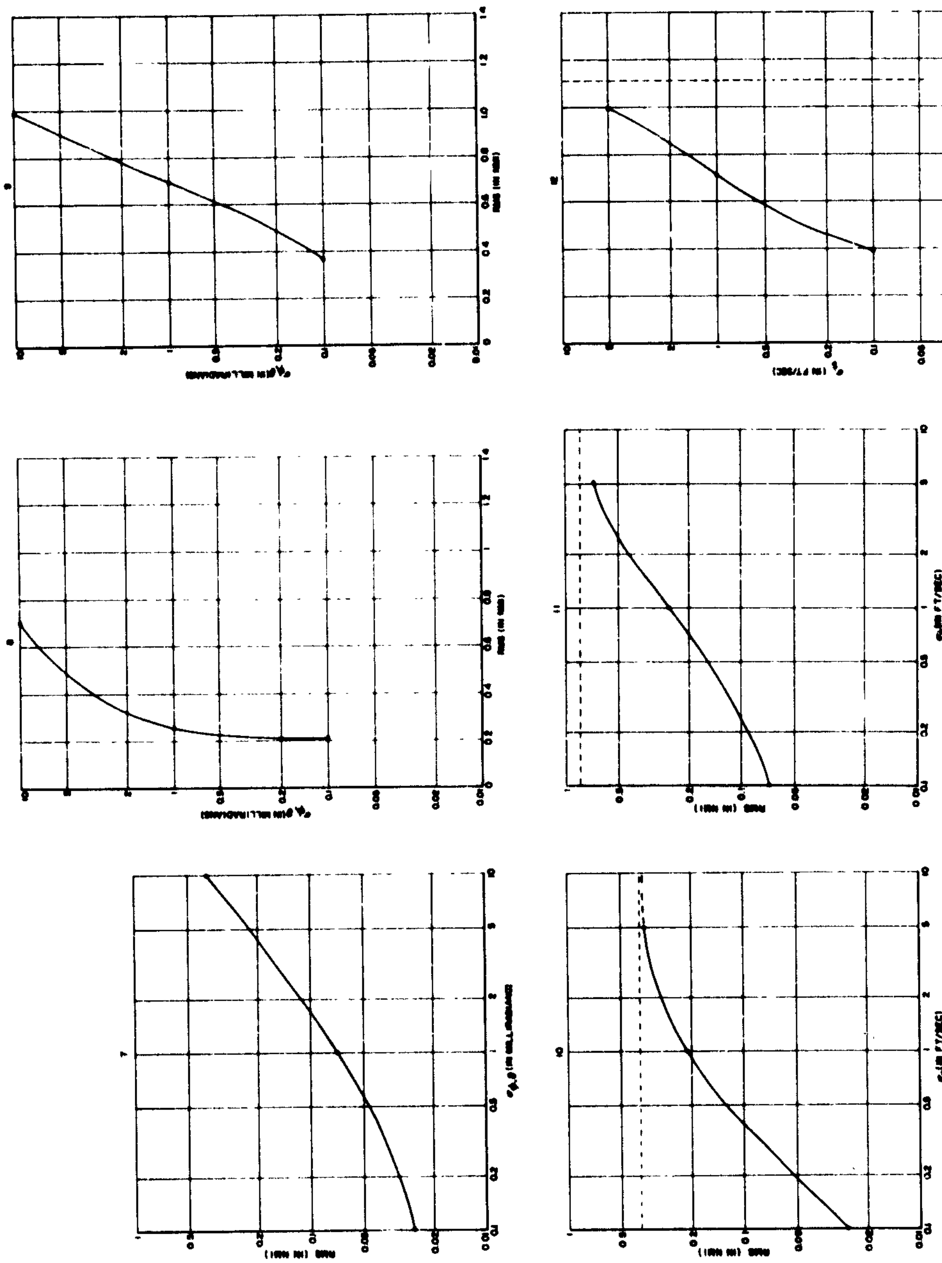

FIG. A-36 125 NMI ORBIT STATION CASE C, $\sigma_S = 300FT$

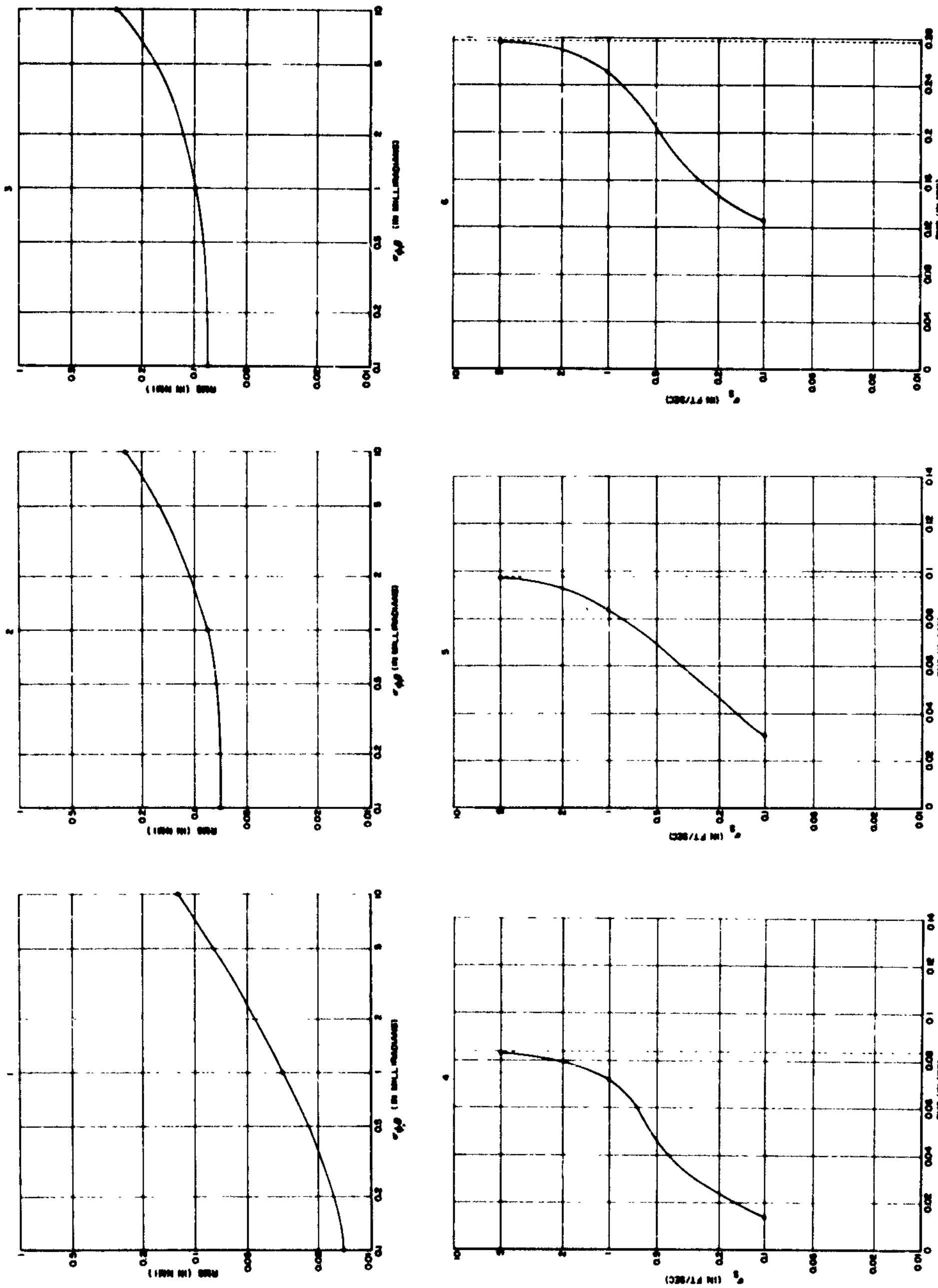

FIG. A-37 125 NMI ORBIT STATION CASE D, σ_S = 50FT

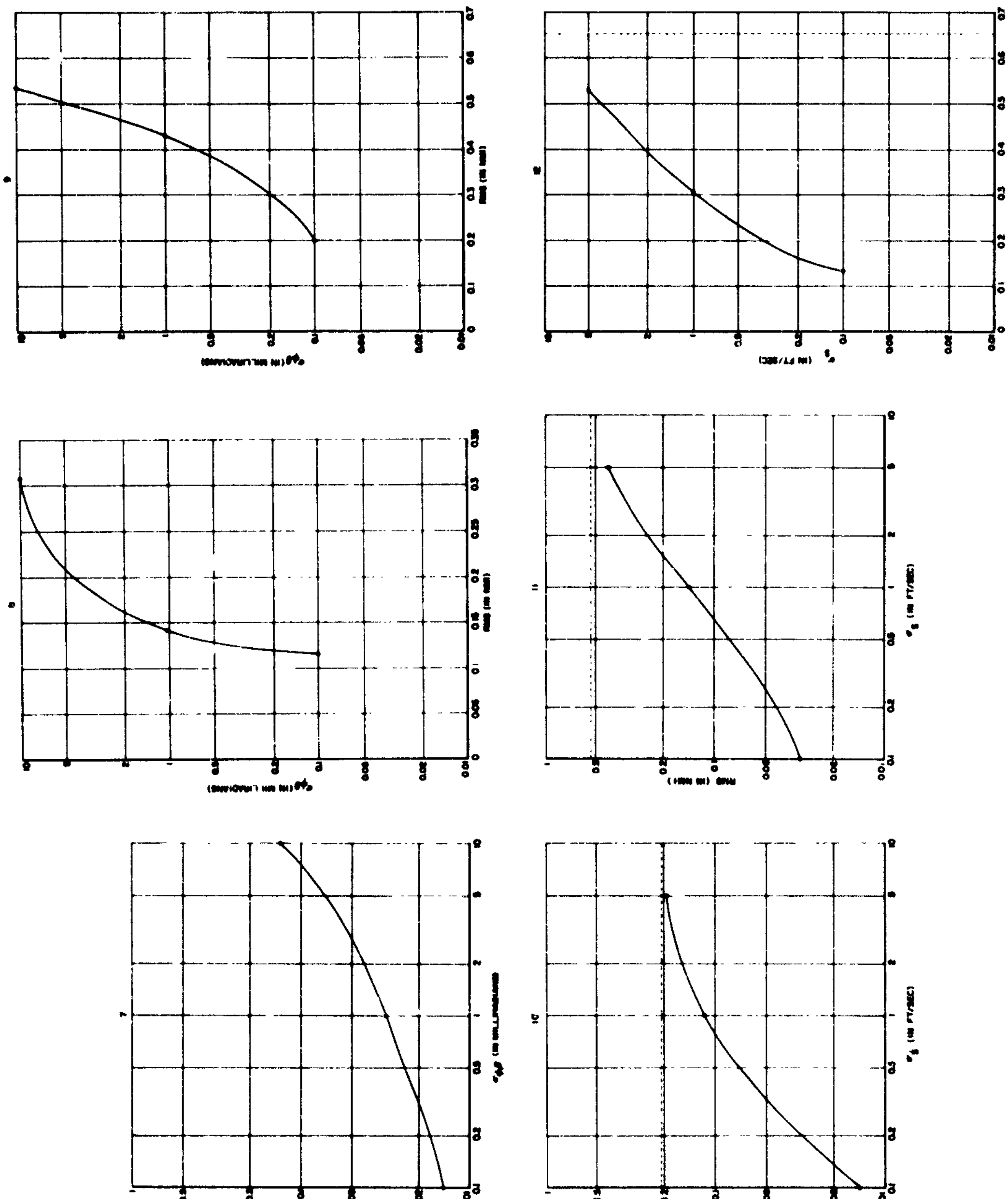

FIG. A-38 125 NMI ORBIT STATION CASE D, σ_S = 300 FT

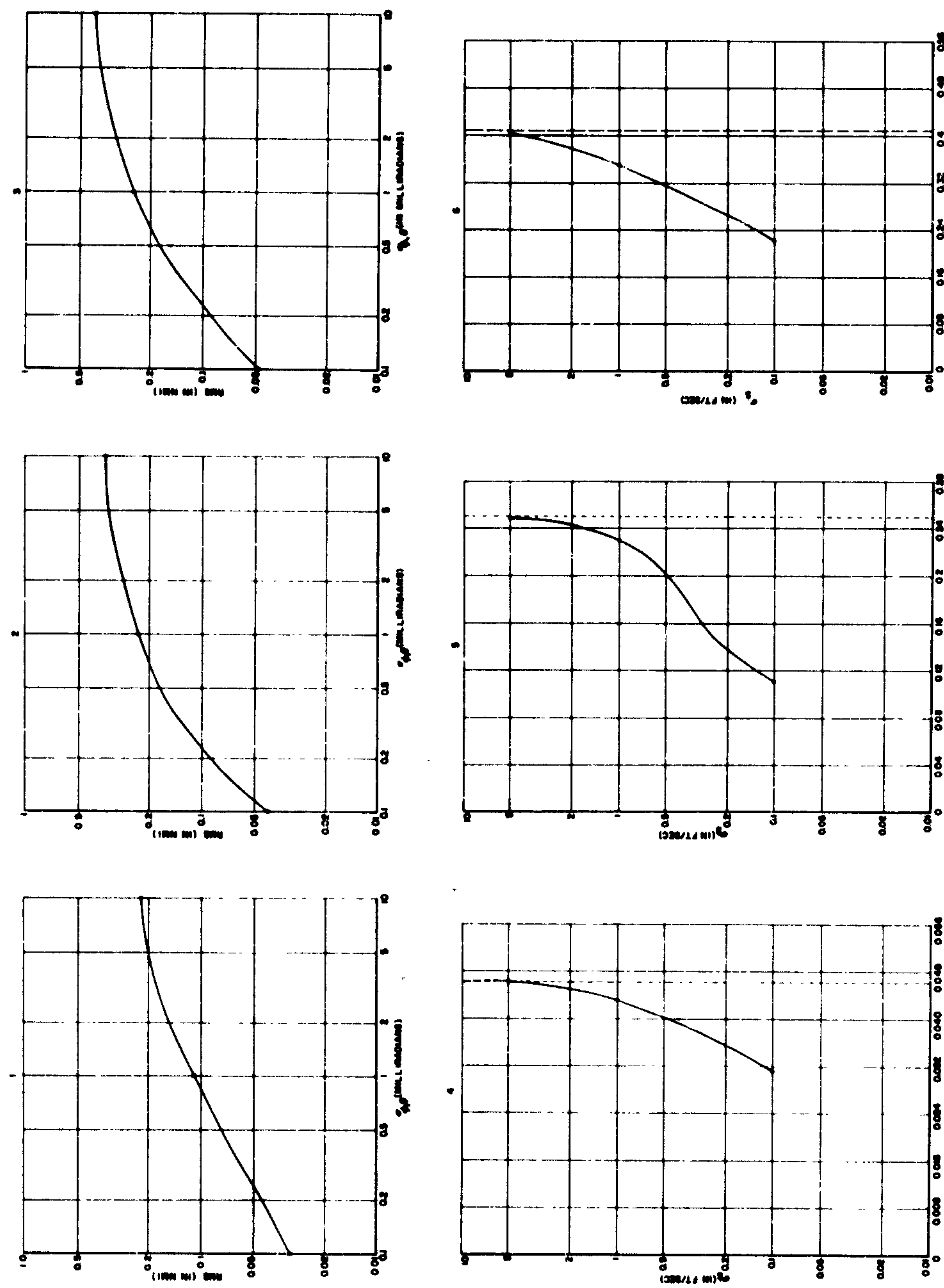

FIG. A-39 125 NMI ORBIT
STATION CASE E, $\sigma_S = 50$ FT

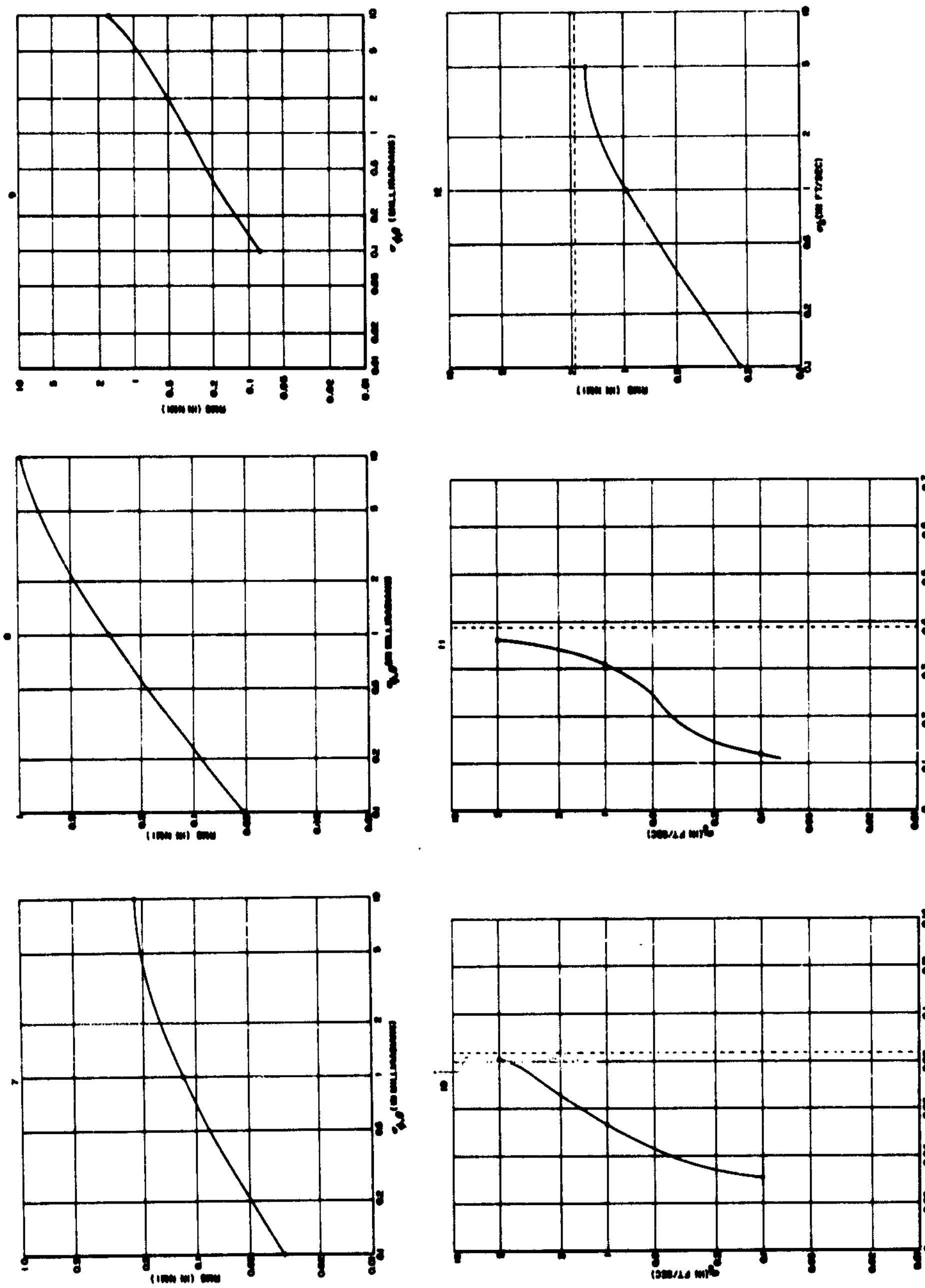

FIG. A-40 125 NMI ORBIT STATION CASE E, $\sigma_S = 300$FT

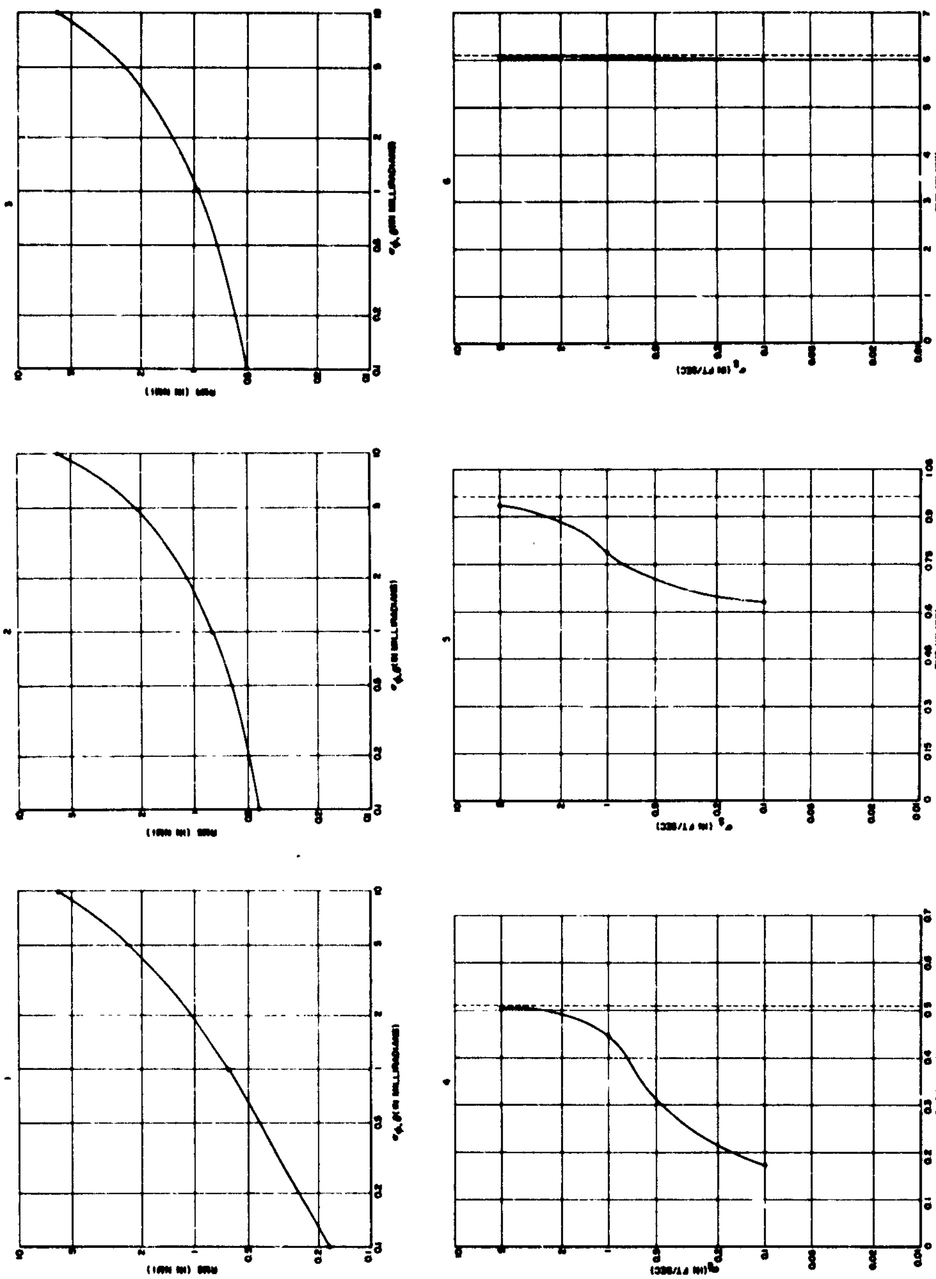

FIG. A-41 125 NMI ORBIT STATION CASE A, $\sigma_S = 50$

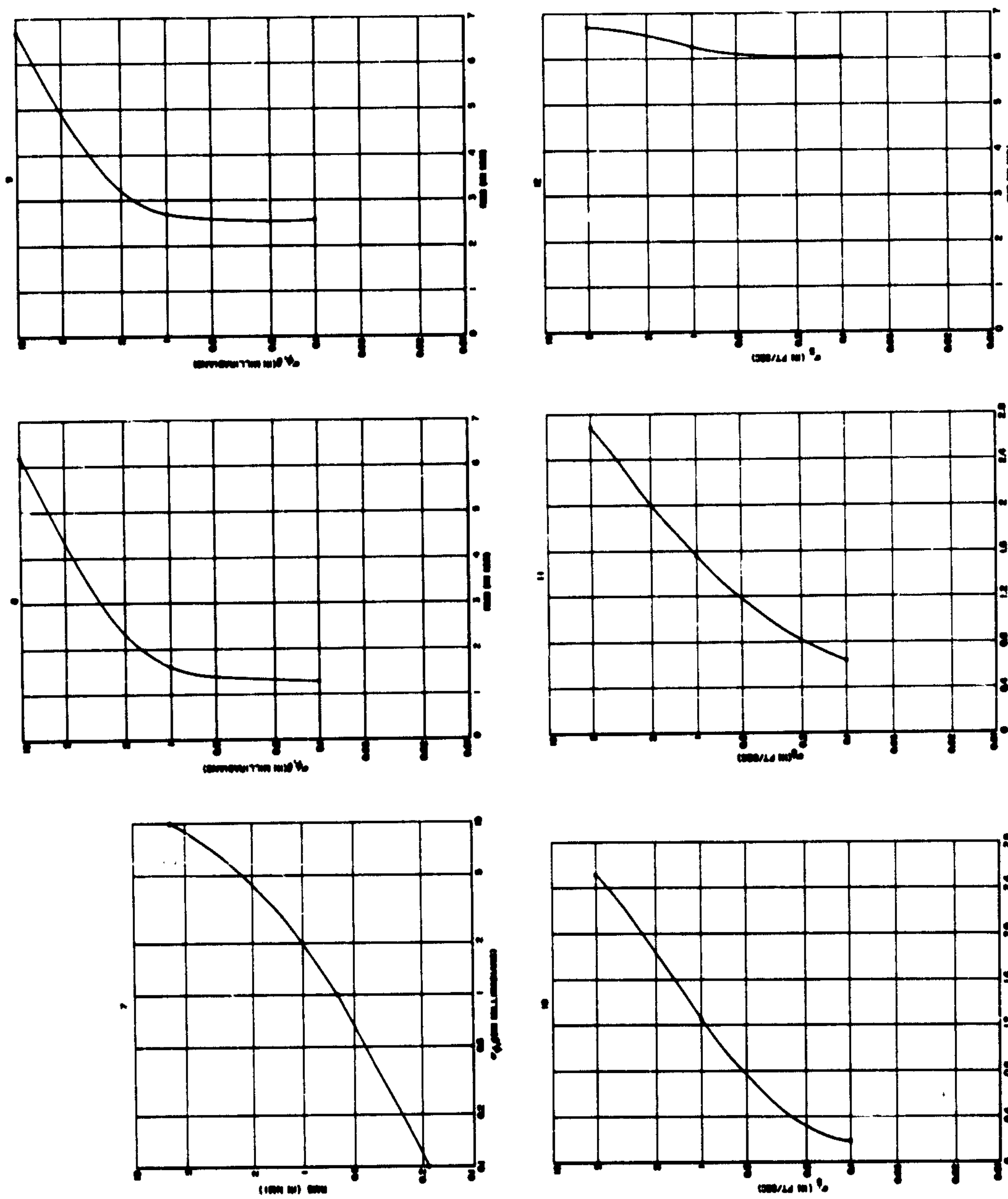

FIG. A-42 125 NMI ORBIT STATION CASE A, $\sigma_S = 50FT$

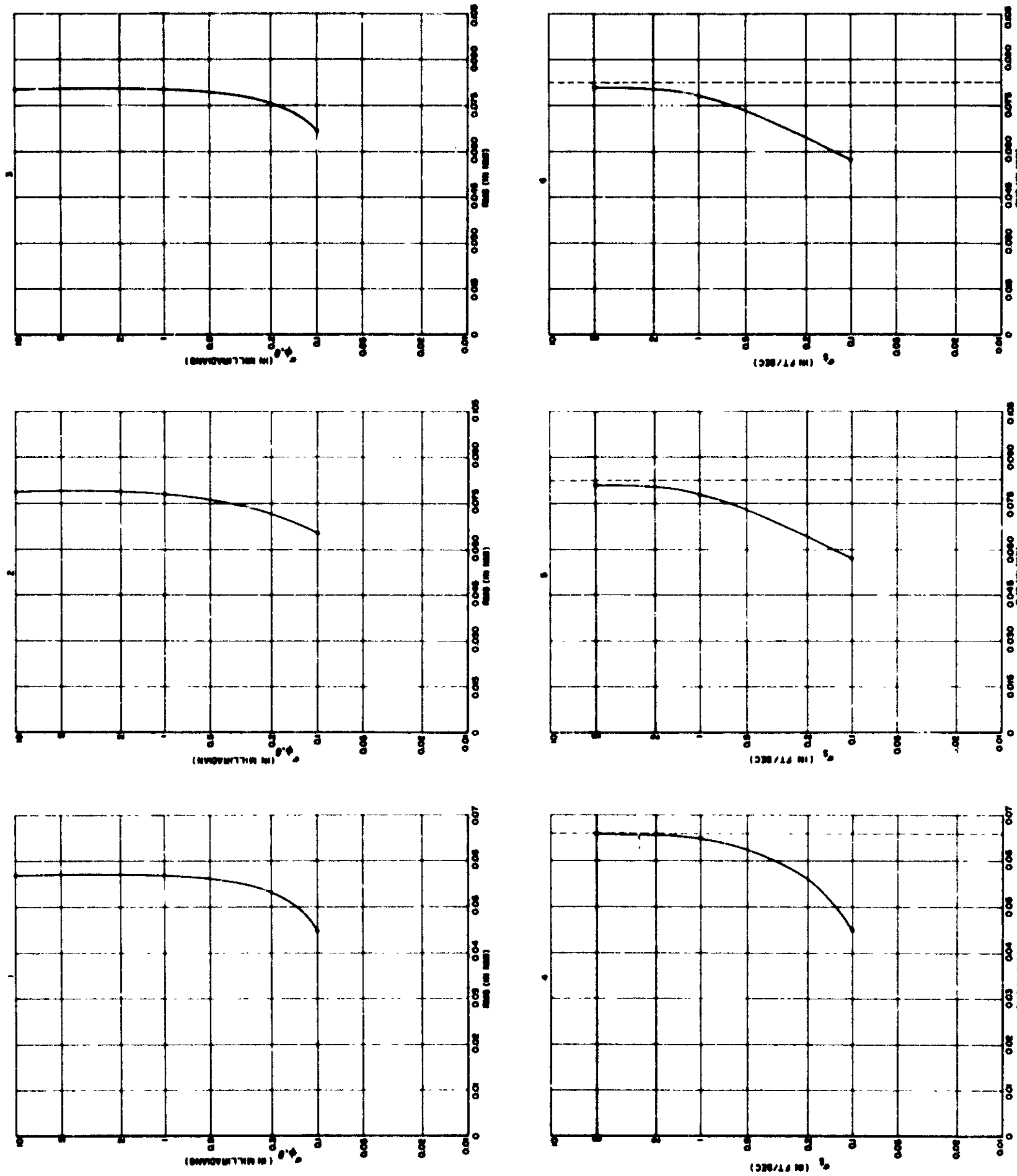

FIG. A-43 2000NMI ORBIT STATION CASE B, σ_S=50FT

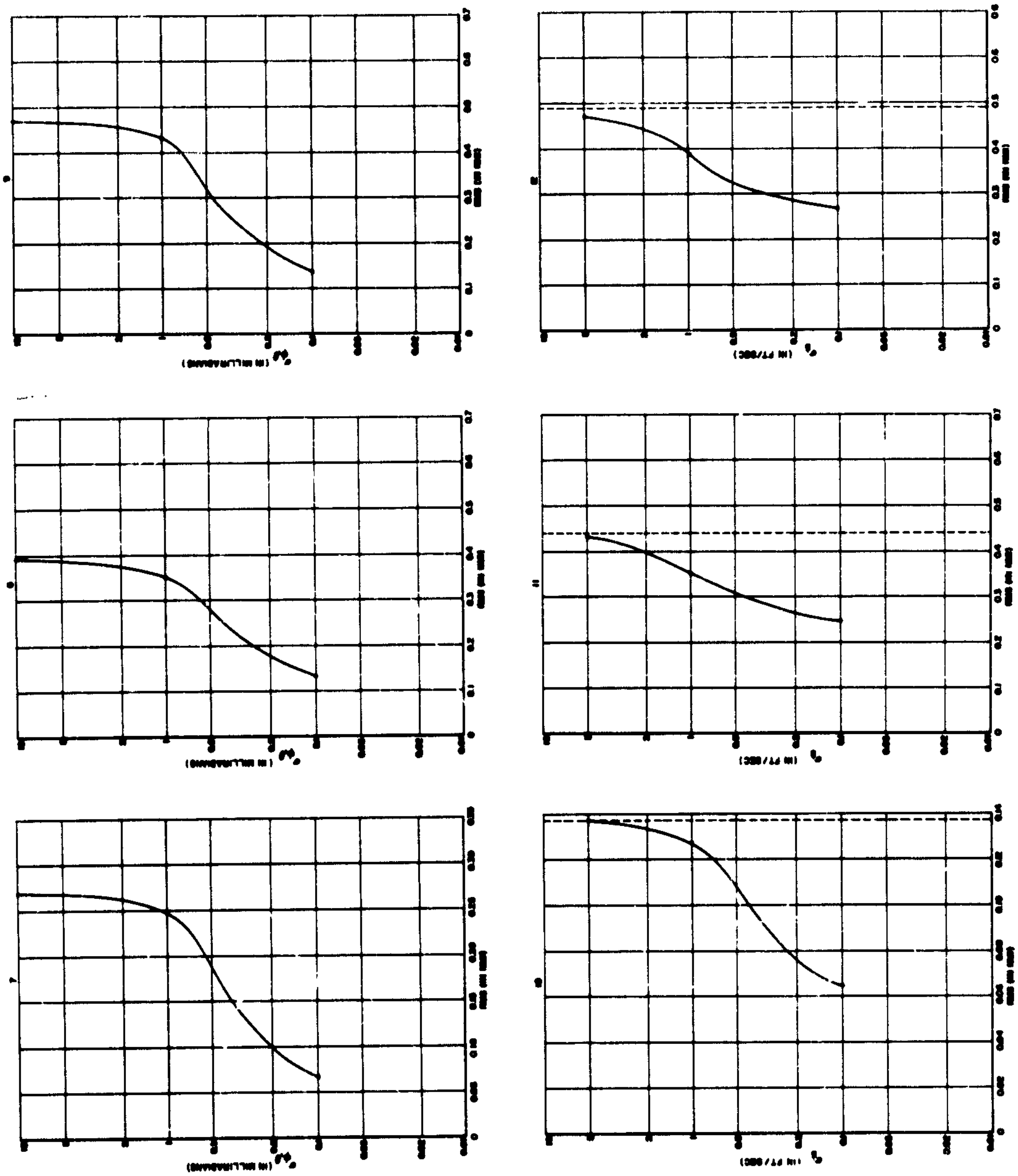

FIG. A-44 2000 NMI ORBIT STATION CASE B, σ_S=300FT

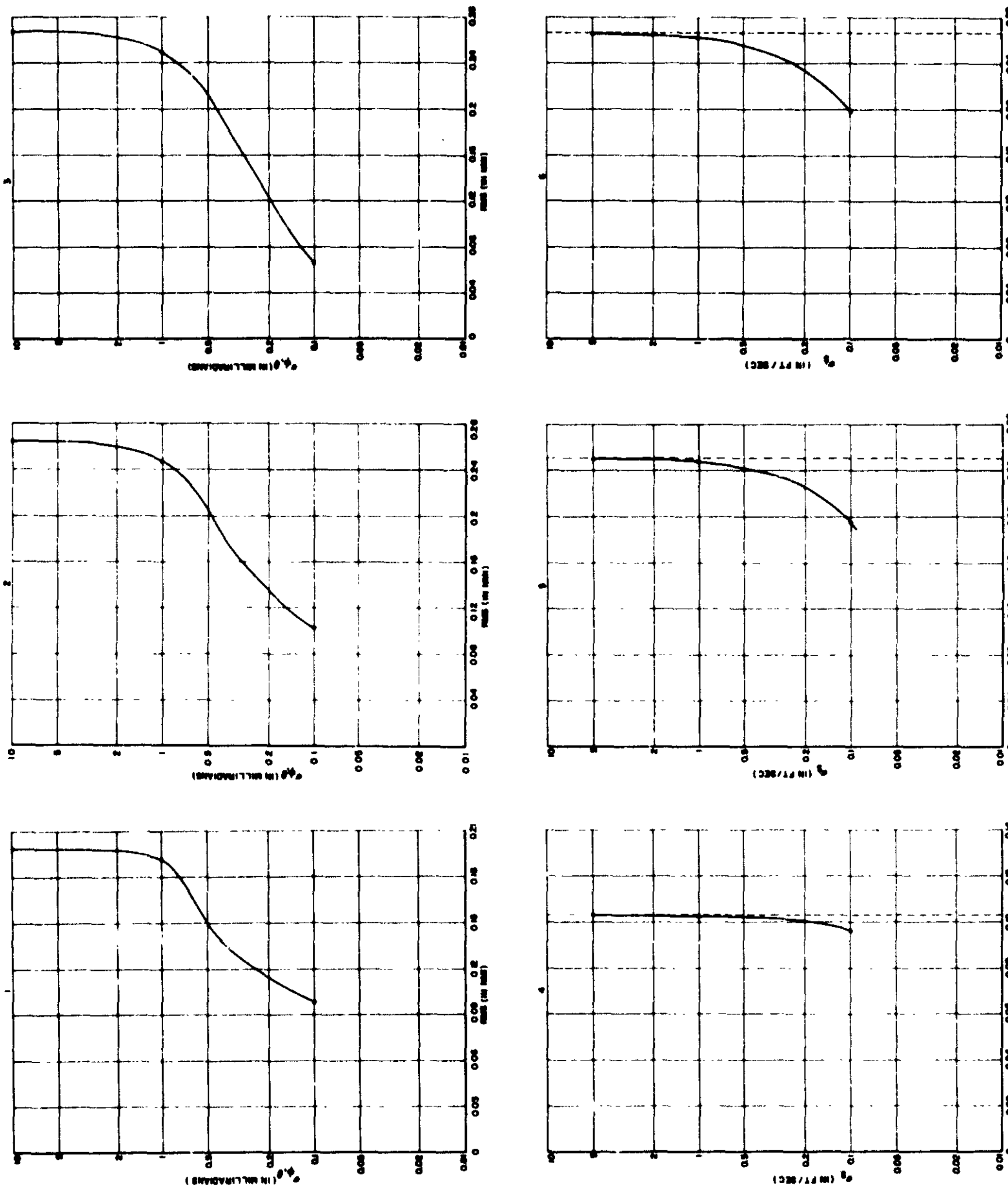

FIG. A-45 2000 NMI ORBIT STATION CASE C, σ_S =50FT

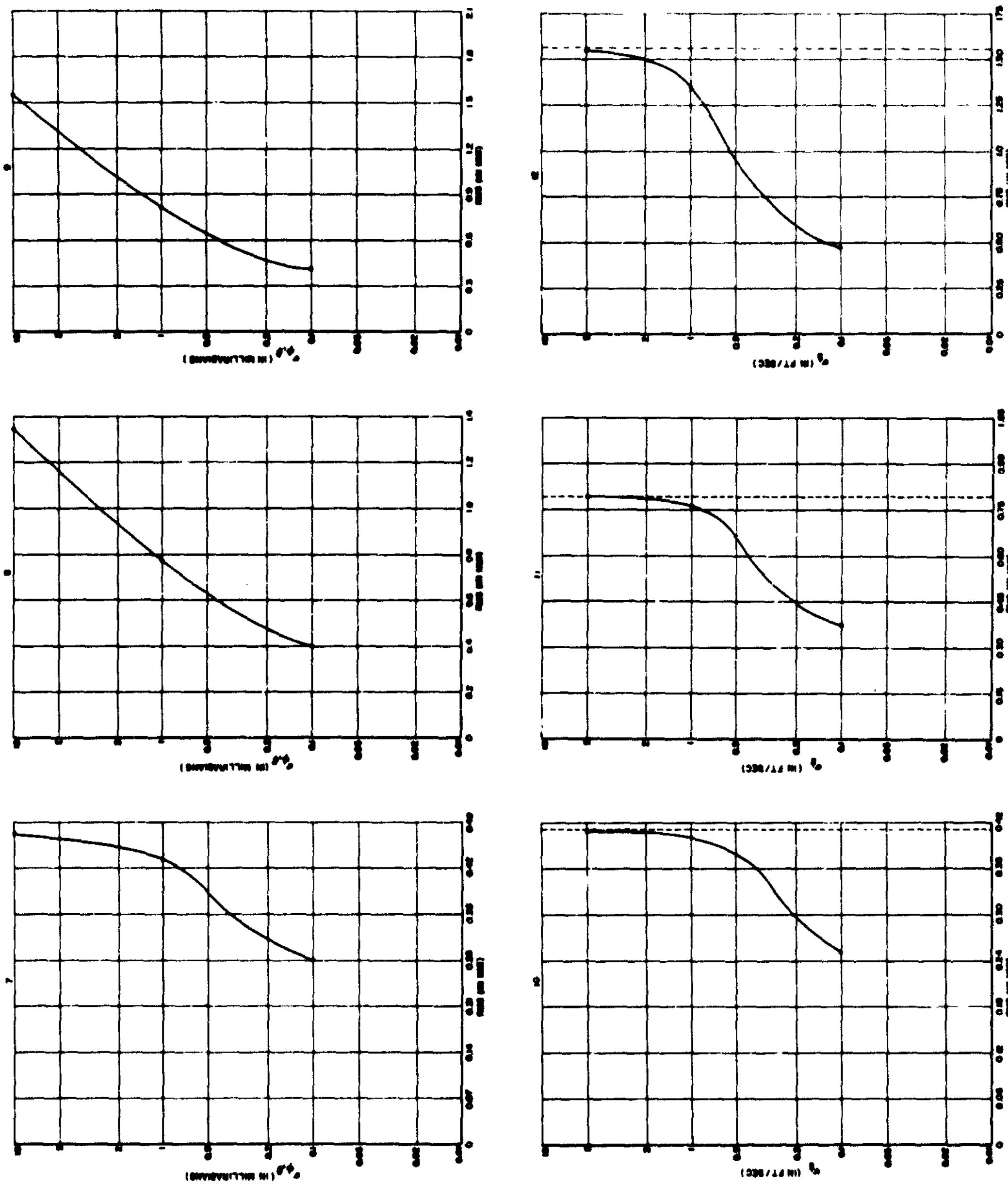

FIG. A-46 2000 NMI ORBIT
STATION CASE C, σ_S = 300FT

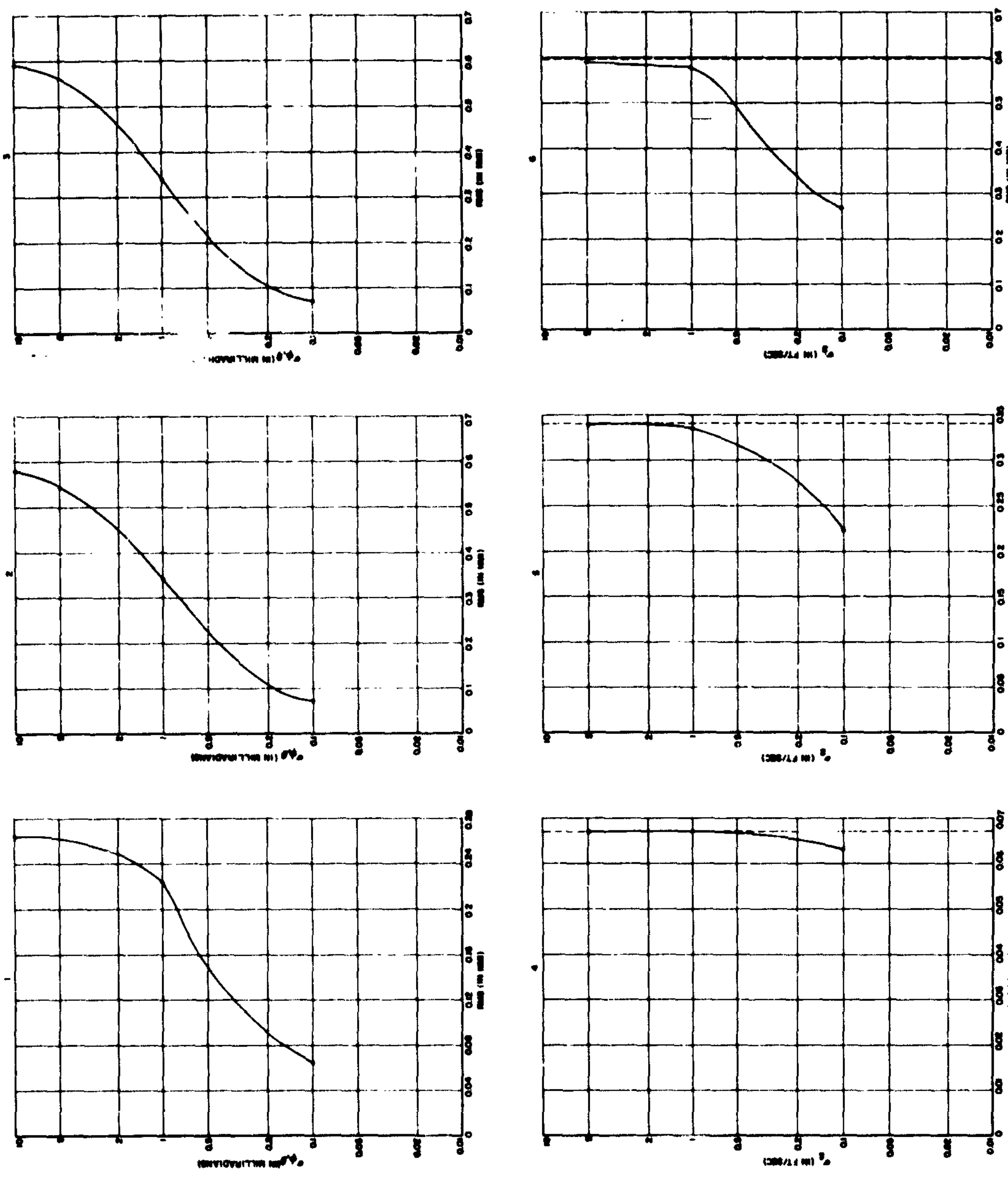

FIG. A-47 2000NMI ORBIT
STATION CASE D, σ_S=50FT

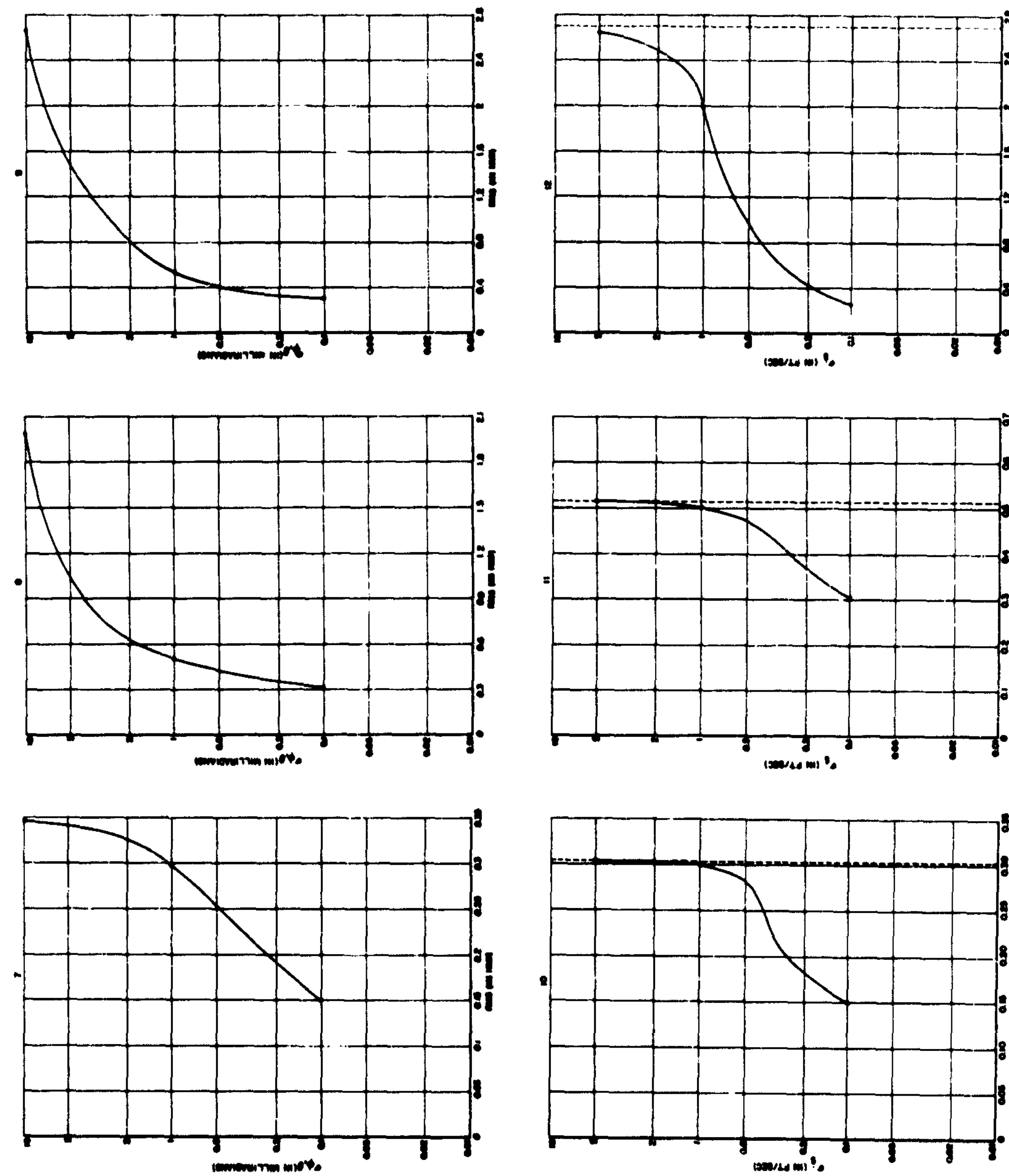

FIG. A-48 2000 NMI ORBIT STATION CASE D, $\sigma_S = 300$FT

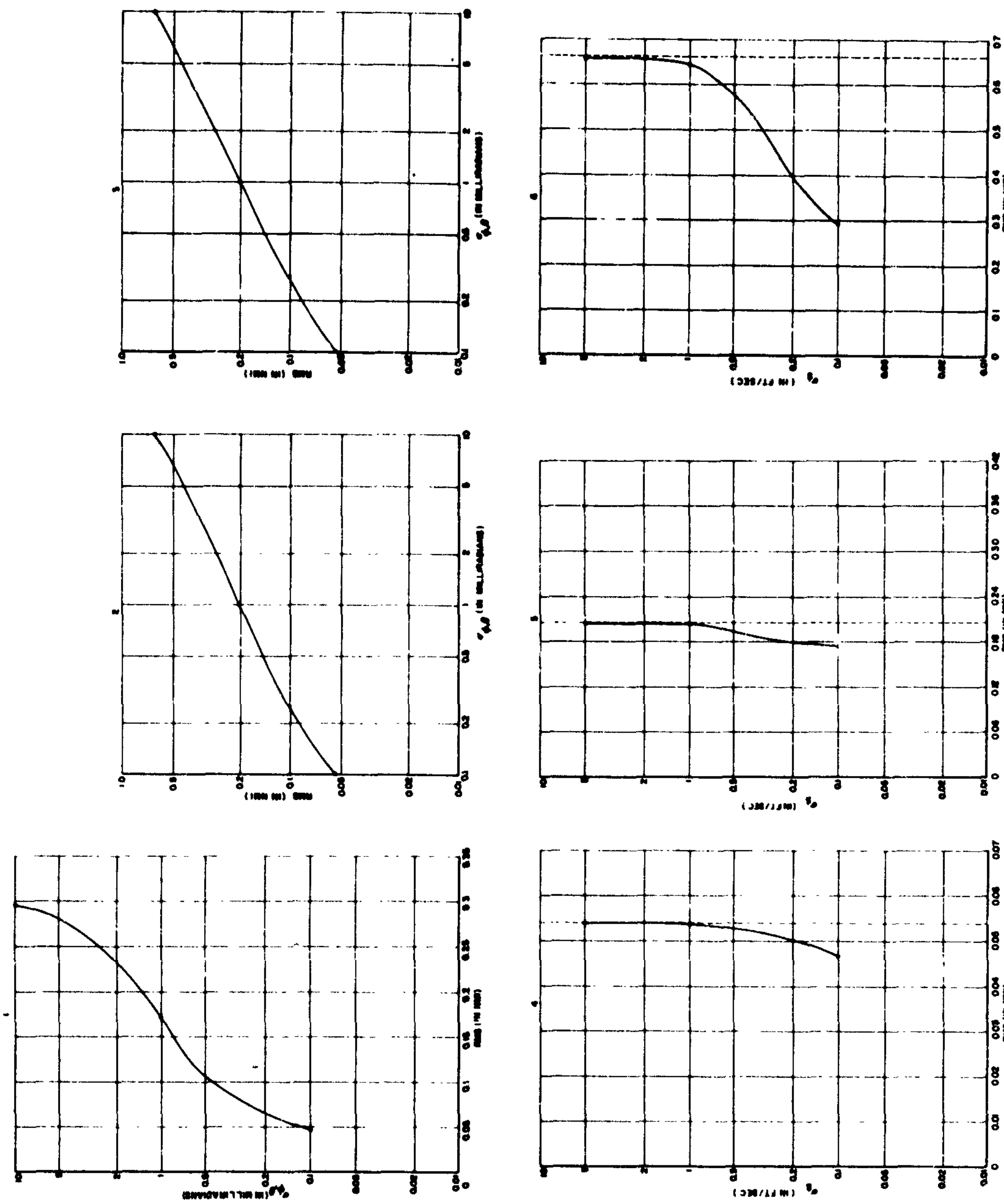

FIG A-49 2000 NMI ORBIT STATION CASE E, $\sigma_S = 50$ FT

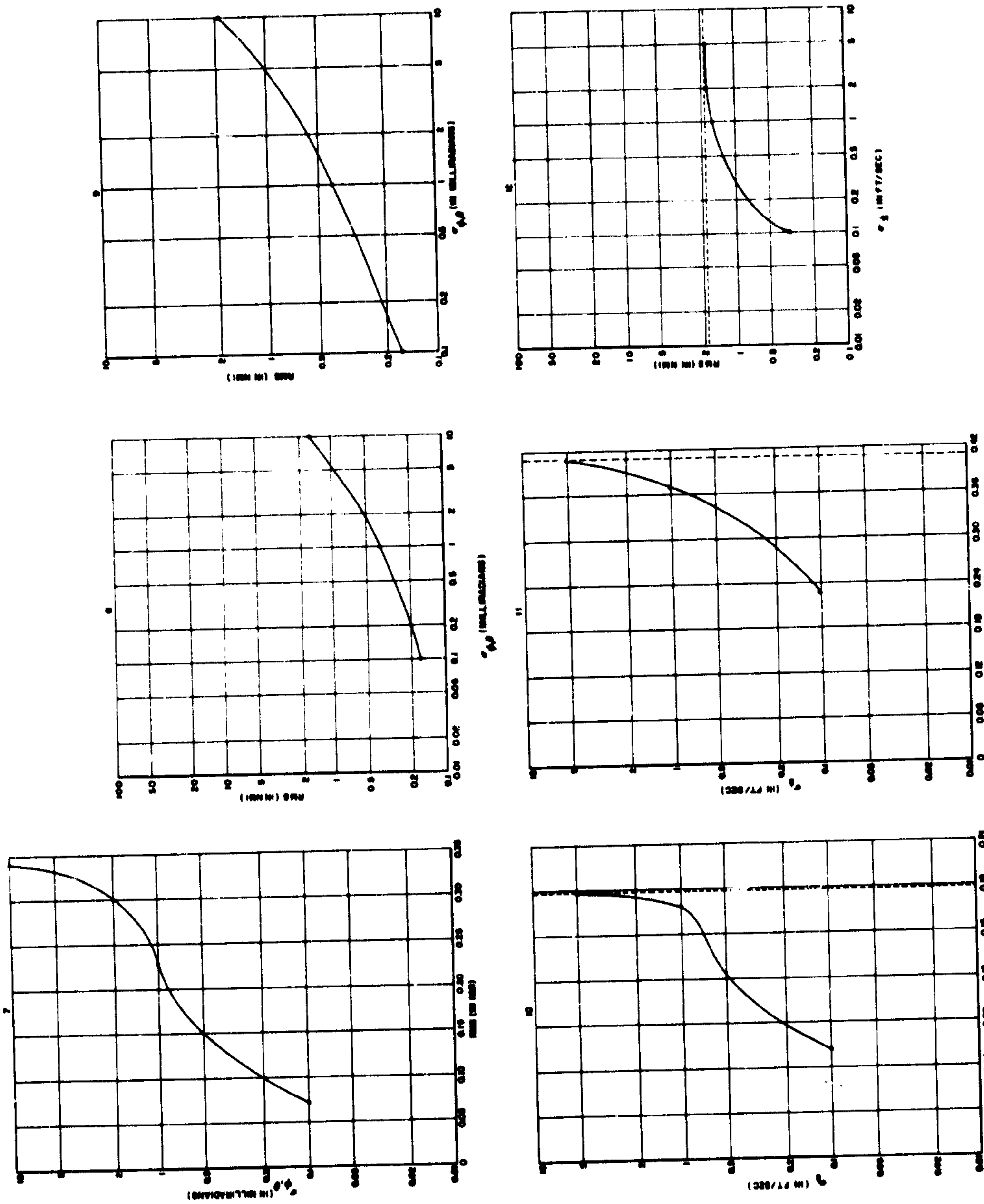

FIG. A-50 2000 NMI ORBIT STATION CASE E, σ_S=300FT

APPENDIX B

TRACKING SENSORS AND ERRORS WITH THEIR CORRESPONDING RMS' s

TABLE B-1

TRACKING SENSORS AND ERRORS

CASE NO.	SENSOR	SENSOR ERROR *
1	$\sigma_S, \sigma_{\phi,\theta}$	50,0.1
2		300,0.1
3		50,1
4		300,1
5		50,10
6		300,10
7	$\sigma_{\dot{S}}, \sigma_{\phi,\theta}$	0.1,0.1
8		0.1,1
9		0.1,10
10		1,0.1
11		1,1
12		1,10
13		5,0.1
14		5,1
15		5,10
16	$\sigma_S, \sigma_{\dot{S}}, \sigma_{\phi,\theta}$	50,0.1,0.1
17		300,0.1,0.1
18		50,0.1,1
19		300,0.1,1
20		50,0.1,10
21		300,0.1,10
22		50,1,0.1
23		300,1,0.1
24		50,1,1
25		300,1,1
26		50,1,10

* Units of σ_S, $\sigma_{\dot{S}}$, and $\sigma_{\phi,\theta}$ are ft, ft/sec, and milliradian, respectively

TABLE B-1 (Cont'd)

CASE NO.	SENSOR	SENSOR ERROR*
27		300,1,10
28		50,5,0.1
29		300,5,0.1
30		50,5,1
31		300,5,1
32		50,5,10
33		300,5,10
34	σ_S	50
35		300
36	$\sigma_{\phi,\theta}$	1
37	$\sigma_{\dot{S}}$	1

* Units of σ_S, $\sigma_{\dot{S}}$, and $\sigma_{\phi,\theta}$ are ft, ft/sec, and milliradian, respectively

[illegible]

[illegible] FOR [illegible] NMI ORBIT

CASE NO.	STATION CASE A	STATION CASE B	STATION CASE C	STATION CASE D	STATION CASE E
1	0.509394	0.132354	0.131558	0.084069	0.046822
2	2.897179	0.149908	0.384478	0.204565	0.082647
3	0.963438	0.663203	0.156191	0.098211	0.249671
4	3.179538	1.282356	0.820113	0.532869	0.383694
5	6.095192	0.767530	0.686128	0.279830	0.409768
6	7.376270	4.348058	1.102109	0.650835	1.909114
7	0.185827	0.044973	0.026510	0.014419	0.031169
8	0.632875	0.169009	0.072088	0.031131	0.119314
9	6.033601	0.197861	0.388083	0.133250	0.221624
10	1.455849	0.129089	0.217119	0.118161	0.053647
11	1.858270	0.449737	0.265109	0.144190	0.311690
12	6.328759	1.690096	0.720888	0.311318	1.193143
13	5.459447	0.153108	0.412474	0.211861	0.083471
14	8.258126	1.146213	1.227797	0.672043	0.399778
15	10.703141	3.303283	1.452421	0.765040	2.850919
16	10.172053	0.044813	0.026095	0.014259	0.030978
17	0.185377	0.044969	0.026499	0.014414	0.031163
18	0.628534	0.140000	0.071887	0.030983	0.109954
19	0.632732	0.167920	0.072083	0.031127	0.119018
20	6.003460	0.154685	0.385235	0.125638	0.220454
21	6.032595	0.196094	0.388002	0.133017	0.221585
22	0.444002	0.126258	0.117219	0.072296	0.042579
23	1.263037	0.128937	0.210085	0.115474	0.053034
24	0.787864	0.378241	0.140927	0.083580	0.229520
25	1.551165	0.445439	0.254063	0.139885	0.306549
26	6.073394	0.403954	0.667299	0.253046	0.348575
27	6.235573	1.134607	0.715680	0.307384	0.979463
28	0.504919	0.132079	0.130879	0.083482	0.046588
29	2.534140	0.146856	0.365323	0.195827	0.079706
30	0.940421	0.636422	0.155442	0.097445	0.248397
31	2.681562	1.111070	0.693435	0.426150	0.353902
32	6.092679	0.727550	0.684984	0.278131	0.405173
33	6.702018	2.075798	0.990529	0.535247	1.623534
34	1317.814305 *	0.768926	4.699293	0.581031	9.336127
35	7862.644187 *	4.613502	28.195535	3.486161	56.017521
36	532.324555 *	1.592786	4.428597	2.237854	0.870029
37	683.230796 *	1.982359	4.762782	1.523960	7.099780

*These values resulted from lack of sufficient tracking data. More meaningful results would be achieved by using equipment sensors which had much better resolution.

TABLE B-3

RMS'S FOR 2000 NMI ORBIT

CASE NO.	STATION CASE A	STATION CASE B	STATION CASE C	STATION CASE D	STATION CASE E
1	0.172470	0.065810	0.102704	0.066955	0.053961
2	0.735132	0.137026	0.410143	0.307669	0.177937
3	1.151709	0.079763	0.249498	0.339144	0.203525
4	1.380522	0.439039	0.794005	0.514312	0.408341
5	10.253282	0.079995	0.266222	0.591635	0.660093
6	11.445522	0.479486	1.558999	2.698574	1.885488
7	2.207410	0.067177	0.406575	0.170649	0.073335
8	2.985630	0.532457	0.738302	0.427855	0.380935
9	14.059290	1.023610	0.901839	0.507200	0.490962
10	4.388341	0.165728	2.041950	1.064413	0.363260
11	22.074099	0.671779	4.065751	1.706495	0.733353
12	29.856300	5.324562	7.883027	4.278552	3.809356
13	10.203264	0.275094	3.804117	1.803660	0.592607
14	38.876061	1.223012	14.726612	6.834448	2.226027
15	126.735377	6.294988	23.036942	10.335214	6.176709
16	0.154846	0.045478	0.097432	0.063280	0.046951
17	0.545719	0.065681	0.279476	0.150211	0.070908
18	1.139173	0.056897	0.191881	0.224202	0.172984
19	1.262353	0.247134	0.443187	0.297550	0.226463
20	6.375297	0.057072	0.197886	0.263733	0.293815
21	6.832455	0.268729	0.472308	0.343644	0.339289
22	0.171844	0.064918	0.102618	0.066905	0.053846
23	0.675916	0.128147	0.400026	0.301520	0.167694
24	1.151535	0.078665	0.248354	0.336905	0.203123
25	1.333804	0.349246	0.766539	0.503544	0.370491
26	10.170017	0.078887	0.264786	0.579547	0.646990
27	11.333039	0.387069	1.355062	1.984322	1.634001
28	0.172444	0.065773	0.102700	0.066953	0.053956
29	0.731723	0.136624	0.409647	0.307411	0.177486
30	1.151702	0.079723	0.249452	0.339053	0.203509
31	1.377255	0.430899	0.792611	0.513817	0.406371
32	10.249906	0.079949	0.266164	0.591137	0.659553
33	11.440809	0.470061	1.547661	2.653109	1.873091
34	254.434372 *	0.079997	0.266413	0.597946	0.695161
35	212.883970 *	0.479982	1.598469	3.587652	4.176934
36	42.407746	3.012928	45.522737	19.468410	6.207450
37	513.068955 *	10.378671	9.033700	5.082902	4.926194

*These values resulted from lack of sufficient tracking data. More meaningful results would be achieved by using equipment sensors which had much better resolution.

DISTRIBUTION LIST

Address	No. of Copies
Commander Space Systems Division Air Force Systems Command Air Force Unit Post Office Los Angeles, California Attn: Technical Data Center	10
USAF Contract Support Detachment No. 3 Philco Corporation Western Development Laboratories Palo Alto, California	1
Philco Corporation Western Development Laboratories Palo Alto, California	88 + 1 reproducible
Philco Corporation Plant 50 4700 Wissahickon Ave. Philadelphia 44, Pennsylvania Attn: D. Kinnier (Engineering)	1
Philco Corporation Plant 37 Union Meeting Road Blue Bell, Pennsylvania Attn: R. Murphy	1
Philco Corporation Computer Division 3900 Welsh Road Willow Grove, Pennsylvania Attn: Librarian	1
	102 + 1 reproducible